UNIVERSITÄT ZU LÜBECK

From the Institue of Experimental Dermatology

of the University of Lübeck

Director: Prof. Dr. rer.nat. Hauke Busch

Studying the hair follicle mesenchyme to identify novel key drivers of hair follicle miniaturization for unraveling new anti- androgenetic alopecia strategies

Dissertation

For Fulfillment of

Requirements

For the Doctoral Degree

Of the University of Lübeck

From the Department of Natural Sciences

Submitted by

Sabrina Altendorf

From Essen

Lübeck 2023

First referee: Prof. Dr. med. vet. habil. Jennifer Hundt

Second referee: Prof. Dr. rer. nat. Rudolf Manz

Date of oral examination: 19.06.2024

Approved for printing: Lübeck, 16.07.2024

Ein Gelehrter in seinem Laboratorium ist nicht nur ein Techniker, er steht auch vor den Naturgesetzen wie ein Kind vor der Märchenwelt.

A scientist in his laboratory is not a mere technician: he is also a child confronting natural phenomena that impress him as though they were fairy tales.

-Marie Curie-

Table of contents

List of abbreviations

°C	degree Celsius
µL	microliter
µm	micrometer
µM	micromolar
μm^2	square micrometer
5α-R	5α- reductase
A	adenine
aff	affected
ALDH1A2	aldehyde dehydrogenase 1 family member A2
AP	alkaline phosphatase
APM	arrector pili muscle
AR	androgen receptor
BAMBI	bone morphogenetic protein and activin membrane bound inhibitor
Bcl- 2	B cell lymphoma- 2
BMP	bone morphogenetic protein
C	cytosine
casp3	cleaved caspase 3
CB1	cannabinoidreceptor 1
cDNA	complementary DNA
CO_2	carbon dioxide
CPM	counts per million reads
CRH	corticotropin releasing hormone
CRHR1	corticotropin releasing hormone receptor 1
CTS	connective tissue sheath
D	day
DAPI	4′,6-Diamidin-2-phenylindol
DC	dermal cup
dH_2O	distilled water
DHRS9	dehydrogenase/ reductase SDR family member 9
DHT	dihydrotestosterone
DKK-1	dickkopf 1
DNA	desoxyribonucleic acid
DP	dermal papilla
DPC	dermal papilla cell
EBF1	early B cell factor transcription factor 1
EDAR2	ectodysplasin A2 receptor
EGF	epidermal growth factor
ELISA	enzyme-linked immunosorbent assay
EPHA5	ephrin type-A receptor 5
EtOH	ethanol
FC	fold change
FDA	food and drug administration
FGF	fibroblast growth factor
FUE	follicular unit extract
G	guanine
Gas6	growth arrest specific protein 6

GWAS	genome wide association study
H	hour
HC	hair cycle
HF	hair follicle
HFSCs	hair follicle stem cells
HGF	hepatocyte growth factor
HM	hair matrix
HMg	germinative hair matrix
HMpc	pre-cortical hair matrix
HRP	horseradish peroxidase
HS	hair shaft
HSD17B6	hydroxysteroid 17-β-dehydrogenase 6
IGF	insulin like growth factor
IGFBP3	insulin like growth factor binding protein 3
IgG	immunoglobulin G
iHF	intermediate hair follicle
IL1α	interleukin 1α
IRS	inner root sheath
KLF8	krüppel like factor 8
LCM	laser capture microdissection
log	logarithm
min	minute
mL	milliliter
mm	millimeter
mpAGA	male pattern androgenetic alopecia
N_2	liquid nitrogen
ng	nanogram
NGF	nerve growth factor
nm	nanometer
nM	nanomolar
occ	occipital
OCT	optimal cutting temperature compound
ON	overnight
ORS	outer root sheath
PAS	periodic acid– Schiff
PBS	phosphate- buffered saline
PC	principle component
PCA	principle component analysis
PET	polyethylene terephthalate
pg	picogram
Pt	patient
PTHLH	parathyroid hormone like hormone
rlog	regularized logarythm
RNA seq	RNA sequencing
RNA	ribonucleic acid
RNA	ribonucleic acid
ROI	region of interest
RORA	retinoic acid receptor related orphan receptor alpha
RT	room temperature
RT-qPCR	real-time quantitative polymerase chain reaction

RUNX1	Runt-related transcription factor 1
SCF	stem cell growth factor
SF-1	steroidogenic factor 1
SG	sebaceous gland
SHH	sonic headgehog
siRNA	small interfering RNA
SNP	single nucleotide polymorphism
SRD5A2	3-Oxo-5α-steroid-4-dehydrogenase-2
StAR	steroidogenic acute regulatory protein
SYT1	synaptotagmin 1
T	testosterone
TBS	tris- buffered saline
TGFß	transforming growth factor beta
TGFß1I1	transforming growth factor beta 1 induced transcript 1
tHF	terminal hair follicle
TNF-α	tumor necrosis factor- α
TOP1	topoisomerase 1
TUNEL	terminal desoxynucleotidyl transferase-mediated deoxyuridine triphosphate -biotin nick end labelling
UV	ultraviolet
VEGF	vascular endothelial growth factor
ver	vertex
WCM	William’s culture medium

1 Introduction

1.1 Background and project overview

Male pattern androgenetic alopecia (mpAGA) is the most prevalent form of hair loss in men. Nearly 80 % of all Caucasian men develop this heritable androgen-dependent form of progressive hair loss by the age of 80 years. Its hallmarks include the step-wise miniaturization of terminal (t) hair follicles (HFs) (terminal-to-vellus conversion via an intermediate stage) and shortening of the anagen phase in developmentally pre-programmed and affected (aff) scalp regions (vertex and frontotemporal). This leads inescapably to balding in these regions and resulting in the pattern characteristic for mpAGA. Until now it remains insufficiently understood how androgens, especially testosterone (T) and its more potent metabolite dihydrotestosterone (DHT), trigger the onset of this disease and maintain its progression via the same androgen receptor (AR).

Therefore, one aim of this project is to understand the role of T in mpAGA by identifying changes in the early gene expression after T treatment.

It is still debated whether the key pathobiological events happen in the mesenchymal (dermal papilla [DP] and dermal cup [DC]) or in the epithelial (germinative and pre-cortical hair matrix [HMg/ HMpc]) compartments. The aim was to produce maximal clinically relevant data where just the single HF compartments of interest are observed and no cells from neighboring compartments alter the gene expression results. t and intermediate (i) HFs from the occipital (occ) and the aff area of mpAGA patients (Pts) where cryosectioned and single compartments where isolated *in situ* by laser capture microdissection (LCM) and analyzed by RNA sequencing (RNAseq). To detect changes in the early gene expression, HFs where cultured with 10 nM T *ex vivo* before performing LCM and RNAseq. After analyzing the retrieved data, the three most interesting genes were defined and two of them were knocked down with small interfering RNA (siRNA) in a HF *ex vivo* culture to examine the direct effects of this knockdown on healthy male occ tHFs.

In addition, to investigate direct morphological effects of T, t/ iHFs from mpAGA Pts, occ and aff scalp areas where isolated from follicular unit extracts (FUEs) and treated with 30 nM T in a HF *ex vivo* organ culture. Furthermore, the effect of T on HF elongation, HM keratinocyte proliferation and apoptosis, DP inductivity, changes in DC, DP and DP-stalk cell number as well as the induction of apoptosis was investigated.

Taken all together, this study shall provide interesting new insights in the pathobiology of mpAGA and the role of T in its development and help to identify novel target genes for potential mpAGA treatment.

1.2 Hair follicle biology

One of the biggest organs of the human body is the skin. It is made up of three major layers, the epidermis, the dermis and the subcutis (see **Figure 1.1**). The most prominent structure in the skin is the HF and its associated sebaceous gland (SG) [1–3]. The product of this complex mini-organ is a long, pigmented hair shaft (HS). It plays an important role in thermoregulation, social communication and diffusion of sebum produced by different glands [4–7]

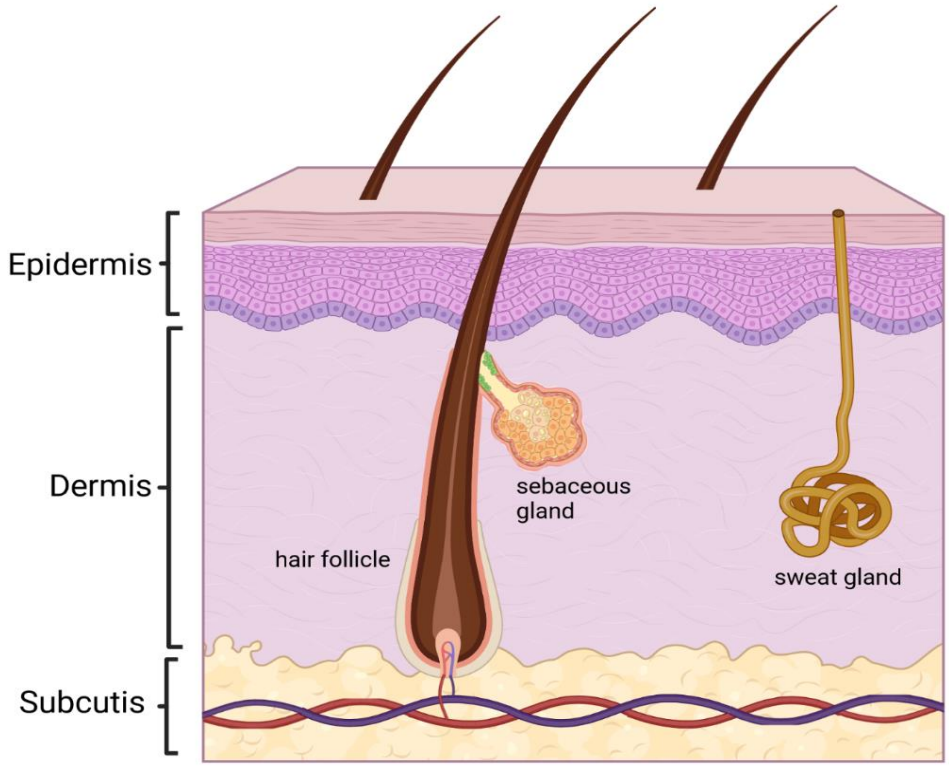

Figure 1.1 Structure of human scalp. The human scalp consists of three major layers, the epidermis, the dermis and the subcutis. The most prominent structures in the human skin are the hair follicles with sebaceous glands, sweat glands and the blood vessels. Figure modified after Grice and Segre. Image was created with biorender.com.

Many different growth factors and their receptors, their antagonists, adhesion molecules, transcription factors mediating a bidirectional cross-talk between cutaneous ectoderm and mesenchyme during embryogenesis, which results in HF formation [4,6,8–10]. After being formed once, the HF self-renews during the hair cycle (HC) [4,6,7,10,11].

1.2.1 Hair follicle anatomy

Following the HF from the epidermis downwards, it starts with the infundibulum where the hair canal opens to the surface of the skin. Afterwards, there is the SG duct, which separates the infundibulum from the isthmus which ends with the insertion of the arrector pili muscle (APM) [6,12]. The APM connects the HF with the upper dermal layers. Under normal circumstances, one FUE (consisting of 3-4 HFs) shares one APM which allows the HF to "erect" during anxiety, anger or stress [13]. Where the APM connects to the HF, the so-called HF bulge is located. It is the HF stem cell niche, containing multipotent epithelial stem cells. These cells are in charge of constantly renewing the HF during the HC [14,15].

Fully developed HFs (HC stage: anagen VI) are composed of mesenchymal and epithelial compartments. The mesenchymal compartments of the HF bulb are an onion-shaped structure consisting of the so-called DP and the surrounding light bulb shaped membrane, the connective tissue sheath (CTS). The DP contains highly specialized and inductive fibroblasts, capillaries, nerve-fibers and collagen bundles. Meanwhile the HMg, the HMpc, the inner root sheath (IRS), the outer root sheath (ORS) and the HS are epithelial compartments. In the HM, the HM keratinocytes are located. These are the most proliferative cells throughout the whole HF which are differentiating into cells of all HF layers except the ORS. By expressing different hair keratins, they produce the HS [6,7,10,16–18]. While the IRS consists of four layers, the companion layer, the Henle's layer, the Huxley's layer and IRS cuticula, the ORS is formally the continuation of the epidermal basal layer [6,7,10,12]. The hair bulb additionally contains the so-called pigmentary unit where active melanocytes are located, which are in charge of transporting melanin to HMpc keratinocytes [19,20].

1.2.2 Hair cycle

Human scalp HFs undergo repetitive cycling with different phases: the growth phase (anagen), the regression phase (catagen) and a relative resting phase (telogen) [21–23]. Under normal conditions, the anagen phase lasts for several years, the catagen phase lasts for one to two weeks and the telogen phase for several months. The DP plays a key role in the maintenance of hair growth [24–27]. DP cells (DPCs) release growth factors and extracellular matrix factors to influence the DP itself by an autocrine effect and also other epithelial cells of the HF with a paracrine effect [23–25]. During the telogen phase, high levels of bone morphogenetic proteins (BMPs), especially BMP-2 and BMP-4 coming from cells outside the HF, are present in the DP. BMP-2 is produced mostly by subcutaneous adipocytes, BMP-4 by extra-follicular dermal fibroblasts [28]. By the presence and interaction of these BMPs with fibroblast growth factor (FGF)-18 (expressed by the HFSCs in mice [29,30]) the HF stays in the resting phase and will not react to the regenerative stimuli such as the Wnt-signaling signals [28]. In a later state of the resting phase, the DPCs start to release growth promoting factors like noggin and sonic hedgehog (SHH) [27,31]. These growth factors are BMP antagonists and cause a decrease in FGF-18 levels and an increase of Wnt activity [8,29,31–34]. This leads to HF regeneration and preparation for entering into the anagen phase again. The onset of the expression of FGF-7 and -10 together with the presence of Shh and noggin lead to the initiation of the Wnt/ β-catenin signaling pathway [32,35]. During anagen phase, insulin like growth factor 1 (IGF1), hepatocyte growth factor (HGF), FGF-7, FGF-10, vascular endothelial growth factors (VEGFs) and stem cell growth factors (SCF) are upregulated in DPCs [31,36–38]. While the anagen HF changes to catagen phase, FGF-5, FGF-22 [39],TGF (transforming growth factor)-β and epidermal growth factors (EGFs) are upregulated in HF keratinocytes. Where these growth factors are upregulated in this transition process in keratinocytes, in the ORS all anti-apoptotic genes such as BCL-2 are downregulated. During catagen, growth factors which are in charge of keeping the HF in anagen are now downregulated [40–43] (see **Figure 1.2**).

Most of the growth factors expressed during the HC are related either to BMP signaling, the SHH signaling pathway or to Wnt/ β-catenin signaling. The SHH signaling pathway is in charge of epithelial cells starting proliferate and initiates the down growth of the HF [44,45]. The Wnt/ ß-catenin signaling pathway is initiating the differentiation of pre-cortex cells at the HS base [46,47]. The BMP signaling pathway is involved in the differentiation and the proliferation of the HF [48].

Besides the DP, the bulge is also necessarily involved in the HC and the resulting hair growth. The bulge area of the HF hosts a niche where quiescent HFSCs are stored until they are

activated for inducing a new HC. As soon as they are activated they leave the niche to become progenitor cells, the so called secondary germ cells, which produce a new HS at anagen onset and also the new hair germ which grows downwards into the dermis [49–51]. HFSCs are activated by Wnt and TGF-β signaling pathways [52].

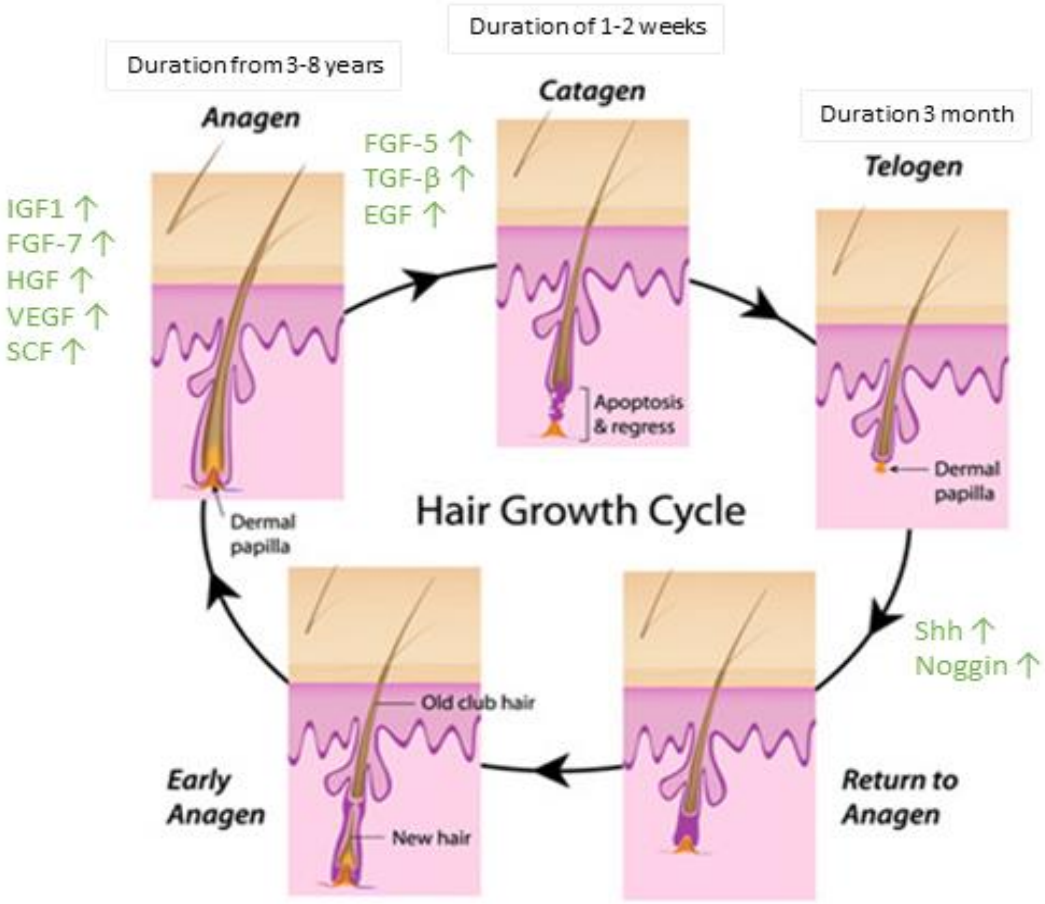

Figure 1.2 Different stages of the human hair cycle. During different stages of the hair cycle, different growth factors (genes) are upregulated to control the maintenance of the different stages: anagen (growth phase, duration 3-8 years), catagen (regression phase, duration 1-2 weeks) and telogen (relative resting phase, duration 3 months). Picture taken from http://topelectrolysisnyc.com and modified. IGF-1= insulin-like growth factore-1, FGF-7= fibroblast growth factor-7, HGF= hepatocyte growth factor, VEGF= vascular endothelial growth factor, SCF= stem cell growth factor, FGF-5= fibroblast growth factor-5, TGF-β= transforming growth factor-β, EGF= epidermal growth factor, Shh= sonic hedgehog.

1.3 Androgenetic alopecia

mpAGA is the most prevalent form of progressive hair loss in humans [53,54]. The exact onset of this disease is not clearly defined, but until the age of 80 almost 80 % of all Caucasian men develop mpAGA [55].

1.3.1 Clinical characteristics

With the onset of puberty, the local and systemic hormonal composition changes, which already initiates in some individuals the onset of mpAGA [55]. The progression of hair loss follows a defined pattern. It usually starts with the thinning of the frontal hair line and is followed by HF miniaturization in the vertex (ver) scalp region, which results in complete frontal/ver baldness (see **Figure 1.3**) [55–57].

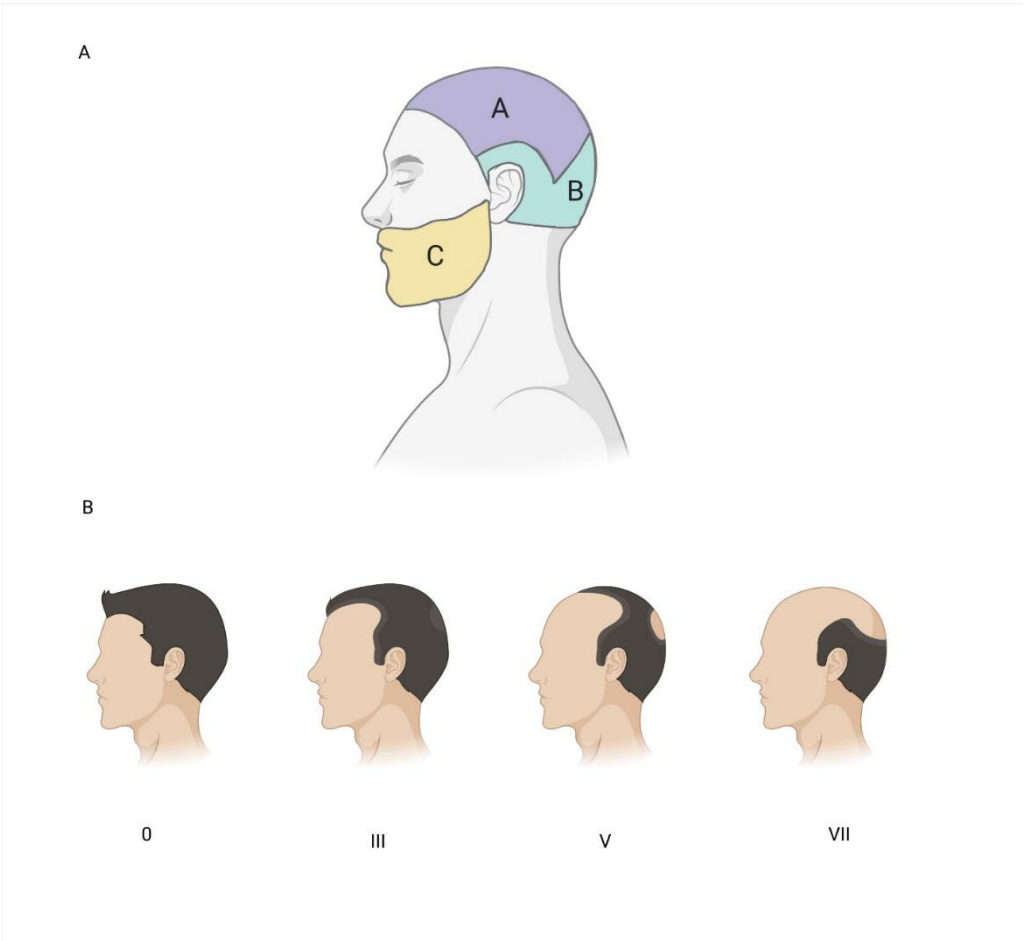

Figure 1.3 The "paradoxical" response of human hair follicles to androgens. A: Area A: Androgen-sensitive area: frontal, and vertex areas where androgens promote terminal-to-vellus hair follicle (HF) transformation. **Area B**: Relatively androgen-insensitive occipital and temporal area where androgens typically do not affect hair growth. **Area C**: Androgen-dependent beard area where androgens promote vellus-to-terminal HF transformation during puberty (as well as in the pubic and axillar region in male and female). **B**: Simplified version of the Norwood-Hamilton scale. Here only stage 0 (healthy), stage III, V and VII are shown. For the complete scale please refer to Norwood et al., 1975; Hamilton et al., 1951 [55,57]. Image was created with biorender.com.

The typical phenotype of mpAGA is defined by two anomalies in HF biology, which can be quantified by phototrichogram [58,59] and visualized by dermoscopy [60]. The first phenomenon is the transformation of tHFs into vellus HFs [61] via an intermediate phase [62]. The other phenomenon is HC related, and induced by premature catagen induction [63–68] resulting in a dramatically increased percentage of telogen HFs in the androgen-sensitive scalp area. While these events take place in the androgen-sensitive areas (frontal, vertex, parietal) of the scalp, the androgen-insensitive areas (occipital, temporal) seem to remain relatively unaffected by testosterone. In addition, there are also androgen-dependent areas (beard, axillary, pubic) where androgens cause a vellus-to-terminal conversion [69]. What causes this “androgen-paradoxon” remains in this moment still unknown.

1.3.2 Histopathology

Comparing a histological image of occ scalp with aff scalp of an mpAGA Pt, the reduction in the number of tHFs in the aff scalp is clearly visible (see **Figure 1.5**). One of the most important histological features of mpAGA is the fibrotic streamer. It appears at the initial position of the former anagen hair bulb, formed by the CTS during its miniaturizaion [70,71].

Despite the fact, mpAGA is known to be a non-inflammatory disease, perifollicular inflammation can often be observed around the epithelium of HFs from the aff area [70,72], as well as mast-cell degranulation in the DC. The released granules contain pro-inflammatory cytokines like tumor necrosis factor α (TNF-α) that activates fibroblasts leading to fibrosis [73,74].

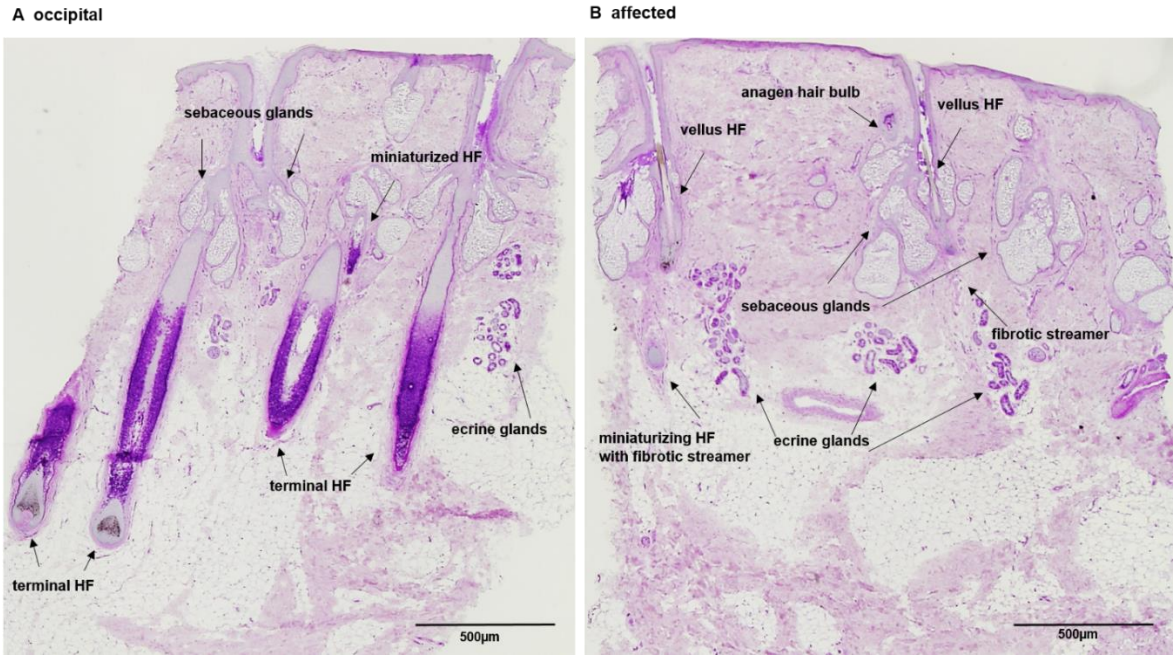

Figure 1.4 Periodic acid-Schiff staining of an occipital and affected scalp section of a male pattern androgenetic alopecia patient. A: Occipital skin section with mostly terminal hair follicles (HFs). Terminal HFs produce pigmented thick hair shafts and are anchored in the adipose tissue or the lower dermis, **B**: Affected skin section of male pattern androgenetic alopecia patients with mostly vellus HFs. Vellus HFs produce thin hair shafts with almost no pigmentation and are confined in the upper part of the dermis with no connection to the arrector pili muscle (For more detailed information see Sinclair, 2016 [75]). HF= hair follicle

1.3.3 The role of androgens

For a long time, androgens have been considered the main guarantor for hair loss in mpAGA [76]. This thought was mainly based on the results of a study that showed, men castrated before puberty are not developing mpAGA unless they are treated with T [55]. Throughout the whole HF [77] T is converted to the much more potent androgen 5α-DHT by an enzyme called 5α- reductase (5α-R) [78]. The general consensus is that the level of circulating T in mpAGA Pts (2-10 ng/mL) [79–84] is in a similar range as in healthy controls (3-15 ng/mL) [85–87]. Although the level of DHT has been reported to be elevated in mpAGA Pts in general [79,83,84] there is even a more detailed differentiation in androgen-sensitive scalp regions and androgen-insensitive scalp regions [78,88]. In addition, the activity of 5α-R was reported to be higher in microdissected HFs from the aff area compared to the occ area [89]. Furthermore, it was shown that the AR is way higher expressed throughout DP fibroblasts from ver and frontotemporal HFs compared to fibroblasts from other scalp regions [89–93]. Until now, no reasonable explanation for the “androgen paradoxon” exists. How can AR signalling lead to exact opposite effects in androgen-sensitive (terminal-to-vellus conversion) and androgen-dependent (vellus-to-terminal conversion) HFs (see **Figure 1.6**)?

In the aff scalp of mpAGA Pts, a protein (steroidogenic acute regulatory protein [StAR]) which is known to be essential for the biosynthesis of T in murine testis [94], was found to be upregulated. In the DP, several transcription factors which regulate StAR activity, like steroidogenic factor-1 (SF-1), are known to be expressed. Therefore, it has been speculated if an intrafollicular conversion of steroids into DHT [95] can be a feature of mpAGA [96].

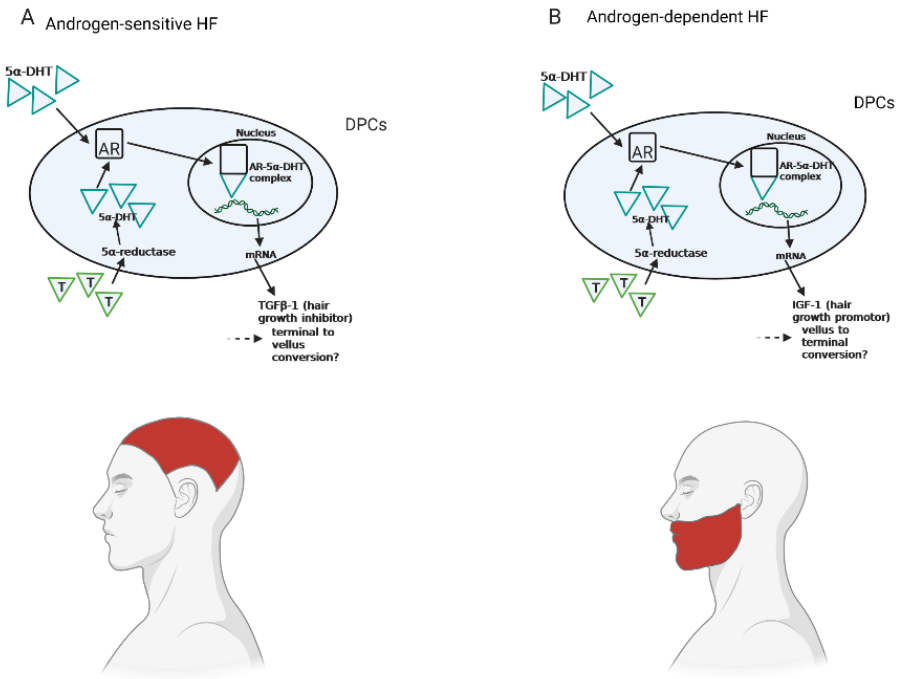

Figure 1.5 Differential androgen effects on dermal papilla cells in distinct human hair follicle populations. 5α-reductase converts testosterone (T) to 5α- dihydrotestosterone (DHT) in both types of hair follicles (HFs) and binds the same androgen receptor (AR). Both, T and 5α-DHT can bind to the AR. After ligand binding, the whole complex translocates into the nucleus where it functions as a transcription factor. **A: Androgen action in androgen-sensitive HFs (Fig.1.4 A, Area A).** The AR-5α-DHT complex stimulates the secretion [97] of transforming growth factor β-1 (TGFβ-1) [26,98]. While TGFβ-1 is a potent hair growth inhibitor and catagen promoter in human scalp HFs *ex vivo* [99], this could explain male pattern androgenetic alopecia -associated telogen effluvium, but does not yet fully explain how this leads to such a complex organ transformation process like the conversion of terminal into vellus HFs. **B: Androgen action in the androgen-dependent HFs (Fig.1.4 A, Area C).** The AR-5α-DHT complex stimulates the secretion [97] of insulin like growth factor-1 (IGF-1) [100]. While IGF-1 is well recognized to be important for anagen maintenance and to inhibit catagen development [101], this could well explain why hair shafts of vellus HFs in the beard region become longer, but – by itself - does not yet convincingly explain the androgen-dependent complex transformation of vellus HFs into terminal HFs. Image was created with biorender.com. 5α-DHT=5α dihydrotestosterone, AR= androgen receptor, T= testosterone, TGFβ-1= transforming growth factor β-1, IGF-1= insulin like growthfactor-1. Image was created with biorender.com.

Dutasteride, an inhibitor for 5α-R was recently discovered as a potential alternative metabolic pathway for the conversion of DHT [102]. It is approved for mpAGA treatment in South Korea and Japan [102–104] and its efficiency was demonstrated in double-blind controlled clinical studies [105]. It was also shown although 5α-R activity was inhibited by dutasteride, DHT can be still be converted. In response to dutasteride treatment a significant genetic variant was found in the DHRS9 (dehydrogenase/ reductase SDR family member 9) gene. The product of this gene, 3α-hydroxysteroid dehydrogenase, synthesizes DHT from 3α-androstandediol. Moreover, another DHT synthesis pathway (also 5α-R independent) was recently discovered. It is mediated by hydroxysteroid 17-β-

dehydrogenase 6 (HSD17B6) that converts 3α-diol to DHT [106,107]. These findings can be the explanation why a high number of Pts does not respond to existing DHT level lowering or 5α-R inhibiting treatments.

1.3.4 Hair cycle dysregulations

Compared to healthy individuals, the different phases of the HC are altered in mpAGA Pts. While the duration of the anagen phase is significantly reduced, the duration of telogen is notably lengthened [63–65]. There is *ex vivo* evidence that androgens promote catagen induction [66–68]. HFs treated with T, show an increased protein expression of TGFβ-2 which is known to be the main catagen promotor. Additionally, a decreased protein expression of IGF-1, which is known to be an anagen maintaining factor was observed in T treated HFs [67,101,108]. In frontal plucked HFs from mpAGA Pts, other HC regulating genes like period circadian regulator 2 (PER2) [109,110] and delta like canonical notch ligand 1 (DLL1) up or down [109,111] were found to be upregulated. All named features can be seen in **Figure 1.7**.

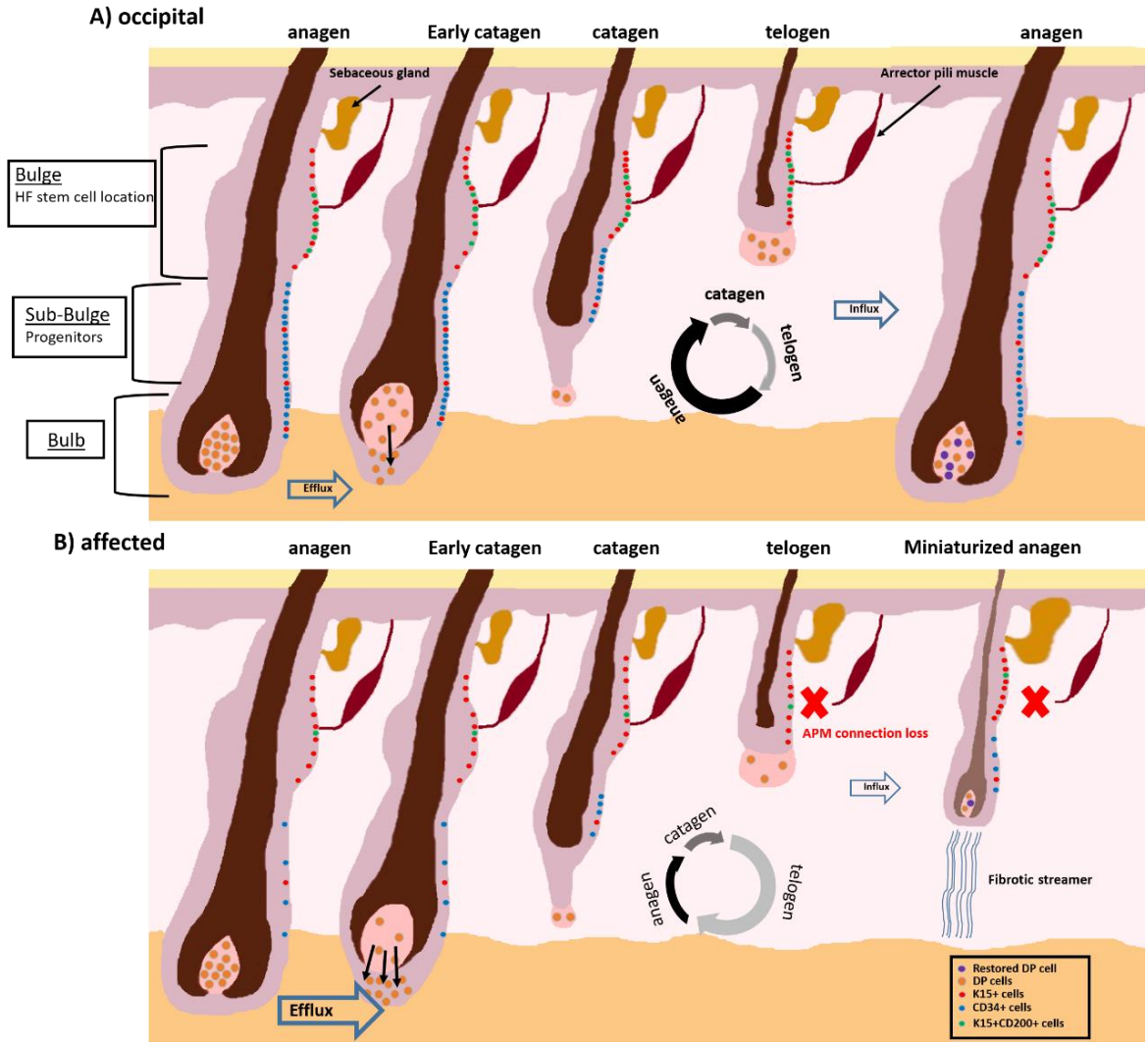

Figure 1.6 Overview of the dysregulations of the hair cycle in male pattern androgenetic alopecia. This scheme of human skin and hair follicles (HFs) shows the difference in the hair cycle between occipital (healthy) and affected male pattern androgenetic alopecia (mpAGA) scalp. The growth phase (anagen), where the hair shaft is produced, the apoptosis-mediated regression phase (catagen) and the master switch phase (telogen) [23,112] which was previously incorrectly defined as relative quiescence, in which the HFs prepare themselves for the initiation of a new hair cycle [112,113]. After the telogen phase, the new anagen onset takes place, where the progenitor cells enter the dermal papilla (DP) and restore the emigrated DP cells. **A) occipital:** In healthy skin the anagen phase is the longest, followed by the short catagen phase and the slightly longer telogen phase [23]. The efflux of dermal papilla cells (DPCs) in the late anagen phase and the influx in the very early anagen phase is balanced in healthy skin [114–116]. **B) affected:** Given that in the androgen-sensitive scalp the activity of 5α reductase (5αR) and the expression of androgen receptor (AR) is higher, compared to the androgen- insensitive scalp. From testosterone converted dihydrotestosterone (DHT) has more impact on the hair cycle than in healthy skin. DHT promotes catagen development in androgen-sensitive scalp HFs. Also hallmarks of mpAGA is the loss of the arrector pili muscle (APM) connection during the miniaturization process [117,118], the enlargement of the sebaceous gland [119], and the formation of thikened firbotic streamers after miniaturization [70,71]. In androgen-sensitive scalp the anagen phase is way shorter and the telogen phase is notably lengthened [63–65]. Also, the efflux and influx of DPCs is impaired in mpAGA [12,120,121]. APM= arrector pili muscle, DP= dermal papilla, K15= keratin 15, CD34= cluster of differentiation 34, CD200= cluster of differentiation 200. Figure was created with Microsoft Paint.

The premature termination of anagen in HFs from the androgen-sensitive scalp area might also be related to inhibition of Wnt signaling [122,123]. Its activity is controlled by secretion of Wnt signaling inhibitors by the DP and determines the length of anagen [124,125]. The downregulation of some of the best known positive Wnt/ β-catenin signaling regulators (BMP and BAMBI) [126,127] as well as the upregulation of the endogenous antagonist of several Wnt molecules, Dickkopf 1 (DKK1) [128–130], in aff scalp regions of mpAGA Pts, shows the scope of the altered HC in mpAGA. *In vitro* experiments of DPCs showed that DHT, accelerates the transcription of DKK1 [129].

Nevertheless, it remains unclear if those gene and protein expression deviations are causing the HF miniaturization and/ or the premature catagen induction, or if they are resulting from the HF transformation and aberrations in the HC.

1.3.5 Cellular and molecular controls of the hair follicle miniaturization

The general assumption is that androgens promote terminal-to-vellus transformation in androgen-sensitive areas of the scalp [55,131,132]. But how this transformation is initiated or executed still remains to be clarified.

The miniaturization process seems to be determined in the anagen hair bulb, linked to cell number, DP size and inductivity of DP fibroblasts [120,133], and not like often speculated in the bulge by the epithelial HFSCs [134]. To further support this hypothesis, a transgenic mouse model to delete DP fibroblasts was designed and supports this claim by showing that DP fibroblasts have influence of HS shape and diameters [135]. Taking these findings into consideration for a possible anti- mpAGA treatment, therapies that prevent the excessive emigration of DP fibroblasts and stabilize their influx from the DC back into the DP during anagen onset, seem to be an attractive class of new anti- mpAGA agents [12,116,120,121]. Moreover, a first clinical trial [136], which tried to restore inductive fibroblasts from the androgen-insensitive DC by injection into androgen-sensitive scalp seemed to be a promising treatment [120,121,136].

1.3.6 Genetic determinants

In the development of mpAGA, androgens as well as genetic factors play a key role [137], as mpAGA is one of the most heritable complex traits [138]. It was shown in twin-studies, that nearly 80 % predisposition to develop mpAGA is inherited [139]. A man with a bald father has a significantly decreased risk to develop mpAGA compared to a man with a bald brother or whose mother has ancestors afflicted by mpAGA. These are evidences for a not only Y-chromosomal inherited complex trait, and support the assumption of a X-chromosomal and autosomal contribution [139–142]. Two X-chromosomal located genes, the AR gene and the ectodysplasin A2 receptor (*EDAR2*) gene have been shown to be involved in mpAGA progression and predisposition [143]. Two particular polymorphisms in the AR gene (CAG and GGN repeats) were shown to influence the transcription activity and resulting from this the AR protein level [144–146]. The chance for a successful finasteride treatment can be lowered by a high number of GGC repeats (>23 counts) in the AR gene, what can also increase the severity of the disease [147]. Another influencing polymorphism was detected in the *SRD5A2* (3-oxo-5α-steroid-4-dehydrogenase-2) gene, which increases the androgen sensitivity [148,149]. Also single nucleotide polymorphisms (SNPs) located on chromosomes 3q26 [150], Xq12 [151] and 20p11 [150,152] (rs6137444, re2180439, rs1998076, rs201571, rs6113491) show strong evidence to be linked to the development of mpAGA.

The largest investigations on involved genes in the pathobiology of mpAGA was done by genome wide association studies (GWAS). One of these identified genes, was topoisomerase 1 (*TOP1*) [138,153,154]. TOP1 is known to be recruited to the AR-regulated enhancer by DHT, and was then speculated to mediate (AR-dependent) gene expression in androgen-sensitive HFs [155]. Although, the *TOP1* gene expression was shown to be downregulated in mpAGA Pts' androgen-sensitive scalp, compared to their androgen-insensitive scalp [156]. Several autosomal located genes, their function and expression in mpAGA aff HFs is not known for all of them, have nevertheless strongly been linked to mpAGA predisposition [109,122,138,150–154,157–160]. These large-scale GWAS brought up risc loci which are present in genes coding for proteins known to be involved in key signaling pathways e.g. HC regulation (FGF5, DKK2, EBF1, RUNX1, KLF8, IGFBP3) [138,149,153,154,161–165], melatonin signaling (RORA) [154], parathyroid hormone signaling (PTHLH) [138,153,154], corticotropin- releasing hormone signaling (CRH, CRHR1) [153,154,166] or have an impact on hair colour (IRF4) [149,167].

The major issues with the previously discussed protein or gene expression studies are the different tissue samples utilized e.g., scalp tissue, plucked HFs or peripheral blood.

1.3.7 Current management

By this time, there are only two food and drug administration (FDA) approved drugs when it comes to mpAGA treatment. One is Finasteride (oral) what is known to be an inhibitor for 5α-R activity and acting as such, decreasing the amount of DHT [168,169]. The other FDA approved drug is Minoxidil (topical) what is known to be a potassium channel opener, which leads to relaxation of vascular smooth muscle and increased blood flow [170]. This increases the nutrition from the vascular system which due to size and distance, iHFs always lacking. Both of these treatments are most effective if applied combined [171,172]. The biggest disadvantage (next to several side effects) is that this therapy requires life-long maintenance.

The fastest and most effective treatment opportunity is hair transplantation surgery with a follow-up treatment of Minoxidil or Finasteride (or a combination of both) [173–175]. Moreover, platelet-rich plasma injections were shown to be successful in some, but not all, treated Pts [176–179]. Also different forms of laser [180,181] and light-based [182] therapies have been shown to be successful in the treatment of mpAGA Pts. The same was shown for cell-based therapies, like injecting dermal sheath cup cells [136] or cytokines secreted by adipose-derived stem cells [183] and cosmetic therapies, like topical caffeine [184,185] or adenosine [186,187].

1.4 Working hypothesis

The following working hypothesis was formulated to guide through the project: Treatment with T induces gene expression changes in HFs from the aff (androgen-sensitive) scalp but has no effect on HFs from the occ (androgen-insensitive) scalp. These lead to changes in the HC by premature catagen induction, reduction of HM keratinocyte proliferation, DP inductivity and DP size by not restoring emigrated DP fibroblasts resulting in a lower number of fibroblasts in the iHFs‘ DP.

1.5 Overall aim and specific questions addressed

The overall aim of this project was to identify genes regulated by T, which are highly involved in mpAGA pathobiology and investigate the aftermath of their knockdown *ex vivo*.

While following this aim as a whole, we also addressed these upcoming specific questions:

1. Is it technically possible to identify *in situ* the transcriptome of i/ tHFs‘ mesenchymal compartments only?
2. Are there differences in the transcriptomic profile in the mesenchymal compartments of i/ tHFs from aff and occ?
3. How does T impact on gene expression changes in different HF types from different scalp locations?
4. What possible candidate genes for the pathobiology of mpAGA could be identified after the short-term treatment with T?
5. Does the protein expression of these possible candidate genes differ throughout different HF types?
6. Is their protein localization equal to the RNA localization?
7. What changes in HF biology related parameters can be detected by silencing those genes?
8. Are there indications of progressing HF miniaturization after the treatment with T?
9. Do HFs in an *ex vivo* culture still convert T to DHT?

1.6 Experimental design

To identify the transcriptomic differences between aff and occ t/ iHFs fresh frozen HFs from mpAGA Pts, 10 µm thick cryosections were collected and the DP and the DC were cut out with LCM technique. From those isolated compartments the RNA was isolated and sent for RNAseq. To investigate what changes in the transcriptomic profile after short-term T treatment, aff and occ t/ iHFs from mpAGA Pts were organ-cultured *ex vivo* in the presence of 10 nM T. In the end, RNA was extracted from those HFs and sent to RNAseq analysis. With the RNAseq data a DESeq2 calculation of Log2 fold change (FC) was performed and genes with a FC <0.5 and >2 and a CPM value of 0.5 where highlighted. The appearance of those genes was checked in the list of highlighted genes from the T treated HFs and then the most interesting ones were picked. The expression of the target gene proteins was checked via immunofluorescence (triple) staining in aff and occ t/ iHFs of mpAGA Pts. The RNA of those genes was localized by *in situ* hybridization in aff and occ t/ iHFs of mpAGA Pts.

To see what impact those candidate genes have on HF biology, these genes where silenced with siRNA. HF elongation, HC staging, HC score as well as proliferation and apoptosis of HM keratinocytes, has been evaluated.

For checking if aff and occ t/ iHFs deriving from mpAGA Pts are suitable for establishing an *ex vivo* model and to see if T treatment progresses HF miniaturization, these HFs were cultured in the presence of 30 nM T for 72 hours and several parameters were evaluated (HF elongation, HC staging, HC score, proliferation and apoptosis of HM keratinocytes, DP inductivity, DP and DC cell number, apoptosis of cells in the DP and DC).

2 Material and Methods

All experiments in this thesis involving human material were performed according to Helsinki guidelines and after written Pts' consent and ethics committee approval.

2.1 Human tissue collection

Human FUEs from the occ and mpAGA aff scalp (see **Figure 2.1**) area were obtained from 42 male Pts diagnosed with mpAGA (age between 28 and 69 years; Norwood-Hamilton stage III – VII) (see **Table 2.1**) as well as FUEs from 19 healthy donors (see **Table 2.1**).
FUEs are 1 mm full skin biopsies extracted in the direction of hair growth to maintain the complete HF structures intact for initial re-transplantation. All donors undergo hair transplantation and donated their "left over" FUEs to the Biobank of Monasterium Laboratory (Münster, Germany) after ethics committee approval and signing the Pts' consent. The plastic surgeon shipped the FUEs in Williams' E medium (Gibco, United Kingdom) on 4 °C to Monasterium Laboratory (Münster, Germany) where they were processed 24 hours (h) after extraction.

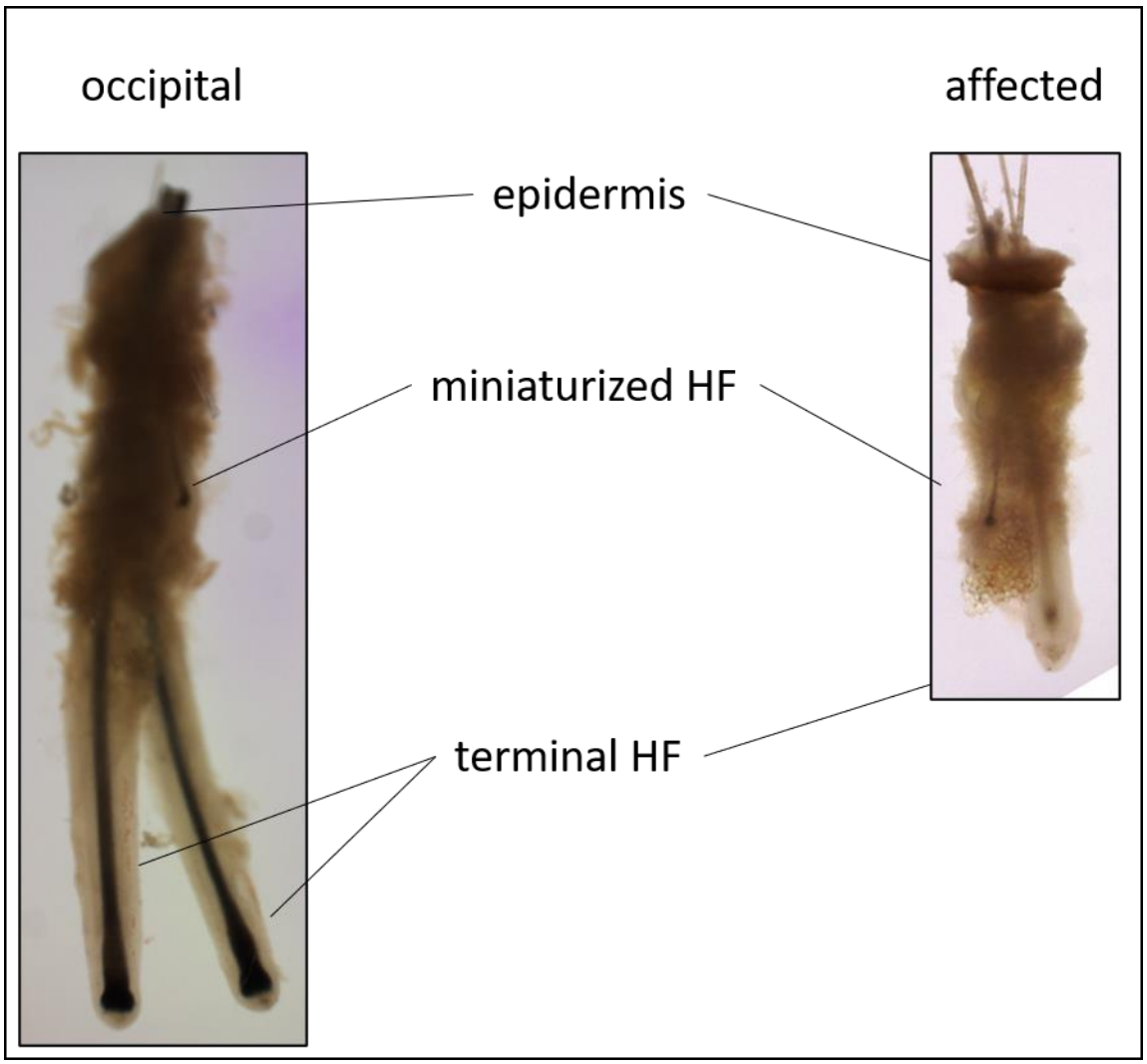

Figure 2.1 Follicular unit extracts from occipital and affected scalp. Clear visible differences in the morphology of follicular unit extracts (FUEs) from occipital and affected scalp of a male pattern androgenetic alopecia (mpAGA) patient. These FUEs were the basis for the microdissection of human hair follicles used in this thesis. HF= hair follicle

Table 2.1 List of all obtained human male pattern androgenetic alopecia samples and healthy donors. This table shows all information about the obtained androgenetic alopecia samples and the healthy donors used as controls. The table includes patients' (Pts) identity, source of the sample origin, usage of sample, skin region where biopsies have been taken, the Pts' gender, age and stage of androgenetic alopecia according to the Norwood-Hamilton scale [55]. Pt= patient, mpAGA= male pattern androgenetic alopecia, AGA= androgenetic alopecia; ID= identity; ♂= male; ♀= female

	Patient ID	Source	Fresh or cultured	Area	Age, sex	AGA stage
mpAGA Pts	Pt 1	Dr. Jiménez Acosta Mediteknia, Las Palmas, Spain	fresh frozen	occipital, affected	48, ♂	IV
	Pt 2	Prof. Rossi, Studio Medico, Rome, Italy	fresh frozen	lesional, non-lesional	60, ♂	IV
	Pt 3	Dr. Jiménez Acosta Mediteknia, Las Palmas, Spain	cultured 6 days with 10nM testosterone	occipital, affected	41, ♂	IV
	Pt 4	Dr. Jiménez Acosta Mediteknia, Las Palmas, Spain	cultured 6 days with 10nM testosterone	occipital, affected	44, ♂	IV
	Pt 5	Dr. Neidl	fresh frozen (overnight shipped)	occipital, affected	37, ♂	V
	Pt 6	Dr. Jiménez Acosta Mediteknia, Las Palmas, Spain	fresh frozen	occipital, affected	37, ♂	V
	Pt 7	Dr. Jiménez Acosta Mediteknia, Las Palmas, Spain	fresh frozen	occipital, affected	45, ♂	IV
	Pt 8	Dr. Jiménez Acosta Mediteknia, Las Palmas, Spain	fresh frozen	occipital, affected	46, ♂	V
	Pt 9	Dr. Jiménez Acosta Mediteknia, Las Palmas, Spain	fresh frozen	occipital, affected	54, ♂	IV
	Pt 10	Dr. Jiménez Acosta Mediteknia, Las Palmas, Spain	fresh frozen	occipital, affected	57, ♂	III/ IV
	Pt 11	Dr. Jiménez Acosta Mediteknia, Las Palmas, Spain	fresh frozen	occipital, affected	47, ♂	V/ VI
	Pt 12	Dr. Jiménez Acosta Mediteknia, Las Palmas, Spain	fresh frozen	occipital, affected	50, ♂	IV
	Pt 13	Dr. Azar, Zentrum für moderne Haartransplantation, Berlin, Germany	fresh frozen	occipital, affected	45, ♂	IV
	Pt 14	Dr. Jiménez Acosta Mediteknia, Las Palmas, Spain	fresh frozen	occipital, affected	41, ♂	V
	Pt 15	Dr. Jiménez Acosta Mediteknia, Las Palmas, Spain	fresh frozen	occipital, affected	32, ♂	III
	Pt 16	Dr. Jiménez Acosta Mediteknia, Las Palmas, Spain	cultured 6 h with 10 nM testosterone	occipital, affected	63, ♂	IV
	Pt 17	Dr. Erdmann, Kosmed Klinik, Hamburg, Germany	cultured 24 h with 10 nM testosterone	occipital, affected	60, ♂	IVa
	Pt 18	Dr. Erdmann, Kosmed Klinik, Hamburg, Germany	cultured 24 h with 10 nM testosterone	occipital, affected	33, ♂	III
	Pt 19	Dr. Jiménez Acosta Mediteknia, Las Palmas, Spain	fresh frozen	occipital, affected	60, ♂	IV
	Pt 20	Dr. Jiménez Acosta Mediteknia, Las Palmas, Spain	fresh frozen	occipital, affected	50, ♂	V
	Pt 21	Dr. Jiménez Acosta Mediteknia, Las Palmas, Spain	fresh frozen	occipital, affected	45, ♂	V

	Pt 22	Dr. Erdmann, Kosmed Klinik, Hamburg, Germany	cultured 24 h with 10 nM testosterone	occipital, affected	28, ♂	III
	Pt 23	Dr. Erdmann, Kosmed Klinik, Hamburg, Germany	cultured 24 h with 10 nM testosterone	occipital, affected	29, ♂	III
	Pt 24	Dr. Jiménez Acosta Mediteknia, Las Palmas, Spain	fresh frozen	occipital, affected	38, ♂	III
	Pt 25	Dr. Jiménez Acosta Mediteknia, Las Palmas, Spain	fresh frozen	occipital, affected	62, ♂	III
	Pt 26	Dr. Jiménez Acosta Mediteknia, Las Palmas, Spain	cultured 24 h with 10 nM testosterone	occipital, affected	36, ♂	IV
	Pt 27	Dr. Jiménez Acosta Mediteknia, Las Palmas, Spain	fresh frozen	occipital, affected	45, ♂	VI-VII
	Pt 28	Dr. Jiménez Acosta Mediteknia, Las Palmas, Spain	fresh frozen	occipital, affected	50, ♂	VII
	Pt 29	Dr. Jiménez Acosta Mediteknia, Las Palmas, Spain	fresh frozen	occipital, affected	50, ♂	Va
	Pt 30	Dr. Erdmann, Kosmed Klinik, Hamburg, Germany	cultured 24 h with 30 nM testosterone	occipital, affected	69, ♂	IV-V
	Pt 31	Dr. Jiménez Acosta Mediteknia, Las Palmas, Spain	fresh frozen	occipital, affected	60, ♂	VII
	Pt 32	Dr. Erdmann, Kosmed Klinik, Hamburg, Germany	cultured 24 h with 30 nM testosterone	occipital, affected	34, ♂	VI- VII
	Pt 33	Dr. Jiménez Acosta Mediteknia, Las Palmas, Spain	fresh frozen	occipital, affected	48, ♂	IV-V
	Pt 34	Dr. Jiménez Acosta Mediteknia, Las Palmas, Spain	fresh frozen	occipital, affected	44, ♂	IV
	Pt 35	Dr. Jiménez Acosta Mediteknia, Las Palmas, Spain	fresh frozen	occipital, affected	43, ♂	VI
	Pt 36	Dr. Jiménez Acosta Mediteknia, Las Palmas, Spain	fresh frozen	occipital, affected	43, ♂	VI
	Pt 37	Dr. Jiménez Acosta Mediteknia, Las Palmas, Spain	fresh frozen	occipital, affected	33, ♂	VI
	Pt 38	Dr. Jiménez Acosta Mediteknia, Las Palmas, Spain	fresh frozen	occipital, affected	50, ♂	V
	Pt 39	Dr. Jiménez Acosta Mediteknia, Las Palmas, Spain	fresh frozen	occipital, affected	25, ♂	VI
	Pt 40	Dr. Jiménez Acosta Mediteknia, Las Palmas, Spain	fresh frozen	occipital, affected	38, ♂	IV
	Pt 41	Dr. Jiménez Acosta Mediteknia, Las Palmas, Spain	fresh frozen in RNA extraction buffer	occipital, affected	51, ♂	VI
	Pt 42	Dr. Jiménez Acosta Mediteknia, Las Palmas, Spain	fresh frozen in RNA extraction buffer	occipital, affected	55, ♂	VI
	Pt 43	Dr. Jiménez Acosta Mediteknia, Las Palmas, Spain	cultured 24 h with 30 nM testosterone	occipital, affected	52, ♂	VI-VII
healthy donors	Pt 44	Dr. Jiménez Acosta Mediteknia, Las Palmas, Spain	siRNA culture	occipital, affected	32, ♂	-
	Pt 45	Dr. Erdmann, Kosmed Klinik, Hamburg, Germany	siRNA culture	occipital, affected	56, ♂	-

	Pt 46	Dr. Erdmann, Kosmed Klinik, Hamburg, Germany	siRNA culture	occipital, affected	27, ♂	-
healthy donors, used for establishing	I	Metropolitan Aesthetics, Berlin, German	Antibody testing	Occipital	69, ♀	-
	II	Schönheitsklinik Dr. Funk, München, Germany	Antibody testing	Occipital	23, ♀	-
	III	Dr. Med Oji, Praxis am Buddenturm, Münster, Germany	Antibody testing	Occipital	45, ♀	-
	IV	Dr. Erdmann, Kosmed Klinik, Hamburg, Germany	Antibody testing	Occipital	23, ♂	-
	V	Dr. Med Oji, Praxis am Buddenturm, Münster, Germany	Antibody testing	Occipital	46, ♂	-
	VI	Schönheitsklinik Dr. Funk, München, Germany	siRNA test culture	Occipital	68, ♂	-
	VII	Schönheitsklinik Dr. Funk, München, Germany	siRNA test culture	Occipital	71, ♂	-
	VIII	Dr. Erdmann, Kosmed Klinik, Hamburg, Germany	Antibody testing, *in situ* hybridization testing	Occipital	47, ♂	-
	IX	Schönheitsklinik Dr. Funk, München, Germany	Antibody testing, *in situ* hybridization testing	Occipital	38, ♂	-
	X	Dr. Med Oji, Praxis am Buddenturm, Münster, Germany	Antibody testing	Occipital	30, ♀	-
	XI	Dr. Med Oji, Praxis am Buddenturm, Münster, Germany	Antibody testing	Occipital	26, ♂	-
	XII	Dr. Med Oji, Praxis am Buddenturm, Münster, Germany	Antibody testing	Occipital	31, ♂	-
	XIII	Dr. Med Oji, Praxis am Buddenturm, Münster, Germany	Antibody testing	Occipital	32, ♂	-
	XIV	Dr. Med Oji, Praxis am Buddenturm, Münster, Germany	Antibody testing	Occipital	22, ♀	-
	XV	Schönheitsklinik Dr. Funk, München, Germany	Antibody testing	Occipital	54, ♀	-
	XVI	Schönheitsklinik Dr. Funk, München, Germany	Antibody testing	Occipital	26, ♂	-

2.1.1 Determination between terminal and intermediate hair follicles

For distinguishing between t and iHFs, different parameters were measured and validated in obtained cryosections to finally categorize them correctly. A tHF needs to fulfill the following criteria: HF bulb anchored deep in the adipose tissue, thick pigmented HS, diameter of the HF bulb at the level of the Auber's line >270 µm (based on Miranda et al.[62]) and DP diameter at the level of the Auber's line >100 µm (based on Miranda et al.[62]) (see **Figure 2.2**). To take the measurements it is very important to validate sections from the middle of the HF to guarantee the exact DP diameter. The Auber's line is defined as a line between the points where the DP is widest ([188]). For iHFs the following criteria were valid: HF bulb anchored not that deep or not at all in the adipose tissue, thin and less pigmented HS compared to tHFs, bulb diameter at the level of the Auber's line <250 µm (based on Miranda et al.[62]) and DP diameter at the level of the Auber's line <80 µm (based on Miranda et al.[62]) (see **Figure 2.2**). Depending on the experiment it was not possible in all cases to validate all four criteria so it was agreed on minimum three out of four of the mentioned parameters need to be in the defined range to categorize the HF correctly.

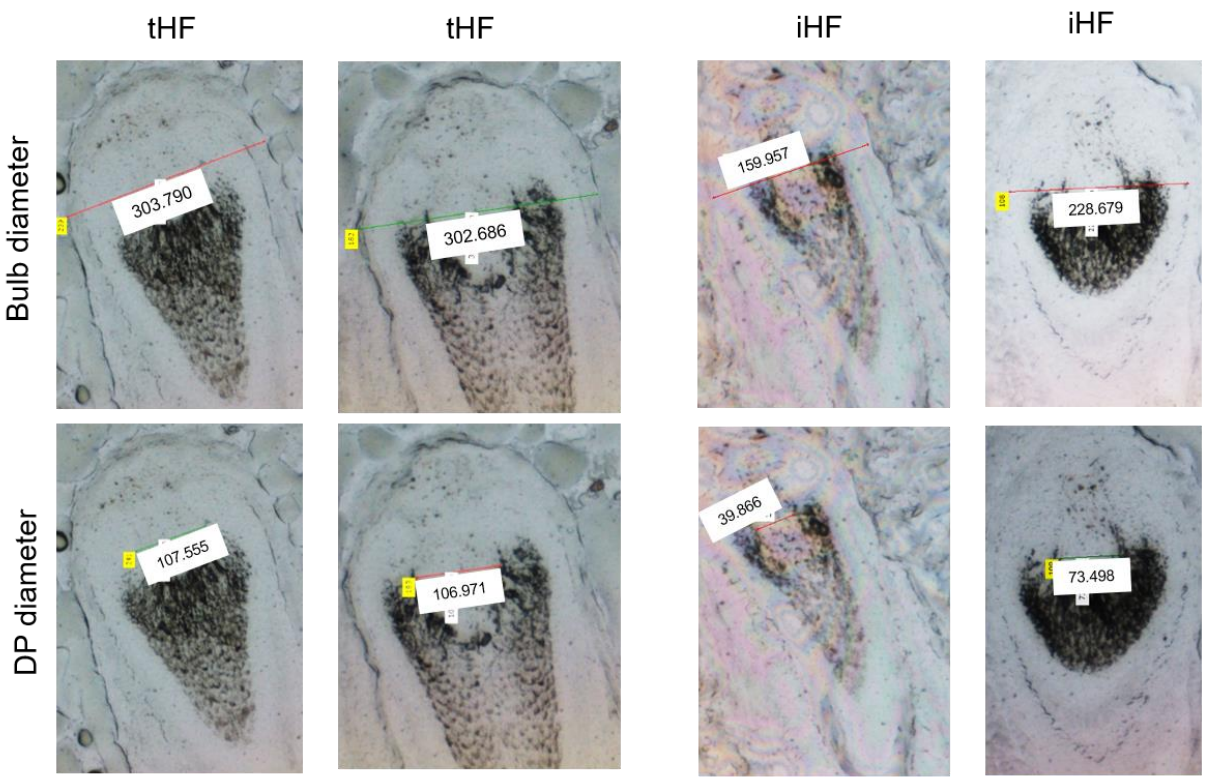

Parameter	Terminal	Intermediate
Bulb diameter at the level of the Auber´s line	> 270µm	< 250µm
DP diameter at the level of the Auber´s line	> 100µm	< 80µm

Figure 2.2 Criteria to distinguish terminal and intermediate hair follicles. The criteria to distinguish terminal (t) and intermediate (i) hair follicles (HFs) is a certain diameter of the bulb and the diameter of the dermal papilla (DP) at the level of the Auber's line. tHF= terminal hair follicle, iHF= intermediate hair follicle, DP= dermal papilla

2.1.2 Sample preparation for laser capture microdissection

For LCM based transcriptome analysis the HFs were microdissected (amputated with a scalpel below the bulge region), embedded in optimal cutting temperature compound (OCT) (Thermo Fisher, Germany) and frozen in liquid nitrogen (N_2) on the day of surgery, then stored at -80 °C. 10 µM thick sections were cut in a RNAse free environment with a Leica 3500 cryostat (Leica, Germany) and were collected on UV-light and RNAse-ZAP (Sigma, USA) pre-treated PET (polyethylene terephthalate) membrane covered glass-slides (Carl Zeiss, Germany). To prevent RNA degradation, the cut sections should not be stored longer than 24 h at -80 °C.

2.1.3 Sample preparation for immunofluorescence staining and *in situ* hybridization

For the localization and visualization of proteins and RNA *in situ,* HFs were microdissected and embedded in OCT on the day of surgery and frozen in N_2. 6µM thick sections were cut with a Leica 3500 cryostat and were collected on superfrost glass-slides (Thermo Fisher, Germany). For *in situ* hybridization, the section needs to be cut and kept in an RNAse free environment. After cutting, slides with the sections can be stored at -80 °C.

2.1.4 Sample preparation for *ex vivo* organ culture

To use HFs for *ex vivo* organ culture they got microdissected on the day of surgery. After amputation they are placed separately in a well of a 48 well plate in 250 µL William's culture medium (WCM). This plate is incubated over night (ON) at 37 °C in an atmosphere of 5 % CO_2 and 95 % air.

2.2 Laser capture microdissection

The complete process of LCM is divided into three separate parts. First, the tissue preparation (described in **2.1.2**), followed by the tissue microdissection (described in this chapter) and RNA isolation (described in **2.3**). For the purpose of this thesis, ultraviolet (UV) based LCM technology was used and executed with the LCM PALM MicroBeam (Zeiss, Germany). The HF section was placed on a PET covered membrane slide. Before thawing the slides, the laser needs to be calibrated to ensure that it has the correct parameters in relation to the surrounding temperature, humidity and the PET membrane of the slide (see **Figure 2.3 A**). After thawing and drying the slide, it was placed in the slide holder of the LCM system. The areas of interest (here DP, DC, HMg and HMpc) were marked visible on the computer screen. It is crucial to mark these areas very precisely to avoid cross-contamination of the surrounding tissue. Afterwards, they were separately cut by an UV laser and finally captured separately in the lid of a 0.5 mL Eppendorf collection tube in 20 µL RNA extraction buffer (Zymo Research, Germany) (see **Figure 2.3 B**). After collecting, the tubes were closed and immediately placed upside down on dry ice, to protect the RNA in the sample.

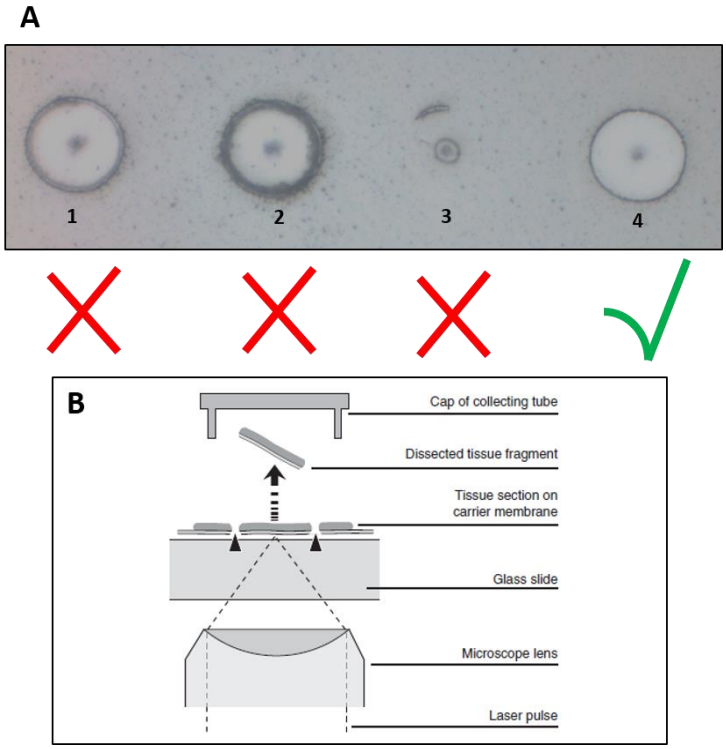

Figure 2.3 Choosing the correct parameters for the laser capture microdissection and its workflow. A: here are shown different cuts of the membrane of a used polyethylene terephthalate (PET) membrane slide. **1** has been cut with too high energy, **2** has a focus chosen too high and **3** has chosen a focus that is too low. Cut **4** has the correct chosen parameters for the cutting energy and focus. **B**: scheme shows the setup in the laser capture microdissection system itself. The laser pulse goes straight through the microscope lens and the glass slide to the PET membrane where the tissue is located. It catapults the dissected tissue directly into the cap of the collection tube, which is filled with 20 µL of RNA extraction buffer.

2.3 RNA isolation

RNA isolation was performed in a, as far as possible, RNAse free designated place. All used materials are dedicated to this place and are just for the purpose of RNA isolation.

2.3.1 RNA isolation from laser capture microdissection derived samples

HF compartments cut with LCM technique are very small, often just consist of a few 100 cells. To isolate the RNA from those samples the Quick-RNA Microprep kit from Zymo research (Zymo research, Germany) was used. This kit worked best when it came to total RNA concentration in the picogram (pg) range. RNA was isolated according to the manufacturer's instructions and stored at –80 °C.

2.3.2 RNA isolation from whole hair follicles

Microdissected HFs were transferred into 100 µL of RNA extraction buffer of the PicoPure™ RNA Isolation Kit from Applied Biosystems (Applied Biosystems, USA). RNA was isolated according to the manufacturer's instructions. RNA was stored at -80 °C. For all used RT-qPCR (real-time quantitative polymerase chain reaction) primers, please see **Table 2.2**.

Table 2.2 All used primers. All primers used for real-time quantitative polymerase chain reaction (RT-qPCR) were ordered from Thermo Fischer. SYT1= Synaptotagmin 1; ALDH1A2= Aldehyde dehydrogenase 1 family member A2; CBR1= Canabinoidreceptor 1; TGFβ1I1= transforming growth factor beta-1-induced transcript 1; EPHA5= Ephrin type-A receptor 5, ACTB= Actin beta

Specificity	System	Source	Ordering number
Human SYT1 Hs00194572_m1	TaqMan	Thermo Fisher	4331182
Human ALDH1A2 Hs00180254_m1	TaqMan	Thermo Fisher	4331182
Human CBR1 Hs00156323_m1	TaqMan	Thermo Fisher	4331182
Human TGFβ1I1 Hs00210887_m1	TaqMan	Thermo Fisher	4331182
Human EPHA5 Hs00300724_m1	TaqMan	Thermo Fisher	4331182
Human ACTB Hs99999903_m1	TaqMan	Thermo Fisher	4331182

2.4 RNA sequencing

After RNA isolation, the samples have been either sent to CeGaT GmbH (Tübingen, Germany) or in the very beginning of the project to the core genomics facility of the University of Münster (Germany). To prepare the samples, the RNA quality and quantity needed to be measured. This was performed with a bioanalyzer (Illumina NovaSeq 6000 sequencing systems). The here obtained results include the isolated amount of RNA in ng/µL and also the RNA integrity number (RIN).

The RIN was created as a quality metric to validate if an RNA sample is intact or mostly degraded. For eukaryotic samples, the RIN is determined by the quantification of the 18S and 28S ribosomal RNA[189]. When RNA concentration and integrity are satisfactory, the cDNA library will be prepared.

For the library preparation, the Takara SMART Seq (Takara, USA) stranded total RNA kit's maximal input was used. RNA-seq was performed with the NovaSeq 6000 device (Illumina, United Kingdom) and 1x75bp method. The obtained raw data was demultiplexed with Illumina bcl2fastq v2.20 and the adapter trimming was first done with the Skewer v0.2. Pico v2 SMART and a second time with the Cutadapt v1.12. In the next step, the trimmed raw data was aligned to the human reference genome (hg19) with the STAR v2.5.2b program and the normalized reads counts have been calculated with the DESeq2 v1.24.0 package.

The normalized read counts were used to compare the different groups of one donor and/or between all obtained donors. For this, the single comparison method was used and the fold change (FC) and CPM (counts per million reads) was calculated manually. Only genes with a FC higher than 2 or lower than 0.5 and of CPM lower than 0.5 have been taken into consideration for evaluation.

2.5 Hair follicle organ culture

i and t mpAGA Pts' HFs from occ and aff were microdissected as previously described and kept ON, one HF per well of a 48 well plate, at 37 °C and 5 % CO_2. On the day of microdissection (day 0 [D0]), pictures of every single HF were taken with a digital microscope (VHX-900F, Keyence, Germany) and at a magnification of 50 x.

After ON incubation, pictures were taken again at a magnification of 50 x and additionally 200 x. The 200 x pictures are for the macroscopic determination of the HC phase. The 50 x pictures of D0 and D1 were measured with the VHX- 5000_900F communication software by Keyence to determine the growth of the HFs. Just HFs in anagen phase VI and with a growth at D1 of > 7 % were used for the following organ cultures.

2.5.1 Testosterone *ex vivo* culture

After choosing HFs for *ex vivo* organ culture, the HFs were divided in eight experimental groups. HFs were cultured in fully supplemented William's E medium (→ WCM, see **Table 2.7**), with adding either 10 nM (RNAseq) or 30 nM (protein expression) T and incubated at 37 °C and 5 % CO_2 for 48 h. After 24 h (D2), 50 µL of the medium was collected and pooled for each condition, centrifuged on full speed for 15 min and the supernatant was frozen at –80 °C. The medium in the culture plate was restored with 50 µL of fresh medium containing the according amount of T. After 48 h of culture duration, the medium was collected and pooled for each condition and treated as on D2. HFs treated with 10 nM T were stored in RNA extraction buffer (ZymoResearch, USA) at -80 °C. HFs treated with 30 nM T were embedded in OCT and frozen at – 80 °C. Pictures of the HFs were additionally taken on D3 for measurement of total HF elongation (50 x) and for macroscopic analysis of the HC phase (200 x) during the culture.

2.5.2 Small interfering RNA culture

After choosing HFs for *ex vivo* organ culture, they were divided in five (knocking down two target genes) or three (knocking down one target gene) experimental groups, depending on the available number of HFs. HFs were cultured in WCM and 1 µM siRNA (scrambled for vehicle (veh) or target gene specific). Three HFs were cultured only in WCM for control expression of the target gene in qRT-PCR. On D2 and D3 of the culture, only pictures on 50 x magnification were taken for HF elongation measurements. On D4 pictures of the HFs were taken for measurement of total HF elongation (50 x) and for macroscopic analysis of the HC phase (200 x) during the culture. From cultures with five experimental groups, all HFs of group #1, #3 and #5, and from three experimental group cultures, HFs from group #1 and #3, were transferred into 100 µL of RNA extraction buffer of the PicoPure™ RNA Isolation Kit from Applied Biosystems (Applied Biosystems, USA) and stored at –80 °C prior to RNA isolation. HFs from the remaining groups were embedded, three HFs at a time, in OCT for further *in situ* hybridization and/or protein expression analysis. For all used siRNAs, see **Table 2.3**.

Table 2.3 All used small interfering RNAs. All used small interfering RNAs (siRNAs) were ordered from Horizon for the Accell system. TGFß1I1= transforming growthfactor beta 1 induced transcript 1, ALDH1A2 = aldehyde dehydrogenase 1 family member A2.

Specificity	System	Source	Ordering number
Human TGFβ1I1	Accell	Horizon	E-006565-00-0010
Human ALDH1A2	Accell	Horizon	E-008118-00-0010

2.6 Immunofluorescence

In OCT embedded HFs were cut on a Leica 3500 cryostat in 5 µm thick sections and collected onto superfrost glass-slides (Thermo Fisher, Germany). For reducing the amount of material needed to analyze all criteria, double and triple stainings were established whenever possible. After cutting, tissue samples were fixed, pre-incubated with blocking and/or permeabilization solution and the primary antibody was added. After ON incubation with the primary antibody, slides were washed again and the secondary antibody was added. After 45 min incubation at room temperature (RT), slides were washed, counterstained with DAPI (4′, 6-Diamidin-2-phenylindol) and mounted with Fluoromount-G (Biozol, Germany). For TUNEL (terminal desoxynucleotidyl transferase-mediated deoxyuridine triphosphate-biotin nick end labelling), fluorescence detection was performed using the ApopTag® Fluorescein *in situ* apoptosis detection kit (Merck Millipore, USA), according to the manufacturer's instructions. Please find all detailed staining information in **Table 2.4**. Detailed information for all used primary and secondary antibodies are shown in **Table 2.5**. Ki-67/TUNEL staining was performed to detect proliferative (Ki-67 positive) and apoptotic (TUNEL positive) cells. The TUNEL staining was additional used to detect the percentage of apoptotic cells in the DP and DC in aff and healthy HFs of mpAGA Pts together with the cleaved caspase 3 (casp3) staining. Both, TUNEL and casp3 are markers for apoptosis but TUNEL technique is known to detect DNA fragmentation. This process not only occurring during apoptosis but also in cells in which DNA damage is induced by other means and can label also non- apoptotic nuclei showing signs of active gene transcription [190,191]. Instead, casp3 is expressed by a cell during the so-called "point of no return" towards apoptosis, even when no morphological changes happened yet [190]. Versican is an exclusive DP marker and is expressed during the anagen phase [192,193]. Versican expression is associated with DP inductivity. ALDH1A2 (aldehyde dehydrogenase 1 family member A2), TGFß1I1 (transforming growth factor beta 1 induced transcript 1), and SYT1 (synaptotagmin 1) are chosen target genes whose protein expression was evaluated in the DP and DC of aff and occ i/tHFs from mpAGA Pts.

All negative controls have been performed in absence of the particular primary antibody. Fluorescence was analyzed on a Keyence Biozero-8000 (Keyence, Germany) microscope. Please find all used primary antibodies in **Table 2.5** and secondary antibodies in **Table 2.6.**

Table 2.4 Detailed information for all performed immunofluorescence stainings. This table shows all information about all single steps of the performed immunofluorescence stainings. Including used washing buffer, fixation solution, antibody concentrations, counterstaining, mounting material, analyzed areas of interest and way of analysis. TUNEL= terminal desoxynucleotidyl transferase-mediated deoxyuridine triphosphate biotin nick end labelling, PBS= phosphate-buffered saline, DAPI= 4′, 6-Diamidin-2-phenylindol; SYT1= Synaptotagmin 1; ALDH1A2= Aldehyde dehydrogenase 1 family member A2; TGFβ1I1= transforming growth factor beta-1-induced transcript 1;

Staining	**Ki-67/ TUNEL**	**Versican**	**Caspase 3**	**ALDH1A2 / TGFβ1I1 / SYT1**		
Washhing buffer	PBS					
Fixation	4 % Paraformaldehyde					
Pre-incubation	10 % Normal goat serum	0.1 % Triton X-100 and 3 % Bovine serum albumin	10 % Normal goat serum	0.1 % Triton X-100 and 10 % Normal goat serum		
Primary antibody	Anti-human Ki-67 (cell signaling) 1:800	Anti-human Versican (DSHB) 1:400	Anti-human cleaved Caspase 3 (Cell signalling) 1:400	Anti-human ALDH1A2 (Thermo Fisher) 1:20	Anti-human TGFβ1I1 (BD Bioscience) 1:50	Anti-human SYT1 (Thermo Fisher) 1:100
Secondary antibody	Goat anti-mouse Rhodamine red (Jackson immuno research) 1:200	Goat anti-mouse Alexa Fluor 546 (Invitrogen) 1:400	Goat anti-rabbit Alexa 488 (Invitrogen) 1:200	Goat anti-rabbit Alexa 488 (Invitrogen) 1:200	Goat anti-mouse Alexa Fluor 546 (Invitrogen) 1:400	Goat anti-rabbit Alexa 647 (Invitrogen) 1:400
Counterstain	DAPI					
Mounting material	Fluoromount-G					
Analyzed areas of interest	Pre-cortical hair matrix, germinative hair matrix	Dermal papilla	Dermal papilla, inductive dermal cup	Dermal papilla, inductive dermal cup		
Quantification method	Counting of postive cells	Measurement of fluoreszcence intensity	Counting of postive cells	Measurement of fluoreszcence intensity		

Table 2.5 Detailed information for all primary antibodies used. ALDH1A2= Aldehyde dehydrogenase 1 family member A2; CB1= Canabinoidreceptor 1; TGFβ1I1= transforming growth factor beta-1-induced transcript 1; EPHA5= Ephrin type-A receptor 5; IgG= immunoglobulin G

Specificity	Clone	Species/ Isotype	Source
Human Synaptotagmin 1	Polyclonal	Rabbit IgG	Thermo Fisher
Human ALDH1A2	Polyclonal	Rabbit IgG	Thermo Fisher
Human CB1	IMG-3C2	Mouse IgG1	ImmunoGenes-ABS Zrt
Human TGFβ1I1	Polyclonal	Mouse IgG1	BD Biosciences
Human EphA5	Polyclonal	Rabbit IgG	Thermo Fisher
Human Ki-67	Polyclonal	Mouse IgG1	Cell Signaling
Human Versican	Polyclonal	Mouse IgG1	DSHB
Human Cleaved caspase 3	Polyclonal	Rabbit IgG	Cell Signaling

Table 2.6 Detailed information for all secondary antibodies used. IgG= immunoglobulin G

Specificity	Clone	Species/Isotype	Source	Conjugated fluorophore
Goat	Polyclonal	Mouse IgG	Life Technologies	Alexa546
Goat	Polyclonal	Rabbit IgG	Life Technologies	Alexa 488
Goat	Polyclonal	Rabbit IgG	Jackson ImmunoResearch Laboratories	Rhodamine red
Goat	Polyclonal	Rabbit IgG	Invitrogen	Alexa 647
Goat	Polyclonal	Mouse IgG	Jackson ImmunoResearch Laboratories	Rhodamine red

2.6.1 Mastering problems coming up during establishing stainings

For this thesis, ALDH1A2, TGFβ1I1 and SYT1 immunofluorescence stainings needed to be established. While establishing these stainings, a lot of difficulties came up and needed to be overcome. Therefore, it needs to be taken into consideration which are the correct blocking steps, the correct washing buffer to use, the necessity of an additional permeabilization step, and the host species of the different antibodies.

The very first step is to find the correct positive control tissue to judge the correct expression pattern and to distinguish from auto fluorescent structures in the skin like blood vessels or nerve endings. For SYT1 it was shown that it is expressed in nerve fibres, so the optimal positive control tissue would be human brain [194] (see **Figure 2.4 A**). The protein expression of ADH1A2 was shown to be in the basal layer of human epidermis (supplier's page) and in human liver (www.proteinatlas.org) (see F**igure 2.4 B**). TGFβ1I1 was shown to be

expressed by human fibroblasts (supplier's page), so as positive control tissue, a section of a human HF DP was used (see **Figure 2.4 C**).

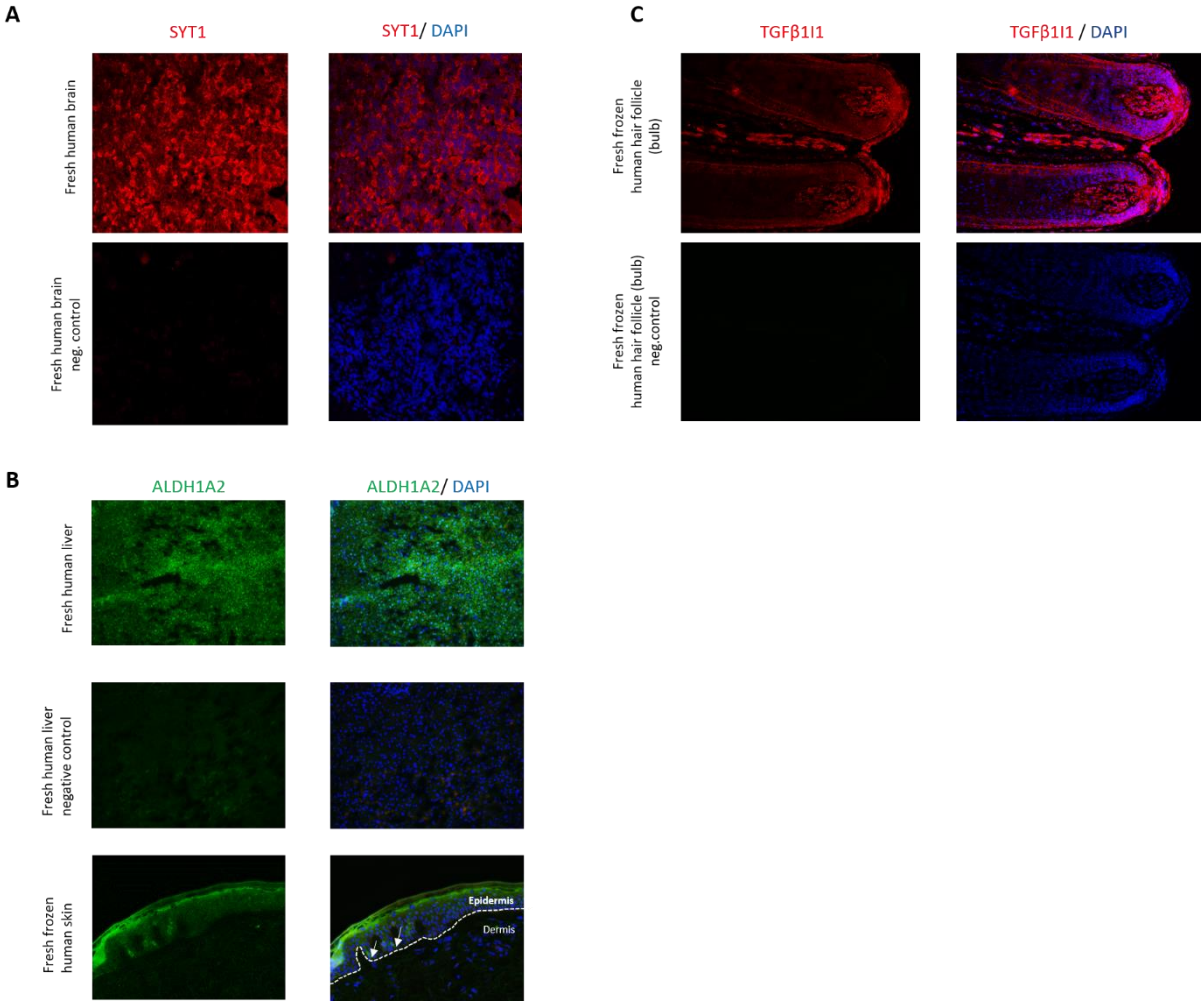

Figure 2.4 Representative images of chosen positive control tissues for establishing immunofluorescence staining protocols. A: Synaptotagmin 1 (SYT1) immunofluorescence staining in human brain sections. **B**: Aldehyde dehydrogenase 1 family member A2 (ALDH1A2) immunofluorescence staining in human liver sections and human skin sections. Arrowheads pointing to positive labeled cells. **C**: Transforming growth factor beta 1 induced transcript 1 (TGFβ1I1) immunofluorescence staining in human hair follicle bulb sections. Displayed scale bars indicating 1 µm. Negative controls have been performed without corresponding primary antibody. SYT1= Synaptotagmin 1; DAPI= 4′,6-Diamidin-2-phenylindol; neg= negative; ALDH1A2= Aldehyde dehydrogenase 1 family member A2; TGFβ1I1= Transforming growth factor beta 1 induced transcript 1

It was also important to find the correct fixation solution for each antibody. After testing several fixation substances, 4%PFA worked best for all tested antibodies. The biggest challenge was to establish a triple staining with these antibodies. Regarding the available number of sections per iHF a triple staining is the only option to detect all three proteins in one Pt. The biggest difficulty was the fact that the host of the ALDH1A2 and SYT1 antibody was rabbit. Due to this fact it was necessary to label every primary antibody immediately with its designated secondary to avoid miss-linking and wrong expression data. Also, an additional blocking step was necessary to add before the incubation with the second primary

rabbit derived antibody. The normally used protocol for a triple staining takes three days. In this case it was necessary to reduce the protocol time to one and a half days. This extreme shortening was necessary because of reduced thickness of the cryo sections. Once the triple staining is established, the correctness of the staining needs to be checked every time. A lot of factors like RT or humidity can influence the binding affinity of the antibodies and cause cross linking between them. Representative pictures of the successful executed protocol and the final proof of its reliability can be seen in **Figure 2.5**.

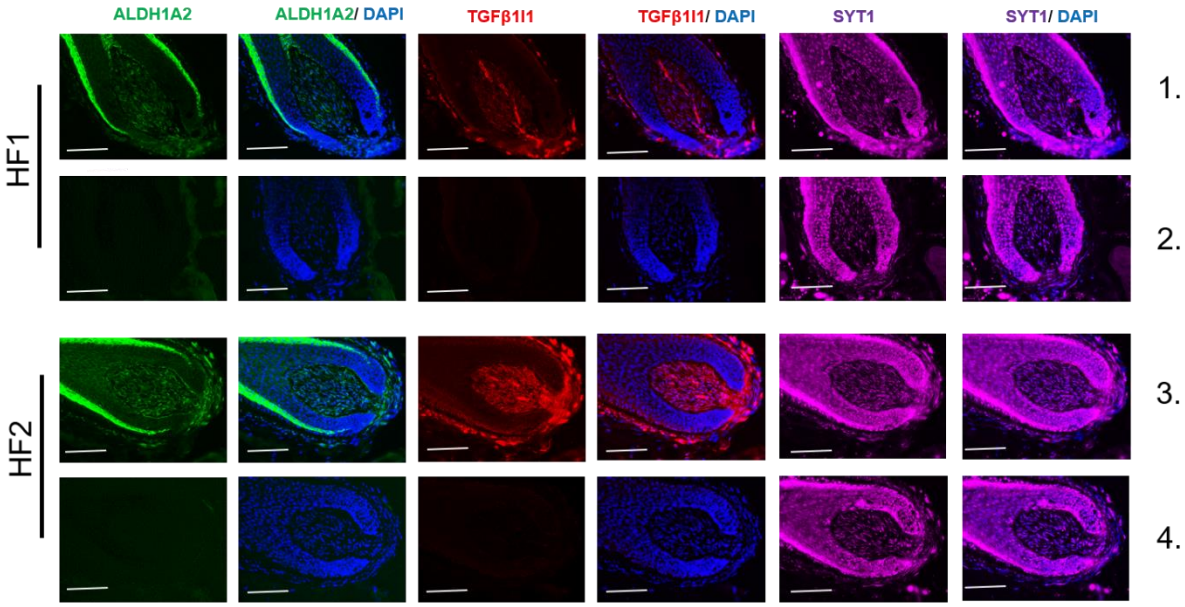

	1. Primary AB (ALDH1A2)	1. Secondary AB	2. Primary AB (TGFß1I1)	2. Secondary AB	3. Primary AB (SYT1)	3. Secondary AB
1. & 3.	√	√	√	√	√	√
2. & 4.	√	/	√	/	√	√

2.7 Histochemistry

Figure 2.5 Representative images of the finally established immunofluorescence triple staining. Row 1 and 3 represent the successful established and executed triple immunofluorescence staining for aldehyde dehydrogenase 1 family member A2 (ALDH1A2), Transforming growth factor beta 1 induced transcript 1 and Synaptotagmin 1 (SYT1). Row 2 and 4 show the final confirmation of the reliability of the protocol which shows no unwanted cross-linking between the SYT1 secondary antibody and the ALDH1A2 primary antibody. So one can confirm that the added blocking step with in between is functional. Stainings has been performed in human hair follicles in skin sections. All displayed scale bars indicating 100 µm. ALDH1A2= aldehyde dehydrogenase 1 family member A2; DAPI= 4′,6-Diamidin-2-phenylindol; TGFβ1I1= Transforming growth factor beta 1 induced transcript 1; SYT1= Synaptotagmin 1; HF= hair follicle, AB= antibody

In OCT embedded HFs were cut with a Leica 3500 cryostat in 5 µm thick sections and collected onto superfrost glass-slides (Thermo Fisher, Germany). Slides were fixed in ice cold acetone and washed with TBS (tris-buffered saline). The alkaline phosphatase (AP) activity solution and the control solution (Levamisole) was prepared according to the suppliers' manual (AP activity substrate Kit SK5300, Vector). After 30 min incubation in 37 °C in the dark, slides were washed and rehydrated with dH2O. AP activity was analysed on a Keyence Biozero-8000 microscope. AP is a marker for DP and its inductivity [195]. The staining is based on a reaction of the AP substrate 5-Bromo- 4-Chloro-3-Indolyl Phosphate (BCIP) with nitroblue tetrazolium (NBT). It forms a NBT diformazan end product that is appearing blue, correlating with the AP enzyme activity *in situ*. Its activity was reported to be highest in the early anagen phase.

2.8 RNAscope *in situ* hybridization

RNAscope® *in situ* hybridization is a technique to target single RNA molecules by signal amplification in intact cells. Here, OCT embedded HFs were sectioned with a Leica 3500 cryostat (5 µm thick) and collected on the same superfrost glass-slides (Thermo Fisher, Germany) as used for immunofluorescence and histochemistry stainings. For RNAscope *in situ* hybridization it is important to prepare the cryostat and all material RNAse free and keep the slides on a low temperature at all the time, to avoid RNA degradation. The sections were fixed in 4 °C cold 4 % paraformaldehyde for two 2 h. After fixing the sections, the slides were washed in PBS and dehydrated by immersing the slides in a chain of Ethanol (EtOH) solutions with increasing concentrations (50 %, 70 % and 100 %). For the antigen retrieval, to reduce unspecific background staining, the slides were incubated with hydrogen peroxide and afterwards incubated with protease IV to permeabilize the cells. After dipping the slides in dH_2O, the corresponding probes were added to each section and incubated for 2 h at 40 °C. Subsequently, the amplification of the first probes were performed according to the supplier's manual, followed by the development of the red (channel 2) signal. Afterwards, the amplification of the second probes were performed and the green (channel 1) signal was developed. Counterstaining was done with Meyer's Hämalaun (Carl Roth, Germany) and slides were mounted with EcoMount (BioCare Medical, USA). *In situ* hybridization was analyzed on a Keyence Biozero-8000 microscope (Keyence, Germany). Please find all use *in situ* hybridization probes in **Table 2.7**.

Table 2.7 All used *in situ* hybridization probes. ALDH1A2= Aldehyde dehydrogenase 1 family member A2; SYT1= Synaptotagmin 1; CNR1= Canabinoidreceptor 1; TGFβ1I1= transforming growth factor beta-1-induced transcript 1

Specificity	System	Source	Ordering number
Human ALDH1A2	RNAscope	ACD/biotechne	Customized
Human Syt1	RNAscope	ACD/biotechne	Customized
Human CNR1	RNAscope	ACD/biotechne	591521
Human TGFβ1I1	RNA scope	ACD/biotechne	Customized

2.9 Dihydrotestosterone enzyme-linked immunosorbent assay

The enzyme-linked immunosorbent assay (ELISA) is a detection method for proteins. Here it was performed to prove that also in HF *ex vivo* organ culture, T is converted to DHT. Therefore, the culture medium was collected on D1, D2 and D3 of the culture, pooled for each group, centrifuged at 4 °C on maximum speed and the supernatant was stored at –80 °C to avoid protein degradation.

The used assay was based on the competitive inhibition enzyme immunoassay technique. The provided 96 well plate was already pre-coated with a goat anti-rabbit secondary antibody. The standards and the organ culture supernatants were added to the well. In the next step, horseradish peroxidase (HRP) conjugated DHT was added to each well. For detection, an antibody specific for DHT as well as an antibody specific for HRP conjugated DHT was added to the wells. After colour development by a substrate solution, the intensity of the colour is opposite to the amount of detected DHT in the samples. The final competitive inhibition is measured between the HRP conjugated DHT and the unlabeled DHT (from the supernatant). The intensity of the colour was measured at 450 nm wave length. **Figure 2.6** shows the principle of the competitive ELISA.

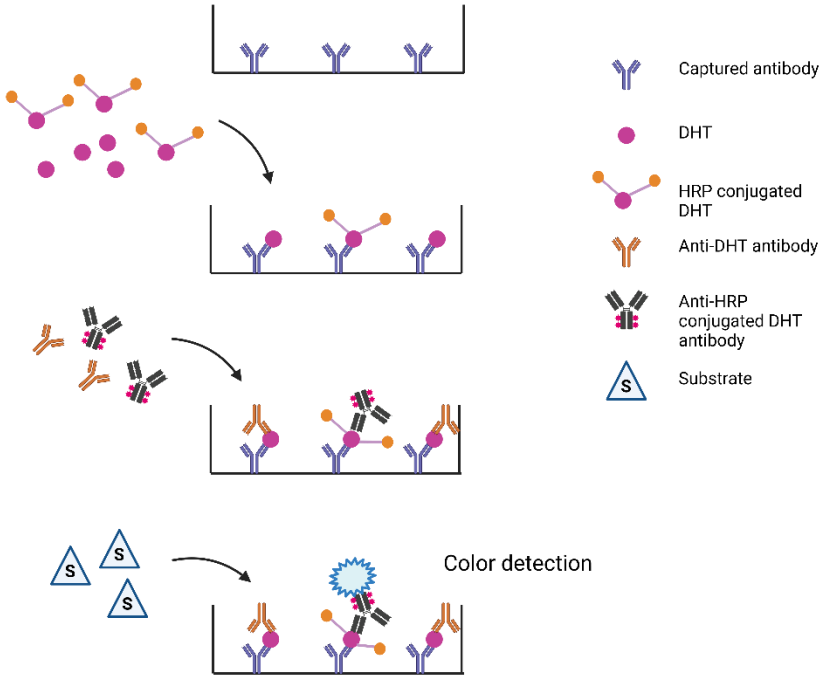

Figure 2.6 Principle of competitive inhibition enzyme-linked immunosorbent assay. A secondary antibody is captured to a solid carrier. The antigen to be tested and a horseradish peroxidase (HRP) conjugated antigen is added to each well. The tested antigen and the conjugated antigen are binding competitively to the immobile antibody. After incubation, antibodies against the unlabeled antigen and the HRP labeled antigen are added to the wells. The substrate added in the next step becomes blue when catalyzing the peroxidase. Absorbance of color can be detected on 450 nm wavelength. The intensity of color developed is positively correlated with the amount of enzyme but reverse proportional to the concentration of the target molecule in the tested sample. Figure created with biorender.com. DHT= dihydrotestosterone, HRP= horseradish peroxidase.

2.10 Microscopy

All microscopic analyses have been performed with a Keyence Biozero-8000 microscope. Pictures for further analyses have been taken with the according filter (bright field for *in situ* hybridization and histochemistry stainings and Cy5, FITC and Texas red filter for immunofluorescence stainings), an optical zoom of 1.6 x and a digital zoom of 20 x.

2.11 Staining analyses

For staining analyses ImageJ was used. For each analysis the corresponding areas of interest (see **Figure 2.7**) have been selected and either the expression intensity, or the number of positive labeled cells was analyzed. The way of analysis for each staining is indicated in **Table 2.4.** For both types of analyses, the corresponding region of interest

(ROI) was drawn onto the image and either the positive labeled cells as well as the present DAPI-labeled cells were counted, or the intensity of fluorescence in the according channel picture was measured. For positive labeled cells, the percentage of positive cells among all cells in this area has been calculated. Pictures of the DAPI-labeled cells have been furthermore used to count the number of cells in a specific area correlated to the area size. Therefore, the number of cells has been counted and the size of the area has been measured with ImageJ.

For all staining analyses statistical analysis was performed as followed using Graph Pad Prism 9: As first the D'Agostino & Pearson omnibus normality test has been performed to check if the values follow the Gaussian distribution. If yes, student's t-test was used to check the data for significance. If Gaussian distribution was not given, Mann-Whitney or Kruscal Wallis test were used to check data for significance.

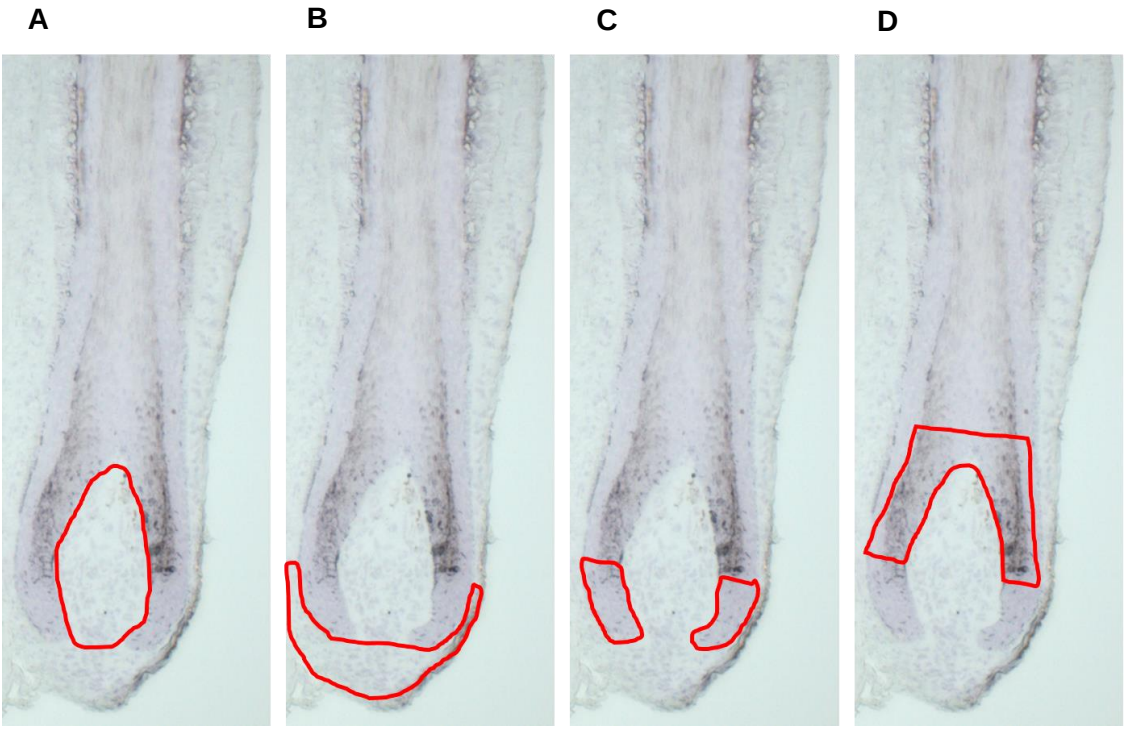

Figure 2.7 Areas of interest for different staining evaluations. Section **A** shows the area of the dermal papilla, which has been evaluated for Versican expression, cleaved caspase 3 positive cells, TUNEL (terminal desoxynucleotidyl transferase-mediated deoxyuridine triphosphate-biotin nick end labelling) positive cells, cannabinoidreceptor 1 (CB1) and ephrin type-A receptor 5 (EPHA5) expression, aldehyde dehydrogenase 1 family member A2 (ALDH1A2), transforming growth factor beta 1 induced transcript 1 (TGFβ1I1) and Synaptotagmin 1 (SYT1) expression and alkaline phosphatase activity. Section **B** shows the area of the inductive dermal cup which has been evaluated for cleaved caspase 3 and TUNEL positive cells, CB1 and EPHA5 expression and ALDH1A2, TGFβ1I1 and SYT1 expression. Section **C** indicates the pre-cortical hair matrix which has been evaluated for Ki-67 and TUNEL positive cells. Section **D** shows the germinative hair matrix which has been evaluated for Ki-67 and TUNEL positive cells.

2.12 Used consumables, kits and chemicals

Table 2.8 shows a detailed list of all prepared buffers and media.

Table 2.8 All used buffers and media.

Buffers and media	
Phosphate-buffered saline (PBS) (pH 7.2)	13 mM NaH2PO4 * H_2O 137 mM NaCl
Tris-buffered saline (TBS) (pH 7.6)	50 mM Tris-Base 151 mM NaCl
Tris-HCL (pH 8.2)	66 mM Tris-Base
William's culture medium (WCM)	William's E Medium, no glutamine 2 mmol/L L-glutamine 10 ng/mL Hydrocortisone 10 µg/mL Insulin 100 U/mL Penicillin 100 µg/mL Streptomycin
10 nM Testosterone culture medium	WCM 10 nM Testosterone in ethanol
30 nM Testosterone culture medium	WCM 30 nM testosterone in methanol
siRNA Transfection medium	WCM 1 µM siRNA

2.13 Used chemicals

Table 2.9 shows details about all used chemicals.

Table 2.9 All used chemicals.

Chemical	Source	Ordering number
Testosterone	Sigma-Aldrich	T1500
DAPI	Sigma-Aldrich	10236276001
4 % Parafomaldehyde	Thermo Fisher	J19943.K2
GNS	Biozol	927503
Fluoromount-G	Biozol	SBA-0100-01
Trizma Hydrochloride	Sigma-Aldrich	T3253
NaOH	Merck Millipore	1064981000
Acetone	Sigma-Aldrich	179124-1L
Faramount	Agilent/DAKO	S302580-2
Triton X-100	Roth	3051.3
Sodiumhydrogenphosphate monohydrate	Merck Millipore	10049-21-5
NaCl	Roth	3957.2
William's E Medium, no glutamine	Thermo Fisher	12551032
L-glutamine	Sigma-Aldrich	G7513
Hydrocortisone	Sigma-Aldrich	H0135
Insulin	Sigma-Aldrich	I9278 – 5ML
Pen/Strep (Penicillin-Streptomycin)	Thermo Fisher	15140122
Ethanol	VWR	1.08543.0250
Methanol	Th.Geyer	1437-2.5L-PE
RNAse Zap	Sigma	R2020-250ML
Eco Mount	BioCare Medical	EM897L

2.14 Used consumables

Table 2.10 shows details about all consumables used.

Table 2.10 All used consumables.

Consumables	Source	Ordering number
Cryo slides	Thermo Fisher	J1800AMNZ
Membrane slides	ZEISS	415190-9051-000
Blades	Pfm medical	207500000
Cryomatrix	Thermo Fisher	6769006
Scalpels	Fisher Scientific	15266778
Barrier pen	Agilent/DAKO	S2002>S200230-2
Coverslips	A. Hartenstein / Laborversandt	0107242
Eppendorf tube 5 mL	Kisker-Biotech	390932A
Eppendorf tube 2 mL	A. Hartenstein / Laborversandt	RSL2
Eppendorf tube 1.5 mL	A. Hartenstein / Laborversandt	RSL1
Eppendorf tube 0.5 mL	A. Hartenstein / Laborversandt	RSL0
Falcon tube 15 mL	Stemcell	352196

Table 2.11 shows details about all used kits.

Table 2.11 All used kits.

Kit	Source	Ordering number
Quick-RNA Microprep Kit	Zymo	R1051
PicoPure™ RNA Isolation Kit	Thermo-Fischer	KIT0204
Human DHT Elisa Kit	Biorbyt/Biozol	orb407091
ApopTag® Fluorescein *In Situ* Apoptosis Detection	Merck Millipore	S7110
Vector® Blue Substrate Kit, Alkaline Phosphatase	Biozol	SK-5300
Tetro™ cDNA Synthesis Kit	Biocat	BIO-65043
RNAscope® 2.5 HD Duplex Detection Reagents	ACD/biotechne PO	322500

3 Results

3.1 The influence of short-term testosterone treatment on hair follicles *ex vivo*

The progressive miniaturization of tHFs in the aff area of mpAGA scalp causes the diseases' typical phenotype. This phenomenon is based on an altered HC, where catagen is prematurely induced what drives the HF to miniaturization. Deriving from certain androgen-based studies, T was assigned to be one of the HF miniaturization driving forces. Therefore, the aim was to investigate the influence of a biological normal T concentration on occ and aff t/iHFs from mpAGA Pts. The serum level of circulating T is reported to be around 3-15 ng/ mL in healthy donors [85–87], and it is reported to not significantly differ in mpAGA Pts [81,83,196].

To investigate the effect of a short-term treatment of mpAGA Pts' HFs, 30 nM T concentration for HF *ex vivo* cultures was chosen. This is in the range of the reported amount and could possibly mimic the *in vivo* circumstances in an *ex vivo* experiment. The HFs were cultured for 48 h with 30 nM T to determine the immediate effects regarding elongation, changes in the HC, proliferation and apoptosis of HM keratinocytes, DP inductivity, altered number of cells in the DP, DC and DP stalk, as well as the apoptosis in the cells of the DC. How the culture was exactly carried out, please refer to **Chapter 2.5**. The aim of this experiment was to understand the immediate changes triggered by T in mpAGA Pts' HFs.

3.1.1 Hair follicles keep their ability to convert testosterone to dihydrotestosterone *ex vivo*

In the human HF, T is converted into its much more potent metabolite 5α-DHT [78]. 5α-DHT can also bind the AR and trigger the same response like T, what is crucial for the pathobiology of mpAGA. To investigate if HFs *ex vivo* are still able to perform this conversion, the culture medium of a 30 nM T treated HF organ cultures was collected and a DHT ELISA was performed (see **Chapter 2.9**). The activity of 5α-R was reported to be higher in aff HFs [89,197,198]. The retrieved results show that exclusively, HFs from the aff scalp convert to to 5α-DHT (see **Figure 3.1**).

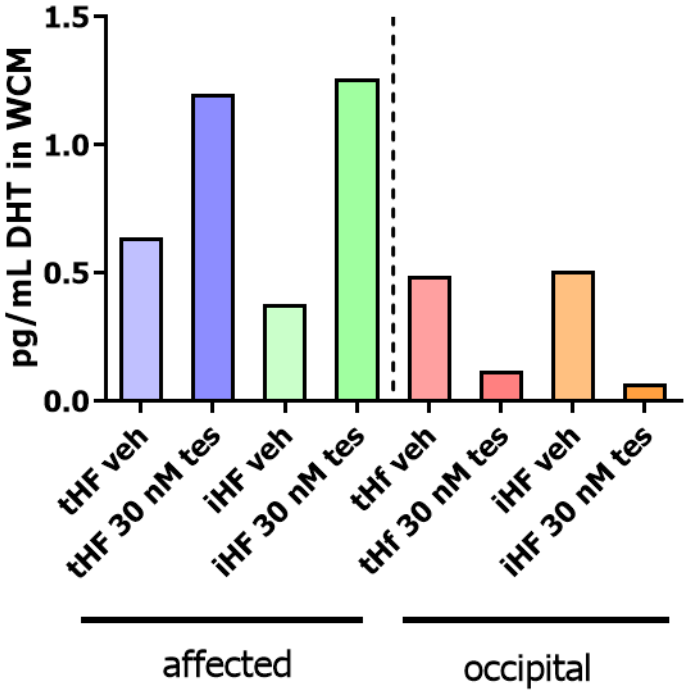

Figure 3.1 Dehydrotestosterone enzyme-linked immunosorbent assay after 48 hours long 30 nM testosterone treatment. This graph shows the concentration of dehydrotestosterone (DHT) released by the hair follicles (HFs) into the culture medium after 48 hours of *ex vivo* treatment with 30 nM testosterone (T). HFs deriving from the affected (aff) scalp of male pattern androgenetic alopecia patients (Pts) converting in culture T to its much more potent metabolite DHT. In contraire, HFs deriving from the occipital (occ) scalp seem to lose this ability. This could be due to the fact, that in the aff scalp the activity of the converting enzyme, 5α reductase, is much higher than in the occ scalp [93, 206, 207]. Graph Pad Prism 9. Mann-Whitney test, ns. HF= hair follicle; t= terminal; i= intermediate; veh= vehicle; tes= testosterone treated; pg= picogram; mL= milliliter; DHT= dehydrotestosterone; WCM= William's culture medium

3.1.2 Short-term testosterone treatment *ex vivo* does not significantly impact on hair follicle elongation

HF miniaturization is one of the hallmarks in mpAGA. So, one could expect to see effects on HF elongation due to the treatment with T. Therefore, the length of each HF was measured directly after isolation (D0), but also on D1 and D3 of the culture. The percentage of growth was calculated and the treatment groups were normalized to their corresponding veh which was normalized to 1. After internal normalization, elongation results of n=3 donors have been pooled together and statistical analysis has been performed using GraphPad Prism 9. Mann-Whitney test has been performed but no significance was detected. The used dose was mimicking the natural, reported, amount of circulating T. To see a reliable effect on HF elongation the dose would need to be higher or the culture time would need to be extended.

As shown in **Figure 3.2**, no effect on HF elongation could be detected between aff and occ t/iHFs of mpAGA Pts.

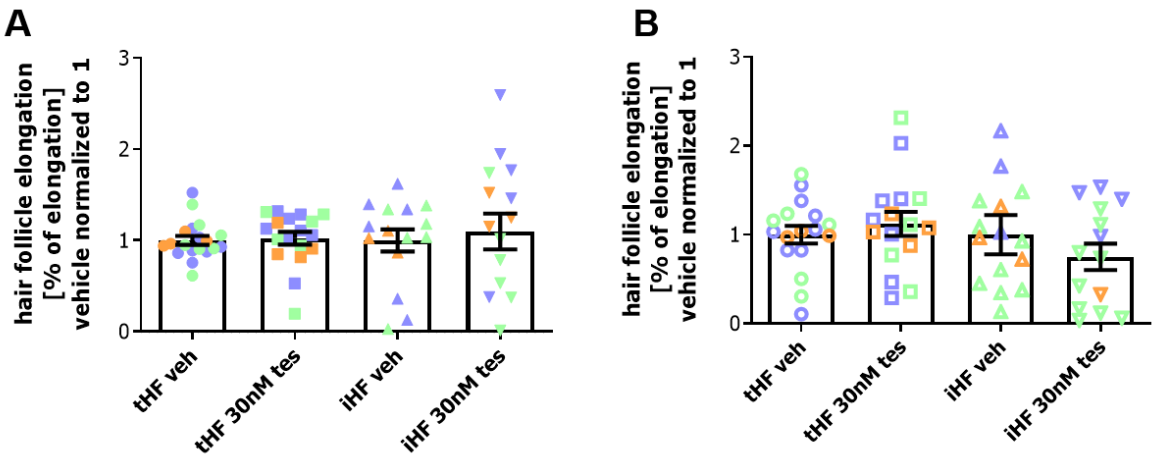

Figure 3.2 Short-term treatment with testosterone *ex vivo* does not significantly impact on hair shaft elongation. A: This graph shows the pooled hair follicle (HF) elongation of terminal (t) and intermediate (i) HFs from the affected (aff) area of n=3 male pattern androgenetic alopecia (mpAGA) patients (Pts). Each treatment group was normalized to its vehicle (veh) and veh was normalized to 1. No significant changes could have been detected regarding the HF elongation in the aff area. **B**: This graph displays the pooled HF elongation of t and i HFs from the occipital area of n=3 mpAGA Pts. Each treatment group was normalized to its veh and veh was normalized to 1. No significant changes could have been detected regarding the HF elongation in the occ area. Mean±SEM, n=11-18 HFs/ group from 3 donors, Pt30 displayed in blue, Pt32 displayed in green, Pt43 displayed in orange. Graph Pad Prism 9. D'Agostino & Pearson omnibus normality test, n too small to determine whether the data follow Gaussian distribution; Mann-Whitney test, ns; Kruskal Wallis test, ns; Dunn's multiple comparison test, vehicle fixed,ns. HFs= hair follicles; t= terminal; i=

3.1.3 Short-term testosterone treatment *ex vivo* does not cause significant changes in the hair cycle

As one of the greatest hallmarks of mpAGA is premature catagen induction [63–68], one could expect a tendential change in HC after 30 nM T treatment *ex vivo*. For assigning each cultured HF to a certain HC stage, the HFs were embedded in OCT and cryosectioned after *ex vivo* culture (see **Chapter 2.1.3**). A Ki-67/ TUNEL staining was performed to observe well known anagen or catagen patterns [199]. Ki-67 labels proliferative cells. In anagen phase, typically the HMg keratinocytes are highly proliferative. In early catagen, the proliferative cells are mostly located in the HMpc. The more the HF goes into catagen, the less keratinocytes are proliferating. Usually, HFs were only subdivided in anagen, early, mid or late catagen. However, it was possible to identify several HFs that on the one hand showed still significant HM keratinocyte proliferation, but on the other hand signs of DP emigration and accumulation of cells in the DP stalk. Those were classified as anagen* (see **Figure 3.3 C**). To decree the HC score, arbitrary values were assigned to each HC phase (anagen= 100, anagen*= 200, early catagen= 300, mid catagen= 400, late catagen= 500, dystrophic catagen= 600). The HC score was calculated and the treatment groups were normalized to their corresponding veh

which was normalized to 1. After normalizing each Pt internally, the results of n= 3 donors were pooled together and statistical analysis has been performed using GraphPad Prism 9. No significance was detected with the Mann-Whitney test. With the chosen concentration of T and the duration of the *ex vivo* culture, it was not possible to detect premature catagen induction or other significant changes in the HC after T treatment. For detecting the expected catagen induction, either the T concentration would need to be elevated, or the duration of the culture would need to be extended (see **Figure 3.3 A, B**).

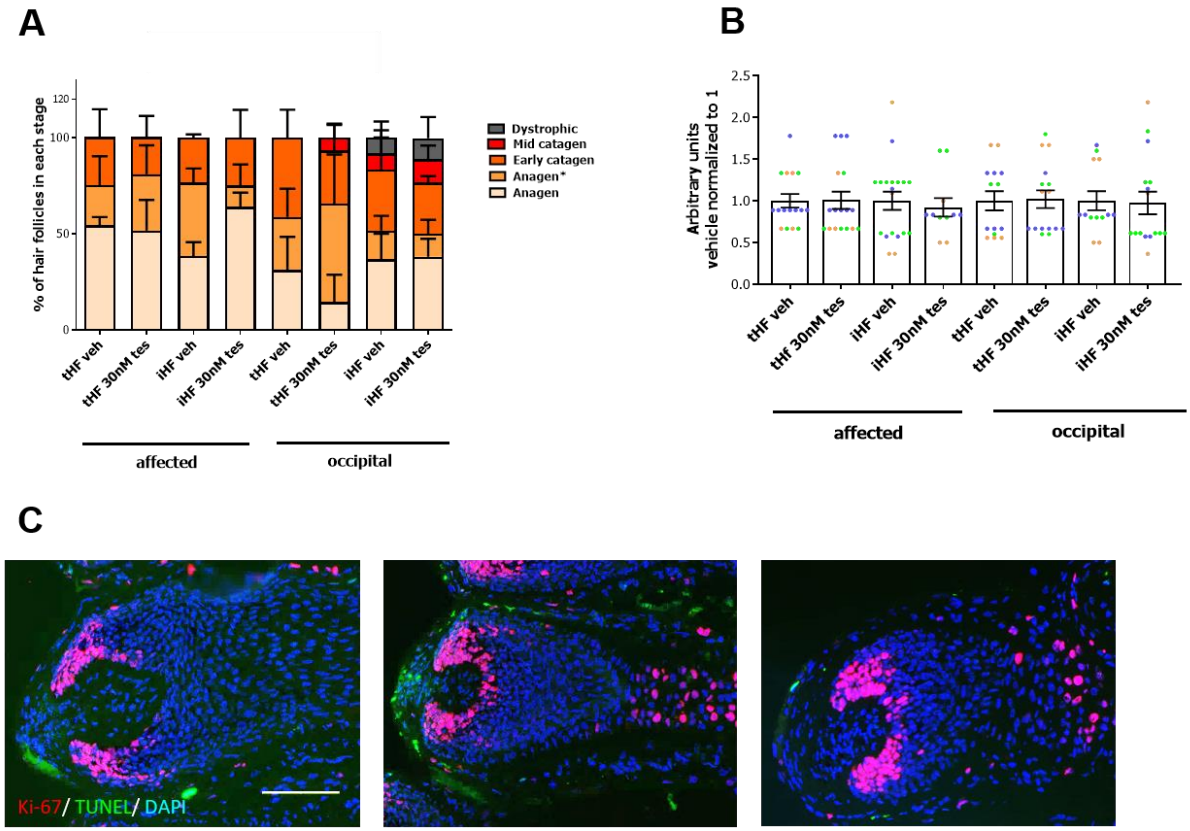

Figure 3.3 Short-term treatment with 30 nM testosterone does not significantly impact on the hair cycle. A: This graph shows the pooled microscopic hair cycle (HC) staging of terminal (t) and intermediate (i) hair follicles (HFs) from the occipital (occ) and affected (aff) area of n= 3 male pattern androgenetic alopecia (mpAGA) patients (Pts). Each treatment group was normalized to its vehicle (veh). No significant changes could have been detected regarding the HC neither in the aff area, nor in the occ area. **B:** This graph displays the pooled HC score of t and iHFs from the occ and aff area of n= 3 mpAGA Pts. Each treatment group was normalized to its veh and veh was normalized to 1. No significant changes could have been detected regarding the HC score in aff or occ t and iHFs after 30 nM testosterone (T) treatment. **C:** Representative images of anagen* HFs after Ki-67/ TUNEL staining. Anagen* HFs fulfilling clear anagen criteria (hair matrix keratinocyte proliferation) as well as early catagen criteria like (dermal papilla cell emigration and accumulation of emigrating cells in the DP stalk). Displayed scale bar indicates 100 µm. Mean±SEM, n= 11-18 HFs/ group from 3 donors, Pt30 displayed in blue, Pt32 displayed in green, Pt43 displayed in orange. Graph Pad Prism 9. D'Agostino & Pearson omnibus normality test, n too small to determine whether the data follow Gaussian distribution; Mann-Whitney test, ns. HF= hair follicle; t= terminal; i= intermediate; aff= affected; tes= testosterone treated; Ki-67= marker of proliferation Ki-67; TUNEL= terminal desoxynucleotidyl transferase-mediated deoxyuridine triphosphate-biotin nick end labelling, DAPI= 4′,6-Diamidin-2-phenylindol. For determining the HC score, arbitrary values are assigned to HFs in different HC stages: anagen= 100, anagen*= 200, early catagen= 300, mid catagen= 400, late catagen= 500, dystrophic catagen= 600

3.1.4 Short-term testosterone treatment *ex vivo* does not induce apoptosis, but increases the proliferation of hair matrix keratinocytes in occipital intermediate hair follicles tendentially

High proliferation in HMg keratinocytes is one criterion to determine HFs in anagen phase. The more the HF goes into catagen phase, the less proliferation can be found in the HM keratinocytes. Therefore, Ki-67/ TUNEL immunofluorescence staining was performed. Proliferative cells could be detected with a Ki-67 antibody. Apoptotic cells were labeled with the TUNEL technique (see **Chapter 2.6**). TUNEL detects DNA fragmentation, and labels, besides cells with an active gene transcription also apoptotic cells [190,191]. For both evaluations, all nuclei in the HMpc and the HMg were counted as well as the Ki-67 and TUNEL positive nuclei. The percentage of all proliferative or apoptotic cells was calculated and the results from n= 3 donors were pooled together. Statistical analysis was performed with GraphPad Prism9. Mann-Whittney test showed significance with a p value <0.05 for the comparison between occ iHF veh and occ iHFs treated with 30 nM T.

The treatment with 30 nM T did not affect the proliferation of HMg and HMpc keratinocytes in aff t/ iHFs or occ tHFs. But surprisingly, T treatment increased the percentage of proliferative HM keratinocytes tendentially in occ iHFs (see **Figure 3.4**). These are unexpected results because up to now the literature claims occipital HFs to be T insensitive [200].

Apoptosis in HMg and HMpc keratinocytes is one criterion to determine HFs in (early) catagen phase. As premature catagen induction is one of the signs for HF miniaturization in mpAGA one could expect to see a higher percentage of apoptotic cells after the treatment of HFs with 30 nM T *ex vivo*. But no increase in the percentage of apoptotic HM keratinocytes was detected in the treated groups (see **Figure 3.4**).

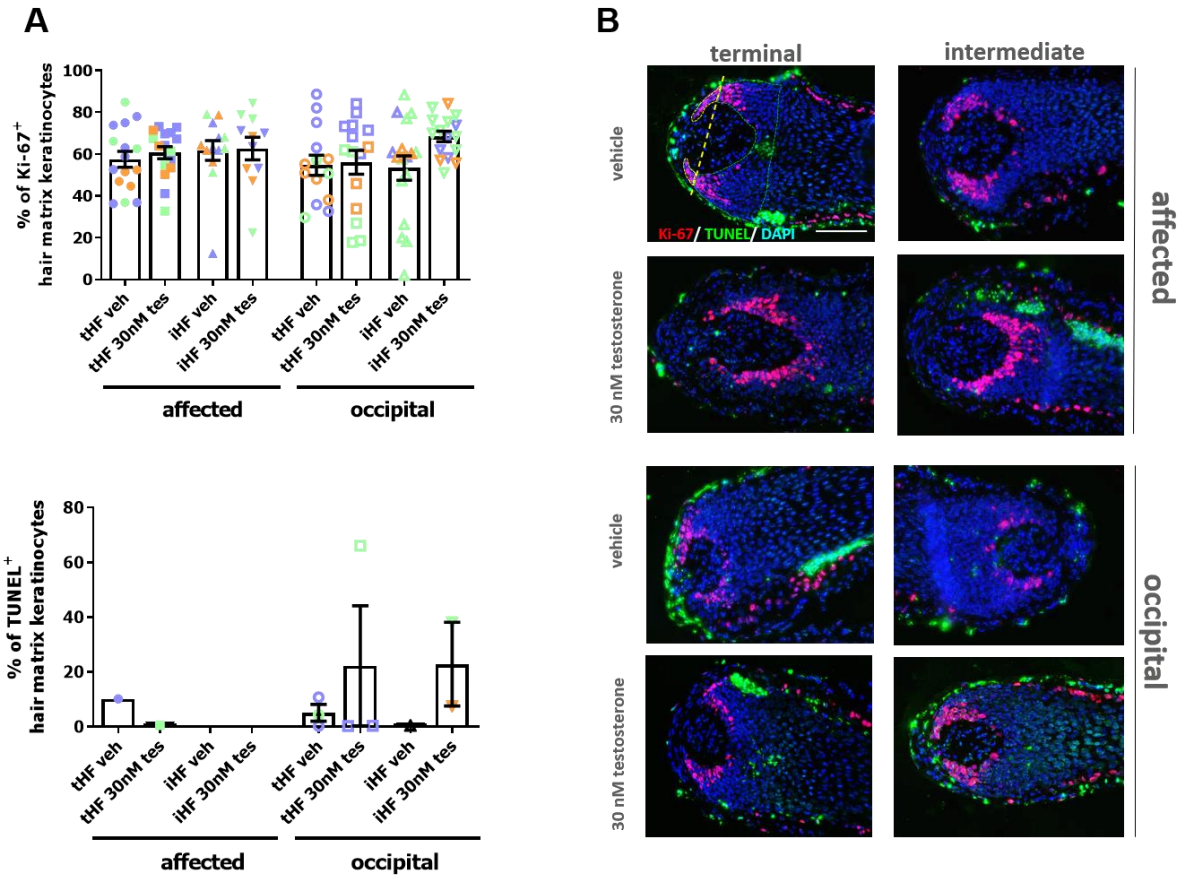

Figure 3.4 Short-term treatment with 30 nM testosterone tendentially increased the proliferation of hair matrix keratinocytes but did not induce apoptosis. A: This graph shows the pooled Ki-67/ TUNEL staining evaluation of terminal and intermediate hair follicles (HFs) from the occipital and affected area of n= 3 male pattern androgenetic alopecia (mpAGA) patients (Pts). Each treatment group was normalized to its vehicle (veh). Proliferation is shown to be tendentially increased after 30 nM testosterone treatment *ex vivo* in occipital intermediate HFs. No changes could have been detected regarding the apoptosis neither in the affected area, nor in the occipital area. **B**: Representative images of Ki-67/ TUNEL staining reflecting the results shown in the graphs of panel **A**. Mean±SEM, n= 11-17 HFs/ group from 3 donors, Pt30 displayed in blue, Pt32 displayed in green, Pt43 displayed in orange. Graph Pad Prism 9. D'Agostino & Pearson omnibus normality test, n too small to determine whether the data follow Gaussian distribution; Mann-Whitney test, ns. Kruskal Wallis test, ns; Dunn's multiple comparison test, vehicle fixed, ns. HF= hair follicle; t= terminal; i= intermediate; veh= vehicle; tes= testosterone treated; Ki-67= marker of proliferation Ki-67; TUNEL= terminal desoxynucleotidyl transferase-mediated deoxyuridine triphosphate-biotin nick end labelling; DAPI= 4′,6-Diamidin-2-phenylindol. Displayed scale bar indicates 100 µm.

3.1.5 Short-term testosterone treatment *ex vivo* significantly decreases dermal papilla inductivity in affected intermediate hair follicles

AP and also versican are well-known markers for the inductivity of DP fibroblasts in mice and humans [50,201–203]. The DP inductivity is highest during anagen phase and decreases during catagen phase [50]. In mpAGA the DP inductivity is reduced, what is caused by the dysregulation of several paracrine factors as BMP-2 and BMP-4 [204].

AP activity was detected via histochemistry analysis (see **Chapter 2.7**) and versican expression was detected via immunofluorescence staining (see **Chapter 2.6**). For both analyses, the DP area was marked (see **Figure 3.5**) and the intensity of expression was measured.

A significant lower (AP activity) and a tendential lower (versican expression) DP inductivity in aff iHFs occ iHFs and aff tHFs was observed, after the treatment with 30 nM T *ex vivo* (see **Figure 3.5**).

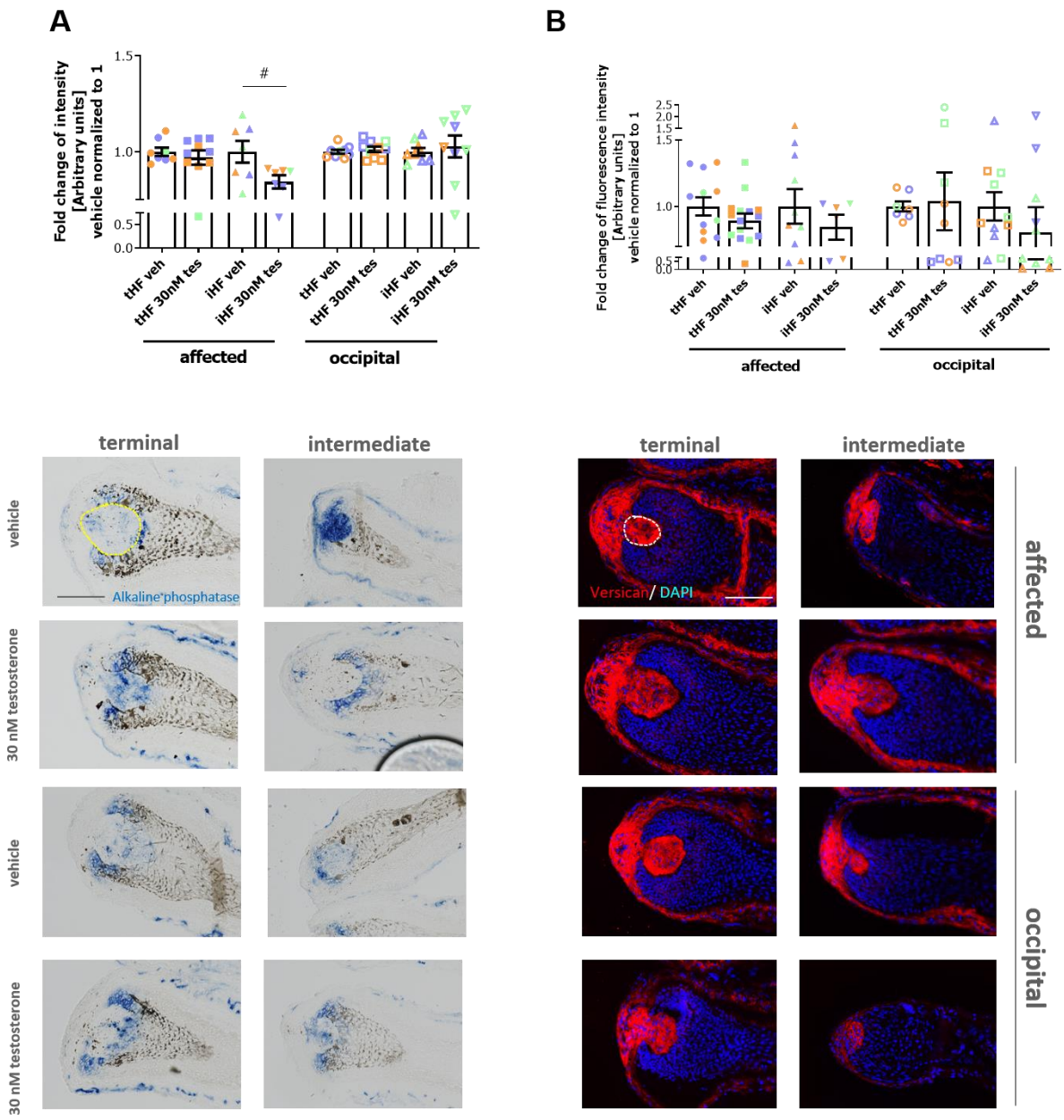

Figure 3.5 Alkaline phosphatase activity and versican expression in occipital and terminal affected and intermediate hair follicles from male pattern androgenetic alopecia patients after 30 nM testosterone treatment *ex vivo*. A: Alkaline phosphatase (AP) activity was measured in the DP as the yellow dotted line indicates. The graph together with the example pictures for AP activity show a significant decrease in intermediate (i) affected (aff) hair follicles (HFs) after 30 nM testosterone (T) treatment from n= 3 male pattern androgenetic alopecia (mpAGA) patients (Pts). Each treatment group was normalized to its corresponding vehicle (veh) and the veh groups were normalized to 1. **B**: Versican expression was measured in the DP as the white dotted line indicates. The expression is clearly tendentially decreased in aff terminal (t) and iHFs and also in occipital (occ) iHFs from n= 3 mpAGA Pts. Each treatment group was normalized to its corresponding veh and the veh groups were normalized to 1. Mean±SEM, n= 11-18 HFs/ group from 3 donors, Pt30 displayed in blue, Pt32 displayed in green, Pt43 displayed in orange. Graph Pad Prism 9. D'Agostino & Pearson omnibus normality test, n too small to determine whether the data follow Gaussian distribution; Mann-Whitney test, ns. Kruskal Wallis test, p<0.0314; Dunn's multiple comparison test, vehicle fixed, #p< 0.05. HF= hair follicle t= terminal; i= intermediate; veh= vehicle; tes= testosterone treated; DAPI= 4′,6-Diamidin-2-phenylindol. Displayed scale bar indicates 100 µm.

Due to the fact, that DP inductivity decreases in catagen HFs naturally, DP inductivity in only anagen aff and occ t/ iHFs after 30 nM T *ex vivo* treatment was examined. The previous shown tendencies (see **Figure 3.5**) were even more prominent when only anagen HFs were analysed (see **Figure 3.6**).

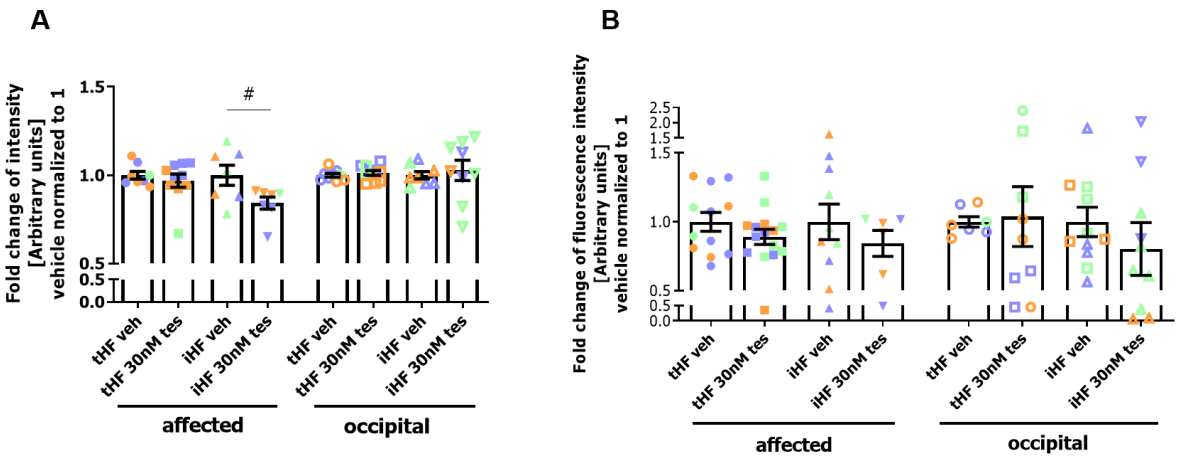

Figure 3.6 Dermal papilla inductivity represented by alkaline phosphatase activity and versican expression in exclusively anagen hair follicles of male pattern androgenetic alopecia pateints. A: Alkaline phosphatase (AP) activity in only anagen affected (aff) and occipital (occ) intermediate (i) and terminal (t) hair follicles (HFs) from male pattern androgenetic alopecia (mpAGA) patients (Pts). AP activity is significantly decreased in aff iHFs after the treatment with 30 nM testosterone (T) *ex vivo* in n= 3 mpAGA Pts. Each treatment group was normalized to its corresponding vehicle (veh) and the veh groups were normalized to 1. **B:** Versican expression in only anagen t/ iHFs from aff and occ of mpAGA Pts. Tendential decreasing can be detected in aff t/ iHFs and in occ iHFs after the treatment with 30 nM T *ex vivo* in n= 3 mpAGA Pts. Each treatment group was normalized to its corresponding veh and the veh groups were normalized to 1. Mean±SEM, n= 6-15 HFs/ group from 3 donors, Pt30 displayed in blue, Pt32 displayed in green, Pt43 displayed in orange. Graph Pad Prism 9. D'Agostino & Pearson omnibus normality test, n too small to determine whether the data follow Gaussian distribution; Mann-Whitney test, ns. Kruskal Wallis test, $p<0.0314$; Dunn's multiple comparison test, vehicle fixed, #$p< 0.05$; Mann-Whitney test, ns. HF= hair follicle t= terminal; i= intermediate; veh= vehicle; tes= testosterone treated.

3.1.6 Short-term testosterone treatment *ex vivo* influences the cell number in the dermal papilla and the inductive dermal cup but has no impact on the cell number in the dermal papilla stalk

In the transition from anagen to catagen, DPCs migrating out of the DP into the DC. Throughout the transition from telogen back to anagen, DPCs are restored and a new DP can be properly formed. This in- and efflux of DPCs is imbalanced in mpAGA aff HFs. Here, one can observe a massive efflux of DPCs from the DP into the DC but almost no influx from the DC back into the DP during the new anagen onset. This is one of the matters for HF miniaturization in mpAGA.

To investigate the influence of 30 nM T treatment *ex vivo* on the number of DPCs, cells in the DP of aff and occ t/ iHFs of mpAGA Pts have been counted and the size of the DP has been measured. The number of cells per μm^2 has been evaluated. For this analysis the immunofluorescence-stained sections of the Ki-67/ TUNEL (see **Chapter 2.6**) staining have been used and the evaluation was carried out only in the DAPI (counterstained) channel pictures. Here, a tendential decrease in DPC number after T treatment in aff iHFs was shwon (see **Figure 3.7**).

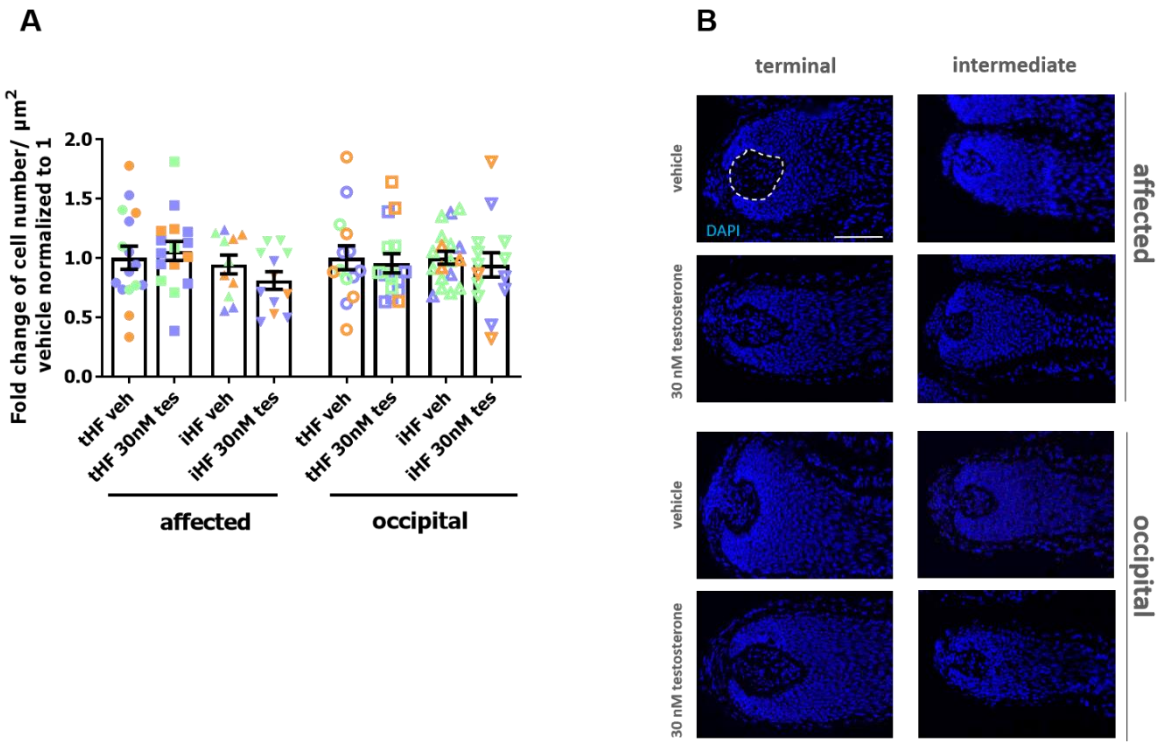

Figure 3.7 Number of cells in the dermal papilla of occipital and affected intermediate and terminal hair follicles of male pattern androgenetic alopecia patients after 30 nM testosterone treatment *ex vivo*. A: The graph shows the fold change of the cell number per µm^2 in the dermal papilla (DP) of occipital (occ) and affected (aff), terminal (t) and intermediate (i) hair follicles (HFs) of male pattern androgenetic alopecia (mpAGA) patients (Pts) after the treatment with 30 nM testosterone (T) *ex vivo*. A tendential decrease in the number of the cells in the DP per µm^2 can be detected in aff iHFs after T treatment in n= 3 mpAGA Pts. **B:** Representative images of DAPI stained HFs with the indicated area (white dotted line) where DP cells have been counted. These images are reflecting the results of the in **A** shown graph and show a tendential decrease in DP cell number per µm^2 in aff iHFs. Mean±SEM, n= 11-18 HFs/ group from 3 donors, Pt30 displayed in blue, Pt32 displayed in green, Pt43 displayed in orange. Graph Pad Prism 9. D'Agostino & Pearson omnibus normality test, data follow Gaussian distribution; unpaired t-test, ns; one-way ANOVA, ns; Dunn's multiple comparison test, vehicle fixed, ns; HF= hair follicle t= terminal; i= intermediate; veh= vehicle; tes= testosterone treated; DAPI= 4′,6-Diamidin-2-phenylindol. Displayed scale bar indicates 100 µm.

Furthermore, the impact of T *ex vivo* treatment on the number of cells in the inductive DC was investigated. Corresponding to the decrease of DPC number in aff iHFs, an increase in cell number in the inductive DC in those HFs could be expected. For this evaluation the same pictures have been taken and the area of the inductive DC has been drawn. Like this, the number of cells per µm^2 was evaluated. Like for the number of DPCs, also the number of cells in the inductive DC decreased after 30 nM T treatment *ex vivo*. In addition, a slight increase in the DC cell number was detected in aff tHFs (see **Figure 3.8**).

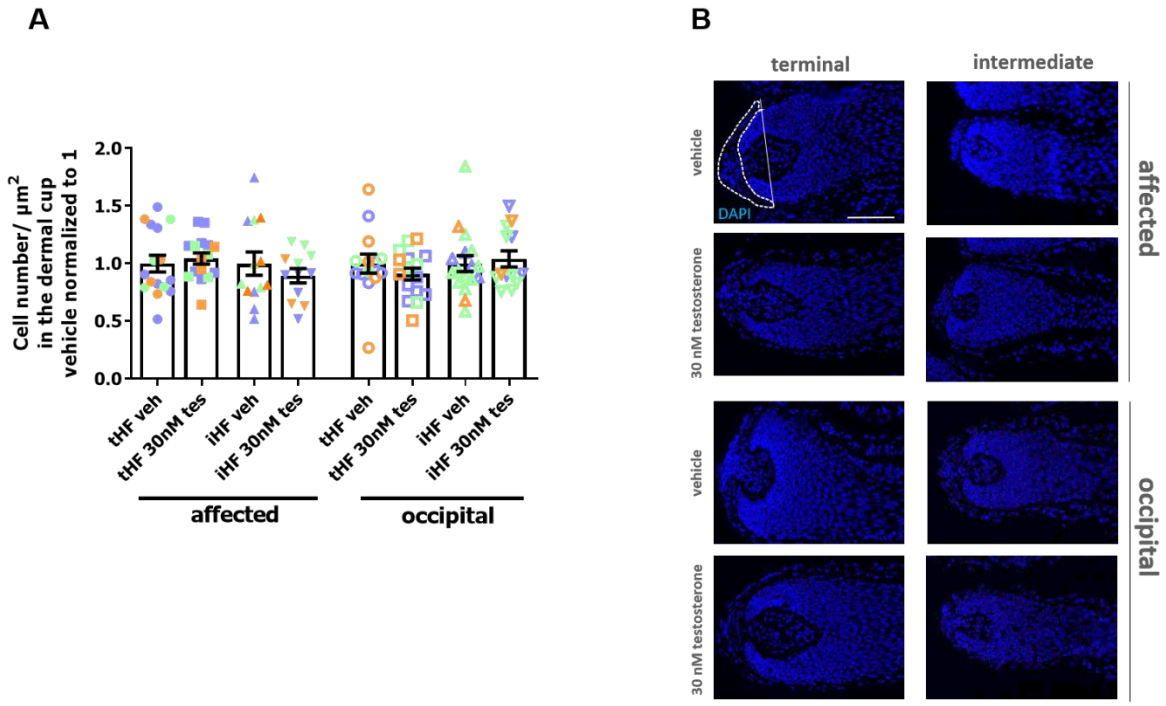

Figure 3.8 Number of cells in the inductive dermal cup of occipital and affected intermediate and terminal hair follicles of male pattern androgenetic alopecia patients after 30 nM testosterone treatment *ex vivo*. A: The graph shows the fold change of the cell number per µm² in the inductive dermal cup (DC) of occipital (occ) and affected (aff), terminal (t) and intermediate (i) hair follicles (HFs) of male pattern androgenetic alopecia (mpAGA) patients (Pts) after the treatment with 30 nM testosterone (T) *ex vivo*. A tendential decrease in the number of the cells in the inductive DC per µm² can be detected in aff iHFs. Furthermore, a tendential increase in number of cells per µm² in the inductive DC of aff tHFs can be detected after T treatment in n= 3 mpAGA Pts. **B:** Representative images of DAPI stained HFs with the indicated area (white dotten line) where inductive DC cells have been counted. These images reflect the results of the in **A** shown graph and display a tendential decrease in inductive DC cell number per µm² in aff iHFs, as well as a tendential increase in cell number in aff tHFs after the treatment with 30 nM T. Mean±SEM, n= 12-17 HFs/ group from 3 donors, Pt30 displayed in blue, Pt32 displayed in green, Pt43 displayed in orange. Graph Pad Prism 9, D'Agostino & Pearson omnibus normality test, data does not follow Gaussian distribution; Kruskal Wallis test, ns; Dunn's multiple comparison test, vehicle fixed, ns. Mann-Whitney test, ns. HF= hair follicle t= terminal; i= intermediate; veh= vehicle; tes= testosterone treated; DAPI= 4′,6-Diamidin-2-phenylindol. Displayed scale bar indicates 100 µm

While 30 nM T treatment seems to have an impact on the number of cells in the DP and the inductive DC, the number of cells in the DP stalk tendentially decreases in the DP stalk of occ tHFs (see **Figure 3.9**). The DP stalk is characterized by the cells which are actively migrating from the DP into the DC. For this evaluation the same images have been evaluated. The area of interest (DP stalk) was drawn in the pictures, the number of cells has been counted and the size of the area was measured. Like this, the number of cells per µm² was evaluated.

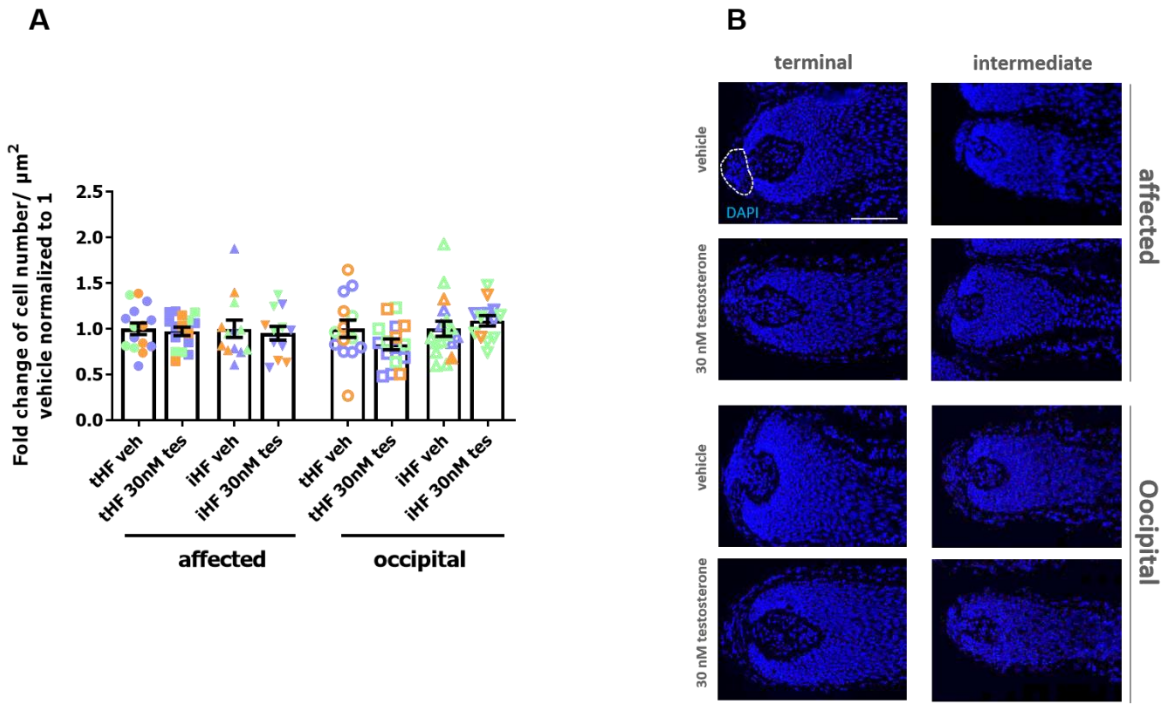

Figure 3.9 Number of cells in the dermal papilla stalk of occipital and affected intermediate and terminal hair follicles of male pattern androgenetic alopecia patients after 30 nM testosterone treatment *ex vivo*. A: The graph shows the fold change of the cell number per µm^2 in the dermal papilla (DP) stalk of occipital (occ) and affected (aff), terminal (t) and intermediate (i) hair follicles (HFs) of male pattern androgenetic alopecia (mpAGA) patients (Pts) after the treatment with 30 nM testosterone (T) *ex vivo*. A tendential decrease in the number of the cells in the DP stalk per µm^2 can be detected in occ tHFs can be detected after T treatment in n= 3 mpAGA Pts. **B:** Representative images of DAPI stained HFs with the indicated area (white dotted line) where DP stalk cells have been counted. These images are reflecting the results of the in **A** shown graph and display a tendential decrease in DP stalk cell number per µm^2 in occ tHFs, after the treatment with 30 nM T. Mean±SEM, n= 12-17 HFs/ group from 3 donors, Pt30 displayed in blue, Pt32 displayed in green, Pt43 displayed in orange. Graph Pad Prism 9, D'Agostino & Pearson omnibus normality test, data does not follow Gaussian distribution; Kruskal Wallis test, ns; Dunn's multiple comparison test, vehicle fixed, ns. Mann-Whitney test, ns. HF= hair follicle t= terminal; i= intermediate; veh= vehicle; tes= testosterone treated; DAPI= 4′,6-Diamidin-2-phenylindol. Displayed scale bar indicates 100 µm.

Due to the fact that the number of DPCs as well as the number of cells in the inductive DC change naturally throughout the HC, the changes in cell number was additionally evaluated in exclusively anagen HFs (see **Figure 3.10**). With this method the results reflect even more reliable the impact of T in mpAGA. When only anagen HFs were observed, the tendential decrease in DPC number in aff iHFs becomes significant and shows it to be a direct effect of the T treatment (see **Figure 3.10 A**). The number of cells in the inductive DC in anagen aff iHFs stays the same, so the previously seen effect in tendential reduction of cell number was due to catagen transition. But when only anagen HFs were evaluated, the increase in number of cells in the inductive DC of aff tHFs gets more prominent what can be considered as an effect caused by the T treatment (see **Figure 3.10 B**). The previously observed tendential decrease in cell number of the DP stalk in occ tHFs is not present anymore when only anagen HFs were taken into consideration (see **Figure 3.10 C**). This can be seen as an HC related

effect when HFs naturally go to catagen. In only anagen HFs the number of DP stalk cells remains the same throughout all evaluated HF types.

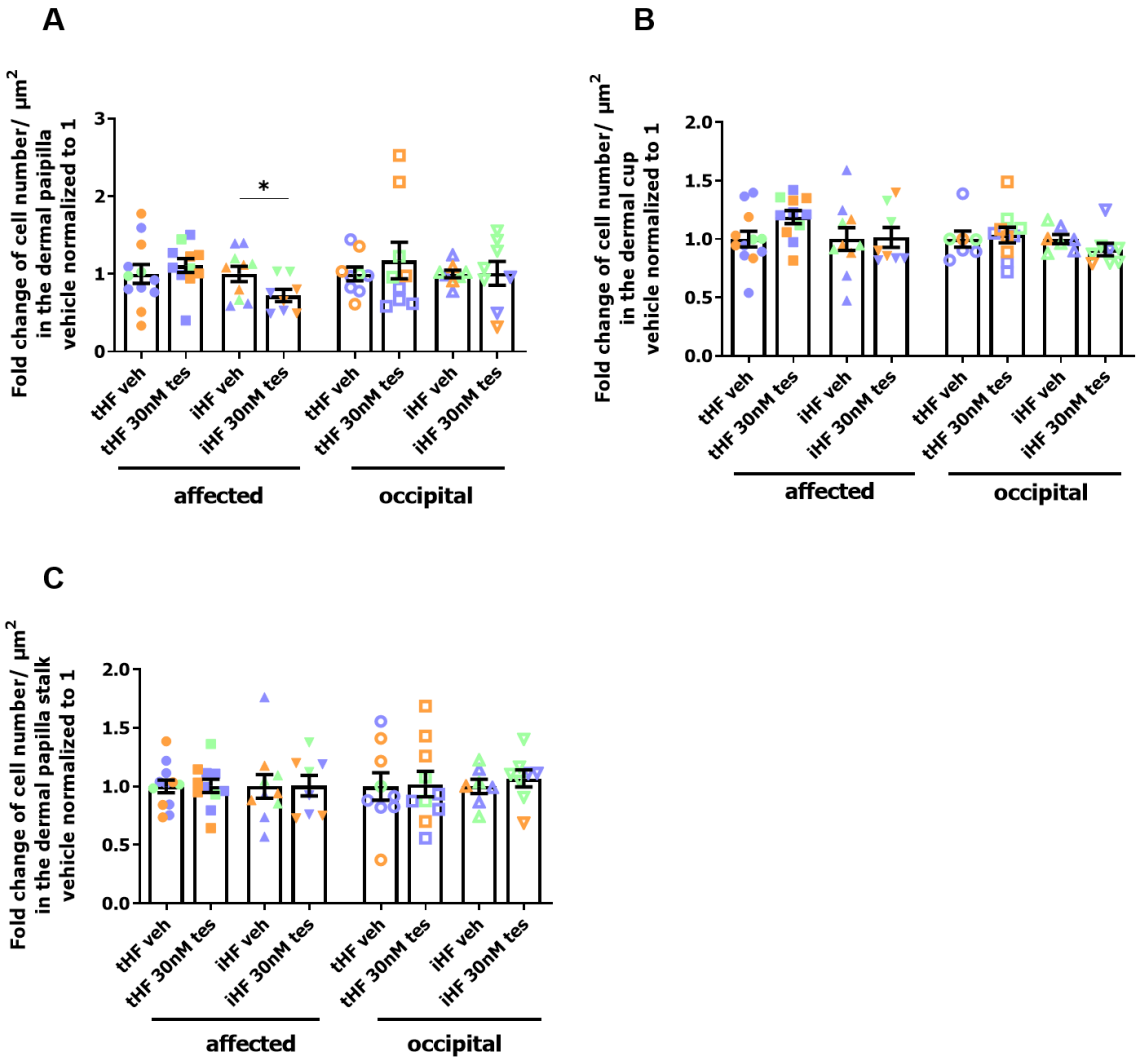

Figure 3.10 The effect of 30 nM testosterone treated affected and occipital terminal and intermediate anagen hair follicles regarding the number of cells in the dermal papilla, the inductive dermal cup and the dermal papilla stalk. A: The graph shows the fold change of the cell number per µm² in the dermal papilla (DP) of occipital (occ) and affected (aff), terminal (t) and intermediate (i) anagen hair follicles (HFs) of male pattern androgenetic alopecia (mpAGA) patients (Pts) after the treatment with 30 nM testosterone (T) *ex vivo*. A significant decrease in the number of the cells in the DP per µm² can be detected in only anagen aff iHFs after T treatment in n= 3 mpAGA Pts**. B:** The graph shows the fold change of the cell number per µm² in the inductive dermal cup (DC) of occ and aff, t/ i anagen HFs of mpAGA Pts after the treatment with 30 nM T *ex vivo*. A tendential increase in number of cells per µm² in the inductive DC of aff tHFs can be detected in only anagen HFs after T treatment in n= 3 mpAGA Pts. **C:** The graph shows the fold change of the cell number per µm² in the DP stalk of occ and aff, t/ i anagen HFs of mpAGA Pts after the treatment with 30 nM T *ex vivo*. No change in the number of the cells in the DP stalk per µm² can be detected in only anagen HFs after T treatment in n= 3 mpAGA Pts. Mean±SEM, n= 7-12 HFs/ group from 3 donors, Pt30 displayed in blue, Pt32 displayed in green, Pt43 displayed in orange. Graph Pad Prism 9. D'Agostino & Pearson omnibus normality test, data does not follow Gaussian distribution; Kruskal Wallis test, ns; Dunn's multiple comparison test, vehicle fixed, ns. Mann-Whitney test, *p< 0.05. HF= hair follicle t= terminal; i= intermediate; veh= vehicle; tes= testosterone treated.

3.1.7 Short-term testosterone treatment *ex vivo* impacts significantly on apoptosis of mesenchymal cells in male pattern androgenetic alopecia patients' hair follicles

Apoptosis is a form of programmed cell death. It is a response to several events happening inside a cell and it is an active and rational "decision" made by the cell to sacrifice for a greater benefit [205,206]. These mentioned events include, besides cell shrinkage and nuclear fragmentation, also chromatin condensation and DNA fragmentation [206]. The validated TUNEL technique is known to detect DNA fragmentation inside the cells [191].

With the transition from anagen to catagen, apoptosis occurs in the epithelial cells of the HF, but in mice and humans, it was never detected in mesenchymal cells under normal circumstances [207–210].

While analysing the Ki-67/ TUNEL staining, in all three Pts, TUNEL positive mesenchymal cells were found, regardless the actual HC stage. TUNEL positive cells are considered to be apoptotic cells.

To investigate if the appearance of TUNEL positive cells is linked to 30 nM T treatment, the total number of cells, as well as just the TUNEL positive cells in the inductive DC have been counted in aff and occ t/ iHFs of mpAGA Pts. The percentage of TUNEL positive cells has been evaluated. Therefore, the immunofluorescence-stained sections of the Ki-67/ TUNEL (see **Chapter 2.6**) staining have been used. A significant increase in percentage of TUNEL positive cells in the DC was detected after T treatment *ex vivo* in aff tHFs, while in aff iHFs, a tendential decrease of the percentage of TUNEL positive cells in the DC was detected. In HFs DCs from the occ area, the opposite effect was caused by 30 nM T treatment *ex vivo*. Here, the percentage of TUNEL positive cells was significantly down regulated in occ tHFs and tendentially upregulated in occ iHFs (see **Figure 3.11 A** and **C**). No changes in the percentage of apoptosis in DP cells of aff and occ t/ iHFs from mpAGA Pts after 30 nM t treatment *ex vivo* could have been detected (see **Figure 3.11 B**).

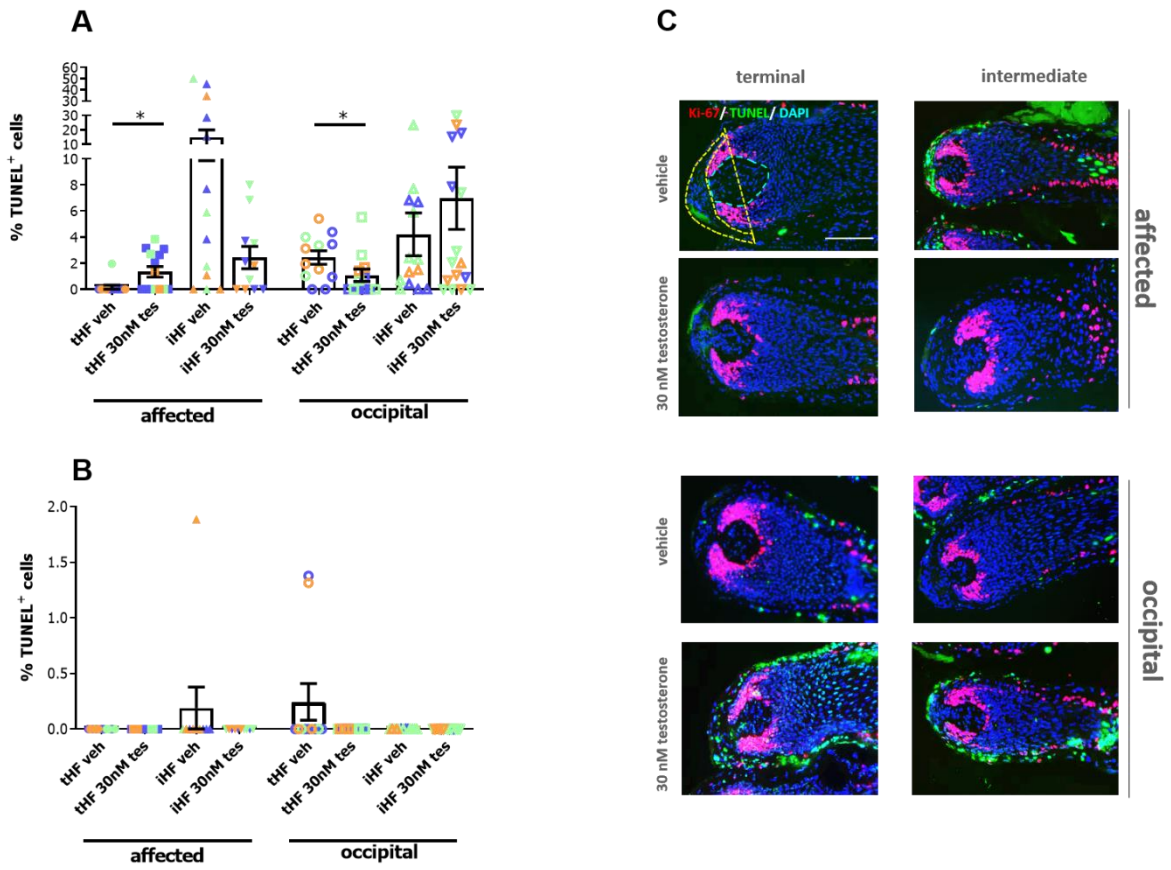

Figure 3.11 The significant effect of 30 nM testosterone on treated affected and occipital terminal and intermediate anagen hair follicles regarding the percentage TUNEL positive cells in the dermal papilla and the inductive dermal cup. A: The graph shows the percentage of TUNEL positive cells in the inductive dermal cup (DC) of occipital (occ) and affected (aff), terminal (t) and intermediate (i) hair follicles (HFs) of male pattern androgenetic alopecia (mpAGA) patients (Pts) after the treatment with 30 nM testosterone (T) *ex vivo*. A significant increase can be detected in the DC of aff tHFs, but a tendential decrease in the percentage of TUNEL positive cells was detected in the DC aff iHFs. In occ tHFs, the percentage of TUNEL positive cells is significantly reduced by T treatment and tendentially increased in occ iHFs DC after T treatment in n= 3 mpAGA Pts. **B:** The graph shows the percentage of TUNEL postitive cells in the dermal papilla (DP) of occ and aff, t/ i HFs of mpAGA Pts after the treatment with 30 nM T *ex vivo*. No TUNEL positive cells could have been detected in n= 3 mpAGA Pts. **C:** Representative images of Ki-67/ TUNEL staining reflecting the results for the percentage of TUNEL positive cells, shown in the graphs of panel **A** and **B**. Mean±SEM, n= 10-16 HFs/ group from n= 3 donors, Pt30 displayed in blue, Pt32 displayed in green, Pt43 displayed in orange. Graph Pad Prism 9. D'Agostino & Pearson omnibus normality test, data does not follow Gaussian distribution; Mann-Whitney test, *p< 0.05. HF= hair follicle t= terminal; i= intermediate; veh= vehicle; tes= testosterone treated; Ki-67= marker of proliferation Ki-67; TUNEL= terminal desoxynucleotidyl transferase-mediated deoxyuridine triphosphate-biotin nick end labelling, DAPI= 4′,6-Diamidin-2-phenylindol. Displayed scale bar indicates 100 µm.

DNA fragmentation detected by the TUNEL technique does not only occur during apoptosis but also in cells in which DNA damage is induced by other means and can label also non-apoptotic nuclei showing signs of active gene transcription [190,191]. During apoptosis cysteinyl-asparate specific proteases (caspases) play key roles [211,212]. To initiate apoptosis, one of the initiator caspases (e.g., caspase 8) is activated by the ligand binding to a TNF receptor. Once activated, the initiator caspases act upon other following caspases (e.g., caspase 3) by cleavage. For this purpose, immunofluorescence staining for cleaved casp3 was performed. Unlike TUNEL, casp-3 is expressed by a cell during the so called “point of no return” towards apoptosis, even when no morphological changes happened yet [190].

To evaluate the effect of 30 nM T treatment *ex vivo* on aff and occ t/ iHFs of mpAGA Pts, the total number of cells as well as the total number of casp-3 positive cells in the designated areas have been counted and the percentage of positive casp-3 cells was calculated.

The observations obtained by the TUNEL evaluation only partially overlap with the results obtained by casp-3 evaluation. In the DC of aff iHFs, only a tendential reduction in the percentage of casp-3 positive cells was detected. Meanwhile, in the DC of occ iHFs a significant reduction of casp-3 positive cells was detected after T treatment. The already observed significant reduction of TUNEL positive cells in the DC of occ tHFs (see **Figure 3.11 A**) overlaps with also a significant reduction of casp-3 positive cells in the DC of occ tHFs (see **Figure 3.12 A**). Surprisingly, casp3 positive cells were significantly increased in the DP of aff tHFs after 30 nM T treatment *ex vivo* (see **Figure 3.12 B**).

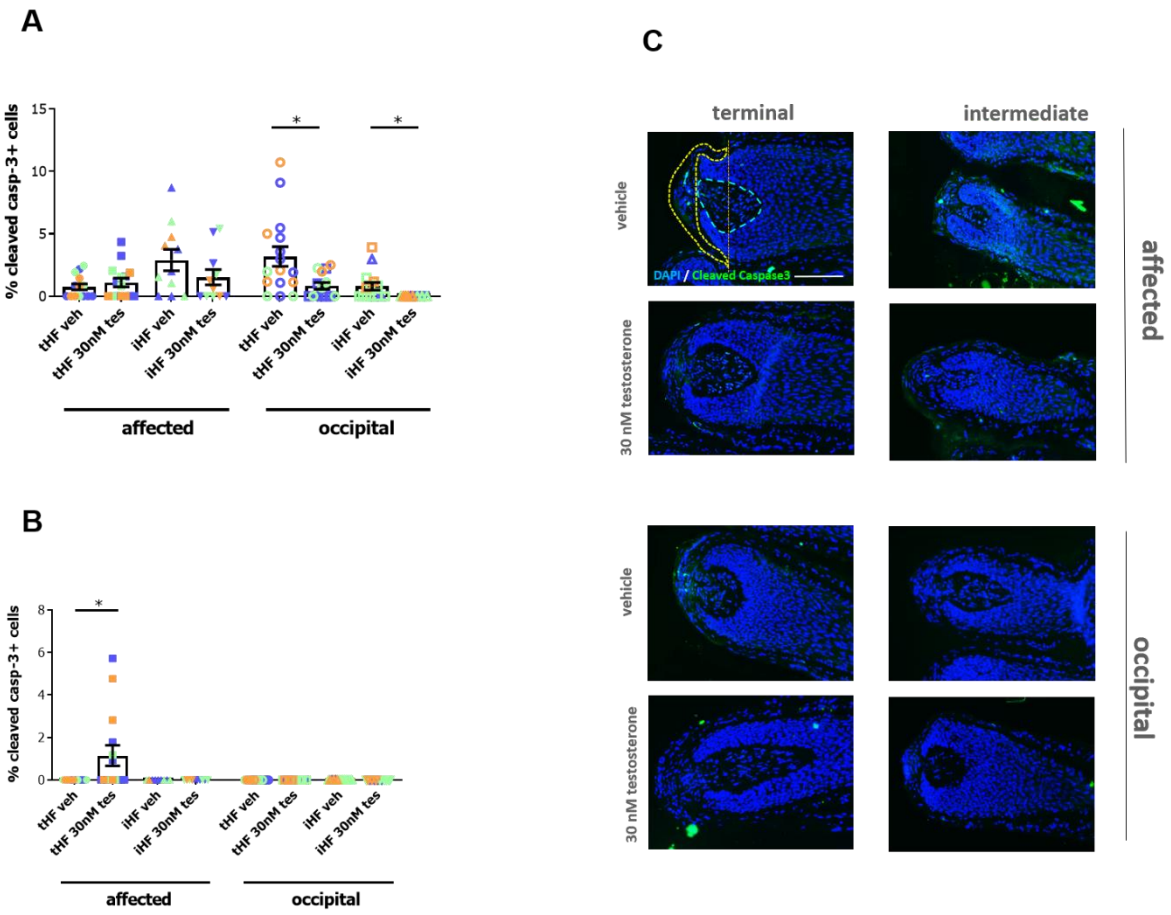

Figure 3.12 The effect of 30 nM testosterone on treated affected and occipital terminal and intermediate anagen hair follicles regarding the percentage cleaved caspase 3 positive cells in the dermal papilla and the inductive dermal cup. **A:** The graph shows the percentage of cleaved caspase 3 (casp-3) positive cells in the inductive dermal cup (DC) of occipital (occ) and affected (aff), terminal (t) and intermediate (i) hair follicles (HFs) of male pattern androgenetic alopecia (mpAGA) patients (Pts) after the treatment with 30 nM testosterone (T) *ex vivo*. A significant reduction the percentage of casp-3 positive cells can be detected in the DC of occ tHFs and also in the DC of occ iHFs after 30 nM T treatment in n= 3 mpAGA Pts. **B:** The graph shows the percentage of casp-3 positive cells in the dermal papilla (DP) of occ and aff, t/ i HFs of mpAGA Pts after the treatment with 30 nM T *ex vivo*. A significant increase in the percentage of casp-3 positive cells in aff iHFs could have been detected in n= 3 mpAGA Pts. **C:** Representative images of casp-3 staining reflecting the results for the percentage of casp3 positive cells, shown in the graphs of panel **A** and **B**. Mean±SEM, n= 10-16 HFs/ group from 3 donors, Pt30 displayed in blue, Pt32 displayed in green, Pt43 displayed in orange. Graph Pad Prism 9. D'Agostino & Pearson omnibus normality test, data does not follow Gaussian distribution; Mann-Whitney test, *p< 0.05. HF= hair follicle t= terminal; i= intermediate; veh= vehicle; tes= testosterone treated; DAPI= 4′,6-Diamidin-2-phenylindol. Displayed scale bar indicates 100 µm.

3.2 Identification of differentially regulated genes in occipital and affected terminal and intermediate hair follicles after short term testosterone treatment

The influence of T is claimed to be the driving force when it comes to HF miniaturization in mpAGA. The naturally appearing concentration of circulating T in the human body is in the range from 3-15 ng/ mL (healthy donors) [85–87] and is known to not differ from the concentration found in mpAGA Pts [80,81,83]. To investigate the influence of T on mpAGA Pts' HFs and the resulting early gene expression changes, a concentration of 10 nM was chosen to mimic the natural appearing concentration of T. How the HF *ex vivo* culture was carried out, please refer to **Chapter 2.5**. Occ and aff t/ iHFs of mpAGA Pts were cultured in 10 nM T containing culture medium for 48 h and then placed in RNA extraction buffer and stored in -80 °C. After isolating the RNA (see **Chapter 2.3**) it was sent to CeGaT GmbH (see **Chapter 2.4**). After cDNA library preparation and RNAseq the normalized read counts for every gene were examined. All genes with a CPM value lower than 0.5 and a calculated FC higher than 2 or lower than 0.5 have been taken into consideration. These criteria allow the comparison of different groups deriving from one donor or all n= 5 donors.

3.2.1 Principle component analysis of occipital and affected terminal and intermediate hair follicles from male pattern androgenetic alopecia patients after short term testosterone treatment

For investigating if short term T treatment has an impact on HFs from mpAGA Pts, HFs were cultured *ex vivo* with 10 nM T for 48 h. RNA was isolated and sent for RNAseq.

After regularized log (rlog) transformation of the obtained raw data (from RNAseq) the dependence of the variance on the mean was minimized for the genes with small counts. The performed principle component analysis (PCA) of all retrieved RNAseq data from all n= 5 donors, revealed three major clusters. The first cluster contains most of the veh samples of Pt17 and Pt22. The second cluster contains most of the 10 nM T treated samples of Pt17 and Pt22. Those two clusters differ mostly in PCA 1 and PCA 2 from each other. The indicated arrows displayed in **Figure 3.13** are always pointing from the veh towards the 10 nM T treated groups. The third and most undefined cluster contains all samples of Pt18, Pt23 and Pt26 (see **Figure 3.13**). Amongst all analysed samples, HFs of Pt17 and Pt22 show similarities in the response to T.

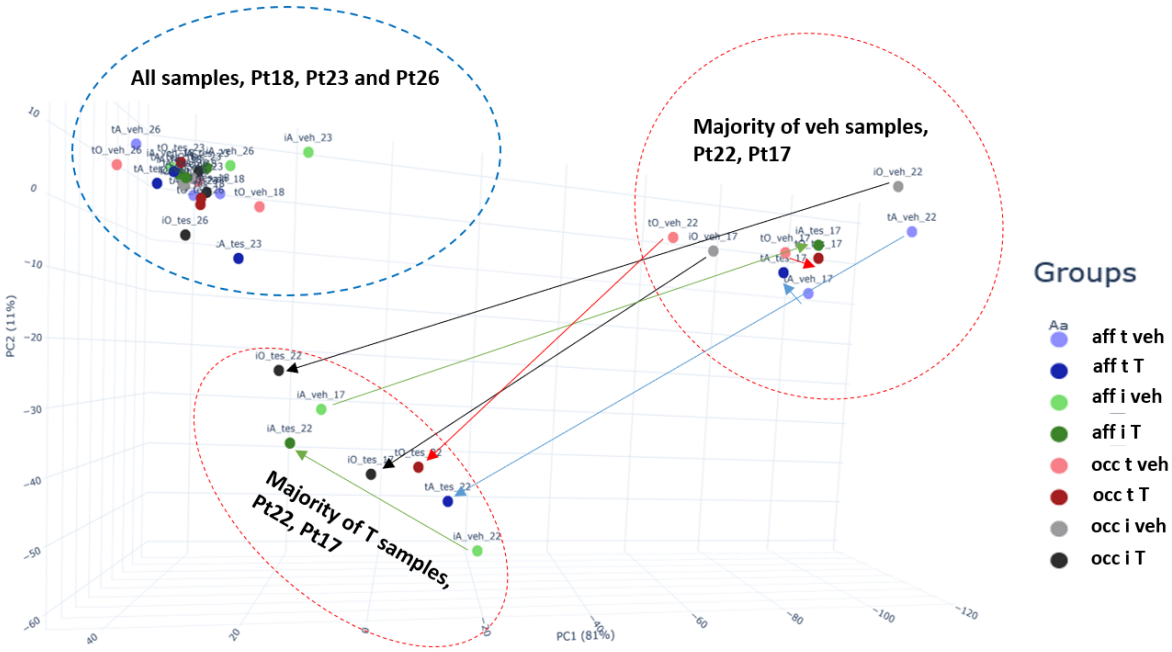

Figure 3.13 Principle component analysis of the RNA sequencing derived data from male pattern androgenetic alopecia patients' hair follicles treated with 10 nM testosterone *ex vivo*. The principle component analysis (PCA) of the RNA sequencing (RNAseq) data obtained from n= 5 patients (Pts) reveals three major clusters. In the first two (red dotted line circle) only samples of Pt17 and Pt22 are present. Those samples segregate mostly in principle component (PC) 1 and 2 by treatment. The indicated arrows are always pointing from the vehicle towards the 10 nM testosterone (T) treated groups and indicating as such the change in PC 1 and 2 by the influence of T *ex vivo*. The third cluster (blue dotted line circle) contains all samples of Pt18, Pt23 and Pt26. Those seem not to differ in PCA 1 or 2 after 10 nM T treatment *ex vivo*. Pt= patient, veh= vehicle, T= testosterone, i= intermediate, t= terminal, aff= affected, occ= occipital, PC (principle component).

Having a closer look on the undefined cluster showing in **Figure 3.13** which contains all samples (veh and 10 nM treated) of Pt18, Pt23 and Pt26, a clear segregation by Pts rather than by treatment can be observed for those three Pts (see **Figure 3.14**). Also here, all displayed arrows pointing from veh to 10 nM treated groups.

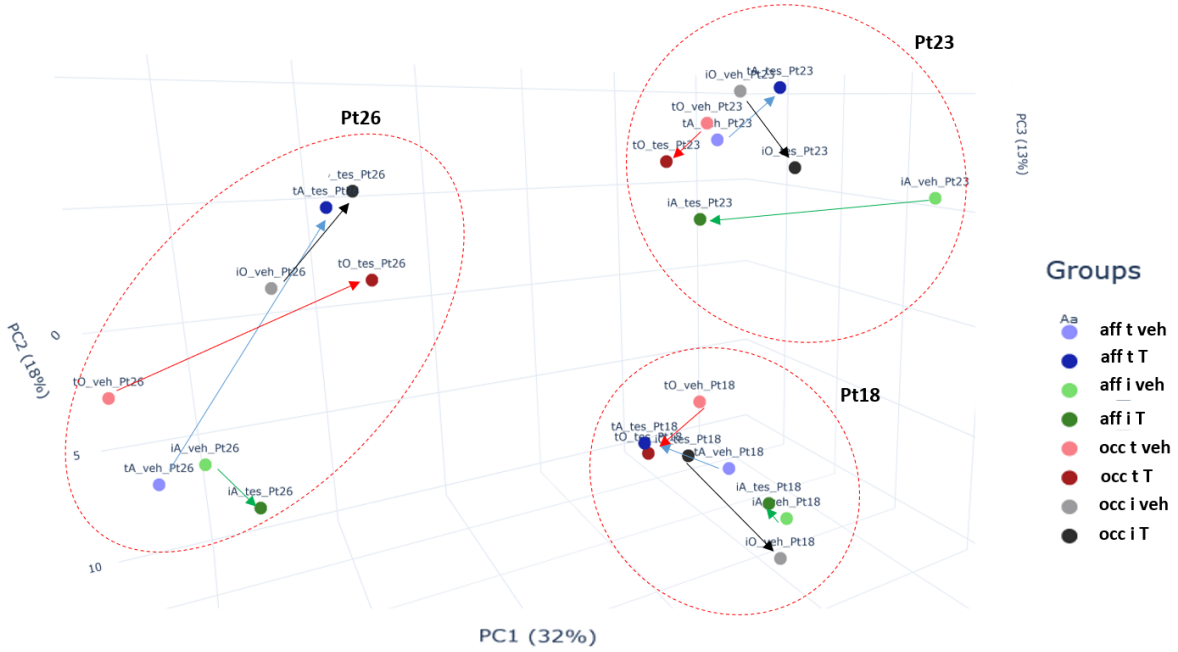

Figure 3.14 Principle component analysis of the RNA sequencing derived data from male pattern androgenetic alopecia patients' hair follicles treated with 10 nM testosterone *ex vivo*. The principle component analysis (PCA) of the RNA sequencing (RNAseq) data obtained from n= 3 patients (Pts) reveals three major clusters. Each cluster contains all samples of one Pt. The indicated arrows are always pointing from the vehicle (veh) towards the 10 nM testosterone (T) treated groups and indicating as such the change in principle component (PC) 1, PC 2 and PC 3 by the influence of T *ex vivo*. These analyzed samples segregate by Pt rather than by treatment. Pt= patient, veh= vehicle, T= testosterone, i= intermediate, t= terminal, aff= affected, occ= occipital.

3.2.2 Analysis of the transcriptomic differences of intermediate and terminal hair follicles from the affected and occipital scalp of male pattern androgenetic alopecia patients after short term testosterone treatment

Changes in the transcriptome of predisposed HFs caused by the influence of T, might be the key to unravel the mechanism behind HF miniaturization in mpAGA. For this purpose, HFs were *ex vivo* cultured with 10 nM T (see **Chapter 2.5**), their RNA was isolated (see **Chapter 2.3**) and sent for RNAseq.

The obtained raw data was processed as described in **Chapter 2.4**. The genes of all n= 5 Pts with a calculated FC higher than 2 and lower than 0.5 as well as a CPM lower than 0.5 were compared by treatment in the respective compartment. The transcriptomic analysis after short term treatment with 10 nM T revealed for aff tHFs 39,582 and for aff iHFs 38,131 differentially regulated genes. Despite the fact, that HFs from the occ scalp are considered to be androgen insensitive, the transcriptomic analysis after 10 nM T *ex vivo* culture revealed for occ tHFs 20,044 and for occ iHFs 42,603 differentially regulated genes. All four comparisons amongst all Pts share 16,301 differentially regulated genes (red ellipse, **Figure 3.15**). These can be

considered to be involved in the “mechanical process” of miniaturization. The differentially regulated genes which are equal in occ tHFs and occ iHFs (490, blue circle, **Figure 3.15**) can be considered to be exclusively involved in the physiological miniaturization (based on HC changes). Genes which appear to be differentially regulated in aff tHFs and aff iHFs (1,175, black circle, **Figure 3.15**) are genes which are exclusively involved in the pathological miniaturization. Due to the fact that the RNAseq after T treatment *ex vivo* can only be considered to be a “snap shot” of gene expression, all of these obtained differentially regulated genes are interesting to elaborate and are potentially the genetical key to HF miniaturization in mpAGA.

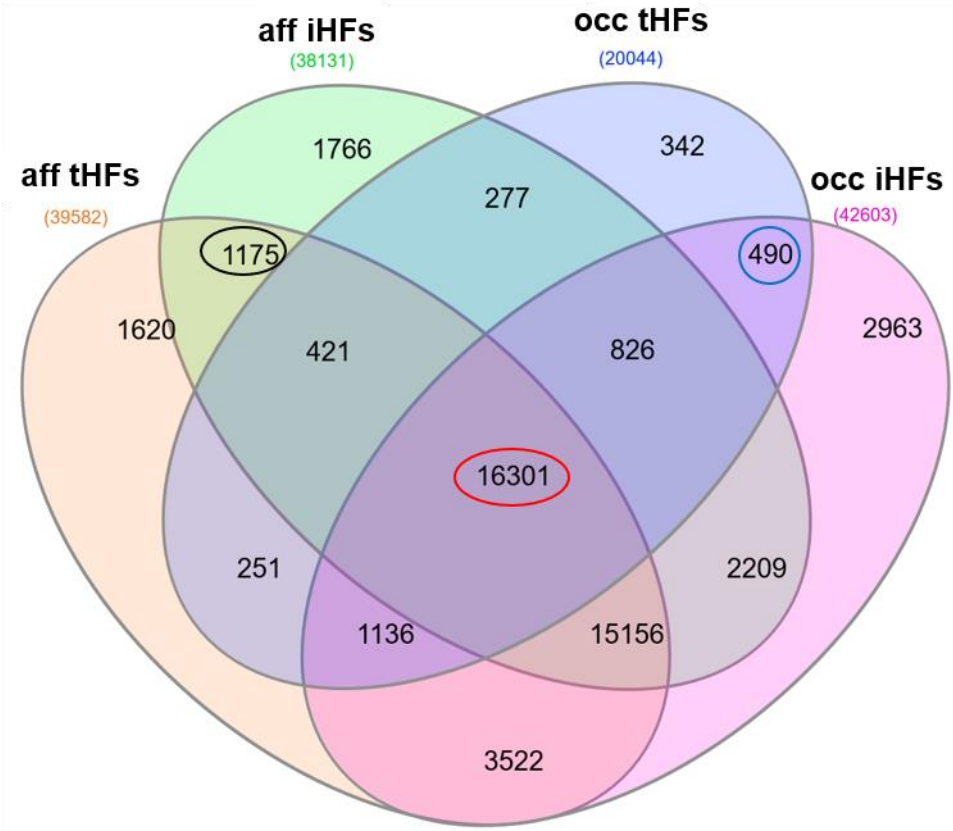

Figure 3.15 Differentially regulated genes after 10 nM testosterone treatment in affected and occipital terminal and intermediate hair follicles of male pattern androgenetic alopecia patients. The short term *ex vixo* treatment of affected (aff) and occipital (occ) terminal (t) and intermediate (i) hair follicles (HFs) of male pattern androgenetic alopecia (mpAGA) patients with 10 nM testosterone (T) revealed 39,582 differentially regulated genes in aff tHFs, 38,131 in aff iHFs, 20,044 in occ tHFs and 42,603 in occ iHFs. 16,301 genes are differentially regulated amongst all tested groups (red ellipse) as a consequence of T treatment. Displayed are also genes involved in physiological miniaturization (490, blue circle) and pathological miniaturization (1,175, black ellipse). Only genes with counts per million (CPM) value lower than 0.5 and fold changes (FCs) higher than 2 and lower than 0.5 have been taken into account for this evaluation.

Genes known to be involved in the core processes of HF biology were found to be differentially regulated in all comparisons of mpAGA Pts HFs after 10nM T treatment (see **Figure 3.15** red ellipse). The heatmap displayed in **Figure 3.16** shows once again, that occ HF show gene reugaltion as response to T treatment and could not be longer considered as “androgen-insensitive”.

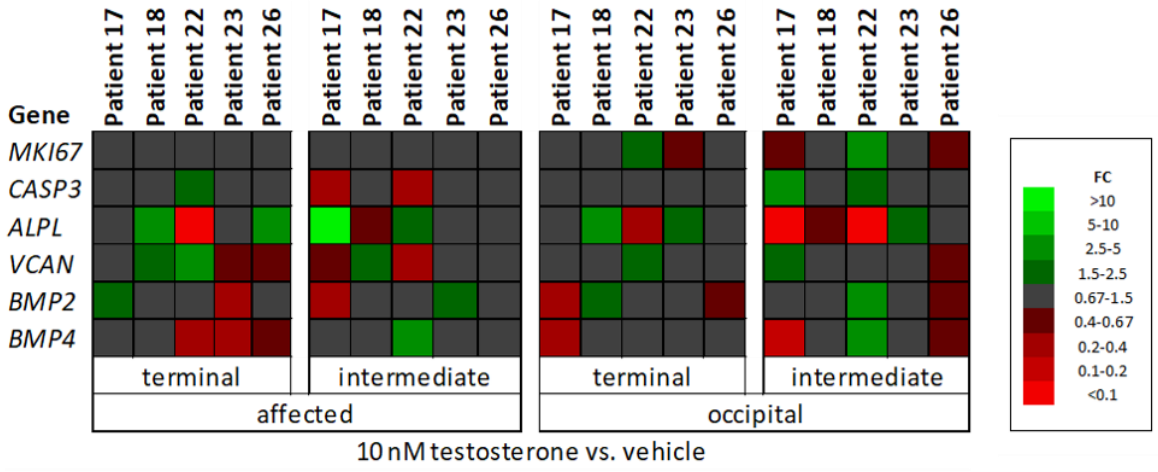

Figure 3.16 Heatmap showing the gene regulation after 10 nM testosterone treatment of hair follicle biology relevant genes in hair follicles from male pattern androgenetic alopecia patients. Genes known to be involved in hair follicle (HF) biology core processes are regulated by 10 nM testosterone (T) treatment. The regulation occurs independent from the physiological phase of the HF or from the location where the HF was harvested from. Shades of green are indicating an upregulation whilst shades of red are indicating a downregulation of the particular gene. Grey indicates no gene regulation. FC= fold change, MKI67= marker of proliferation Ki-67, Casp3= caspase 3, ALPL= alkaline phosphatase, VCAN= versican, BMP2= bone morphogenetic protein 2, BMP4= bone morphogenetic protein 4.

3.3 Identification of differentially regulated genes in different compartments of occipital and affected terminal and intermediate hair follicles of male pattern androgenetic alopecia patients

The characterization of the transcriptomic profile of t and iHFs deriving from the aff and the occ area of mpAGA scalp is necessary to understand the basics of the disease development and occurrence. Herefor, mpAGA Pts' HFs were extracted from the scalp (see **Chapter 2.1**), embedded in OCT and cryosectioned (see **Chapter 2.1.2**). After drying the sections completely, the determination between t and iHFs was performed according to the criteria mentioned in **Chapter 2.1.1.** After successful LCM performance (see **Chapter 2.2**), the RNA was isolated (see **Chapter 2.3.1**) and sent to the core facility of genomics (University of Münster) and to CeGaT (see **Chapter 2.4**). To perform the final bioinformatic analysis, a n= 3 per sequenced compartment is mandatory.

After the compartments have passed the necessary controls (see **Chapter 3.3.1**) only genes of their results with a CPM lower than 0.5 and a calculated FC lower than 0.5 or higher than 2 have been taken into account. To be even more restrictive, genes which only appear in 66.6 % of the Pts (for every analysed compartment separately) were bioinformatically analysed (see **Chapter 3.3.2**).

3.3.1 Principle component analysis of occipital and affected terminal and intermediate hair follicles' dermal papillae and dermal cups from male pattern androgenetic alopecia patients

To perform the *in situ* transcriptomic analysis of four particular compartments (DP, DC, HMg and HMpc), mpAGA Pts' HF compartments were isolated with the LCM technique and RNAseq was performed. Not for all samples RNAseq was successful, due to the very low obtained amount of RNA (20~200 pg). All samples where the library preparation was successful and RNAseq could have been performed are displayed in **Table 3.1.**

Table 3.1 Overview of all sequenced compartment samples with a successful library preparation. x= sequenced at CeGaT GmbH (Tübingen, Germany), o= sequenced in core facility of genomics (University of Münster, Germany). t= terminal, i= intermediate, DP= dermal papilla, DC= dermal cup, HMg= germinative hair matrix, HMpc= pre-cortical hair matrix

	Compatment															
	occipital								vertex							
Patient	tDP	tDC	tHMg	tHMpc	iDP	iDC	iHMg	iHMpc	tDP	tDC	tHMg	tHMpc	iDP	iDC	iHMg	iHMpc
2	x	o	o	o									o	o	o	o
5	o	o	o	o									o	o	o	o
8	x	x	x	x	x	x	x	x	x	x	x	x	x	x	x	x
9																
10	x			x	x			x	x			x	x			x
13	x	x	x	x	x	x	x	x		x	x	x	x	x	x	x
15	x	x	x	x	x	x	x	x			x		x	x	x	x
19	x			x	x			x	x			x	x			x
20	x			x	x			x	x			x	x			x
24	x	x		x	x	x	x		x	x	x	x	x	x		x
25	x	x	x	x	x		x	x	x	x	x	x	x	x	x	x

All the obtained raw data from successful sequenced compartments (see **Table 3.1**) was rlog transformed to minimize the variance of the means for genes with small counts and a PCA was performed. For this PCA (see **Figure 3.17**) all identified genes of all successfully sequenced compartments were taken into account. This analysis shows that samples of Pt2 and 5 (without tDP of Pt2) cluster together (red ellipse) and differ in PC 2 and PC 3 from all other samples (blue ellipse) (see **Figure 3.17**).

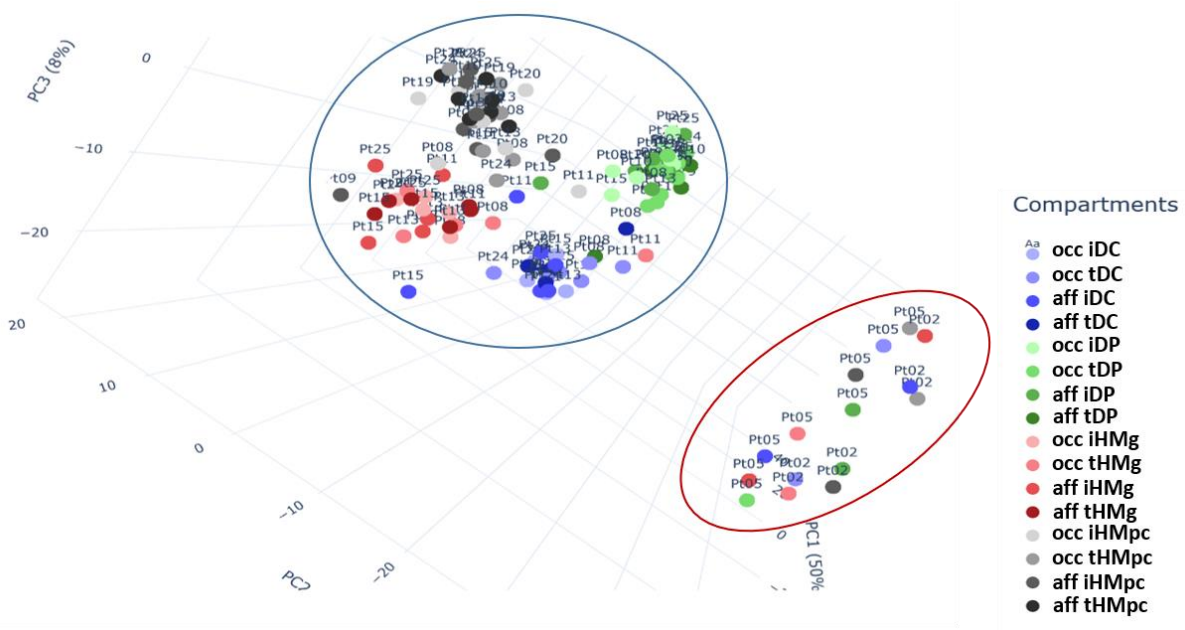

Figure 3.17 Principle component analysis of the RNA sequencing derived data from all fresh frozen male pattern androgenetic alopecia patients' hair follicles. The principle component analysis (PCA) of the RNA sequencing (RNAseq) data obtained from all fresh frozen hair follicles (HFs) reveals two major clusters. The left cluster (blue ellipse) contains all samples sequenced at CeGaT GmbH (Tübingen, Germany). The right cluster (red ellipse) contains all samples sequenced in the core facility of genomics (University of Münster, Germany). Pt= patient, i= intermediate, t= terminal, aff= affected, occ= occipital, DC= dermal cup, DP= dermal papilla, HMg= germinative hair matrix, HMpc= pre-cortical hair matrix.

For this reason, along with the fact that not all HF types were collected from Pt2 and Pt5, the samples sequenced at the University of Münster were omitted in the following evaluation. Having a closer look on the remaining samples of the blue encircled cluster in **Figure 3.17**, it is clearly visible that some samples are not grouping with the other samples deriving from the corresponding compartment (see red ellipses in **Figure 3.18**). These are namely aff iDC of Pt24, aff iHMpc of Pt9 and aff tDP of Pt8. These three samples have been also omitted from the pool of samples.

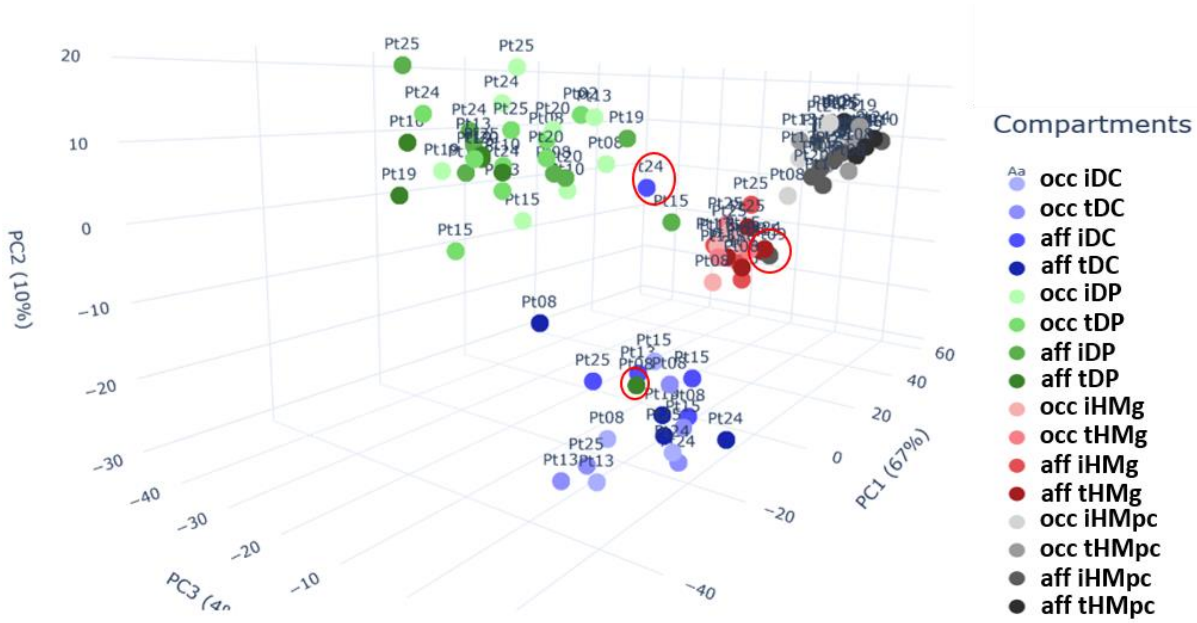

Figure 3.18 Principle component analysis of the RNA sequencing derived data from fresh frozen male pattern androgenetic alopecia patients' hair follicles sequenced at CeGaT GmbH. The principle component analysis (PCA) of the RNA sequencing (RNAseq) data obtained from fresh frozen hair follicles (HFs) reveals four major clusters. All here displayed results were sequenced at CeGaT GmbH (Tübingen, Germany). Four major clusters are visible, but the red marked samples are not grouping with the rest of the samples of their corresponding compartment. Pt= patient, i= intermediate, t= terminal, aff= affected, occ= occipital, DC= dermal cup, DP= dermal papilla, HMg= germinative hair matrix, HMpc= pre-cortical hair matrix.

After omitting the samples sequenced at the University of Münster (encircled red in **Figure 3.17**) and the three samples encircled in red in **Figure 3.18** which are not grouping with the other samples of their corresponding compartment, a last PCA was performed to observe the remaining samples (see **Figure 3.19**). This final PCA revealed that the selected samples for bioinformatics´ analysis cluster per compartments, importantly, this PCA confirms that mesenchymal (DP and DC) and epithelial (HMg and HMpc) compartments have a different transcriptome. Instead, no visible clusters appear for location where HFs were harvested (aff/ occ), or for the type of HFs (i/ t). This further highlights the importance of analysing the different HF compartments separately.

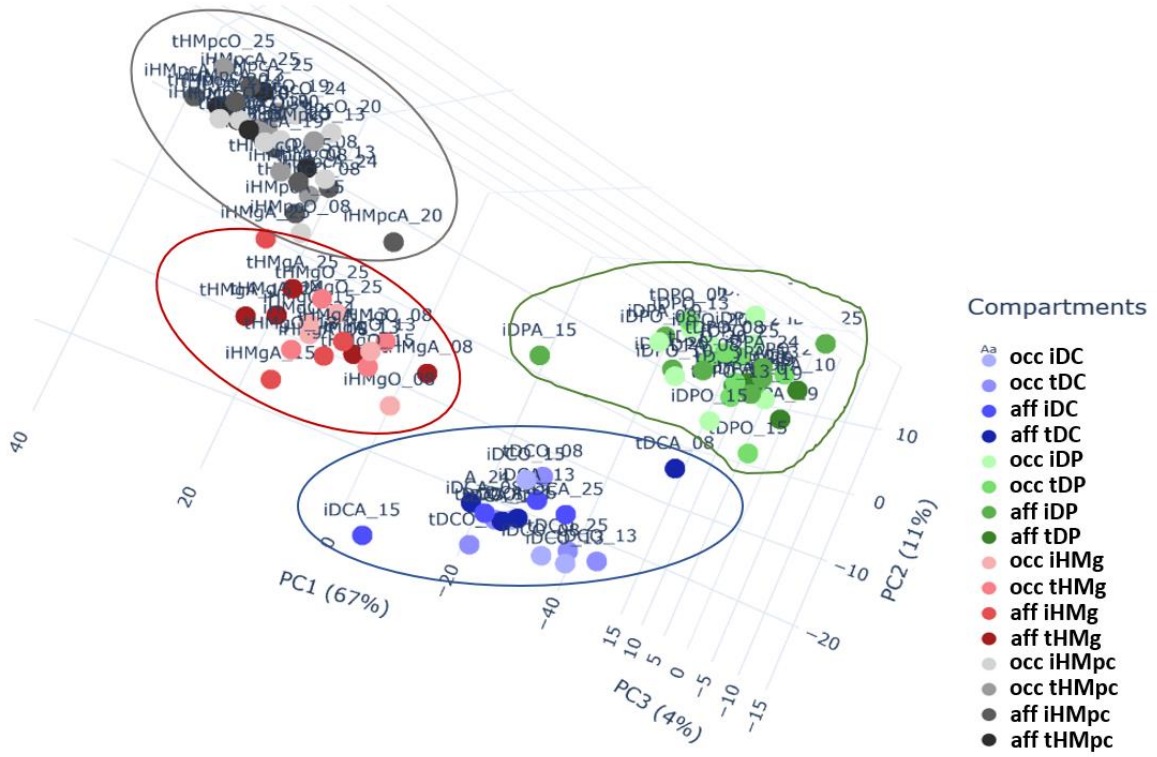

Figure 3.19 Final principle component analysis of the RNA sequencing derived data from fresh frozen male pattern androgenetic alopecia patients' hair follicles sequenced at CeGaT GmbH. The principle component analysis (PCA) of the RNA sequencing (RNAseq) data obtained from fresh frozen hair follicles (HFs) reveals four major clusters. All here displayed results were sequenced at CeGaT GmbH (Tübingen, Germany). Four major clusters are visible, dermal papilla (green ellipse), dermal cup (blue ellipse), germinative hair matrix (red ellipse) and pre-cortical hair matrix (grey ellipse). Samples cluster by compartment but no visible pattern for hair follicle location (affected/ occipital) or type (intermediate/ terminal) can be seen. Pt= patient, i= intermediate, t= terminal, aff= affected, occ= occipital, DC= dermal cup, DP= dermal papilla, HMg= germinative hair matrix, HMpc= pre-cortical hair matrix.

All samples displayed in **Figure 3.19** are summarized in **Table 3.2**.

Table 3.2 Final overview of laser capture mircrodissection-isolated samples for which RNAseq results passed all controls. t= terminal, i= intermediate, DP= dermal papilla, DC= dermal cup, HMg= germinative hair matrix, HMpc= pre-cortical hair matrix

	Compatment															
	occipital								vertex							
Patient	tDP	tDC	tHMg	tHMpc	iDP	iDC	iHMg	iHMpc	tDP	tDC	tHMg	tHMpc	iDP	iDC	iHMg	iHMpc
2	x															
8	x	x	x	x	x	x	x	x		x	x	x	x	x	x	x
10	x			x	x			x	x			x	x			x
13	x	x	x	x	x	x	x	x		x	x	x	x	x	x	x
15	x	x	x	x	x	x	x	x			x		x	x	x	x
19	x			x	x			x	x			x	x			x
20	x			x	x			x	x			x	x			x
24	x	x			x	x	x	x	x	x	x	x	x			x
25	x	x	x	x	x		x	x	x	x	x	x	x	x	x	x

3.3.2 Identification of differentially regulated genes in occipital and affected terminal and intermediate hair follicles' designated mesenchymal compartments

The identification of differentially regulated genes is a powerful method to get insights in the pathobiology of certain diseases. As it was previously shown in the literature, the pathobiology of mpAGA encloses gene expression changes in the whole HF but mostly in the mesenchymal compartments. For this reason, the obtained data from the RNAseq (see **Chapter 3.3**) was bioinformatically analysed. Due to the fact that most known processes in the HF take place or originate in the cells of the DP, the main focus was put on the genes which are differentially regulated in the DP and DC compartments of the mpAGA Pts' aff and occ t/ iHFs. Therefore, the obtained raw data was normalized and only genes with a CPM value lower than 0.5 and a calculated FC lower than 0.5 and higher than 2 were taken into account for the following evaluation. Furthermore, it was not distinguished if a gene transcript was found to be up regulated (CPM< 0.5, FC> 2) or down regulated (CPM< 0.5, FC< 0.5), because this *in situ* analysis needs to be seen as a snapshot of gene expression. To examine differentially related genes, certain comparisons need to be done. Here, differentially regulated genes of respective compartments from aff tHFs have been compared to them from occ tHFs which might give an idea of the "baseline" for either the physiological or the pathological miniaturization. Furthermore, differentially regulated genes of distinct HF compartments between occ iHFs and occ tHFs have been compared, what represents the differentially regulated genes involved in the physiological miniaturization process. Further, differentially regulated genes were compared between aff iHF compartments and aff tHF compartments, what is understood as transcriptomic changes during pathological miniaturization. Lastly, genes which are differentially regulated between aff iHF compartments occ iHF compartments have been compared, what shows the transcriptomic differences between both kinds of miniaturized HFs. For the comparison between aff tDP and occ tDP a total number of 199,963 differentially regulated genes were found while for the comparison between aff iDP and occ iDP 30,230 genes were found to be differentially regulated. The physiological miniaturization comparison revealed 25,260 differentially regulated genes, while pathological miniaturization scored with a total number of 21,038 differentially regulated genes. Surprisingly, a higher number of differentially regulated genes was found in the DC compared to the DP in all comparisons (see **Figure 3.20**). In the DC there were 43,004 differentially regulated genes for the "baseline" of miniaturization comparison, 43,440 for the physiological miniaturization, 33,315 for the pathological miniaturization and 42,893 differentially regulated genes examined between both kinds of miniaturized HFs.

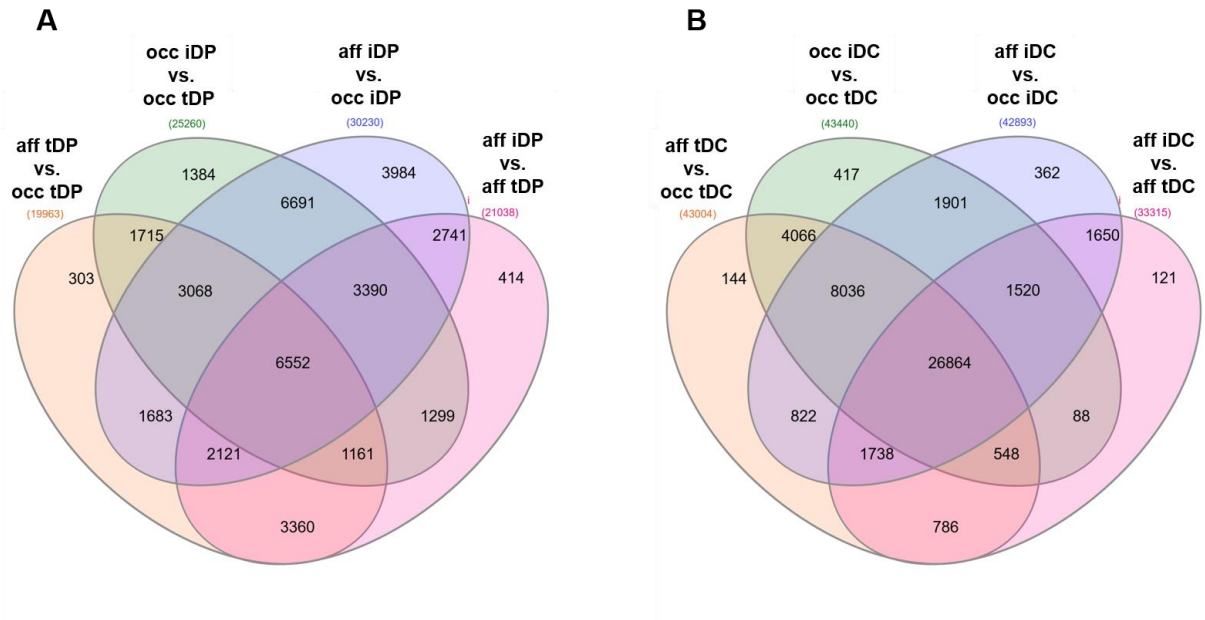

Figure 3.20 Differentially regulated genes in different comparisons of affected and occipital terminal and intermediate hair follicles of male pattern androgenetic alopecia patients. **A:** Differentially regulated genes in the dermal papilla (DP) of affected (aff) and occipital (occ) intermediate (i) and terminal (t) hair follicles (HFs) of male pattern androgenetic alopecia (mpAGA) patients (Pts) in different comparisons. Aff tDP versus occ tDP revealed 19,963 differentially regulated genes which represent the different "baselines" of either pathological or physiological miniaturization. Occ iDP versus occ tDP represents the genes involved in physiological miniaturization and revealed 25,260 differentially regulated genes. Aff iDP versus occ iDP revealed 30,230 differentially regulated genes which are found in iHFs' DPs after both ways of miniaturization. Lastly, aff iDP versus aff tDP represents the genes involved in pathological miniaturization and revealed 25,260 differentially regulated genes. Only genes with a counts per million (CPM) value lower than 0.5 and fold changes (FCs) higher than 2 and lower than 0.5 have been taken into account for this evaluation. **B:** Differentially regulated genes in the dermal cup (DC) of aff and occ i/tHFs of mpAGA Pts in different comparisons. Aff tDC versus occ tDC revealed 43,004 differentially regulated genes which represent the different "baselines" of either pathological or physiological miniaturization. Occ iDC versus occ tDC represents the genes involved in physiological miniaturization and revealed 43,440 differentially regulated genes. Aff iDC versus occ iDC revealed 42,893 differentially regulated genes which are found in iHFs' DPs after both ways of miniaturization. Lastly, aff iDC versus aff tDC represents the genes involved in pathological miniaturization and revealed 33,315 differentially regulated genes. Only genes with a counts per million (CPM) value lower than 0.5 and fold changes (FCs) higher than 2 and lower than 0.5 have been taken into account for this evaluation.

Due to the fact, that for both, DP and DC such a high number of differentially regulated genes have been identified, it was decided to implement another, more restrictive cut-off. So only genes from the previous shown comparisons (see **Figure 3.20**) which appear differentially regulated in minimum of 66.6 % of the Pts were taken into account for further evaluation (see **Figure 3.21**). The final evaluation of differentially regulated genes in the DP and the DC of mpAGA Pts was started from a clearly reduced number of genes.

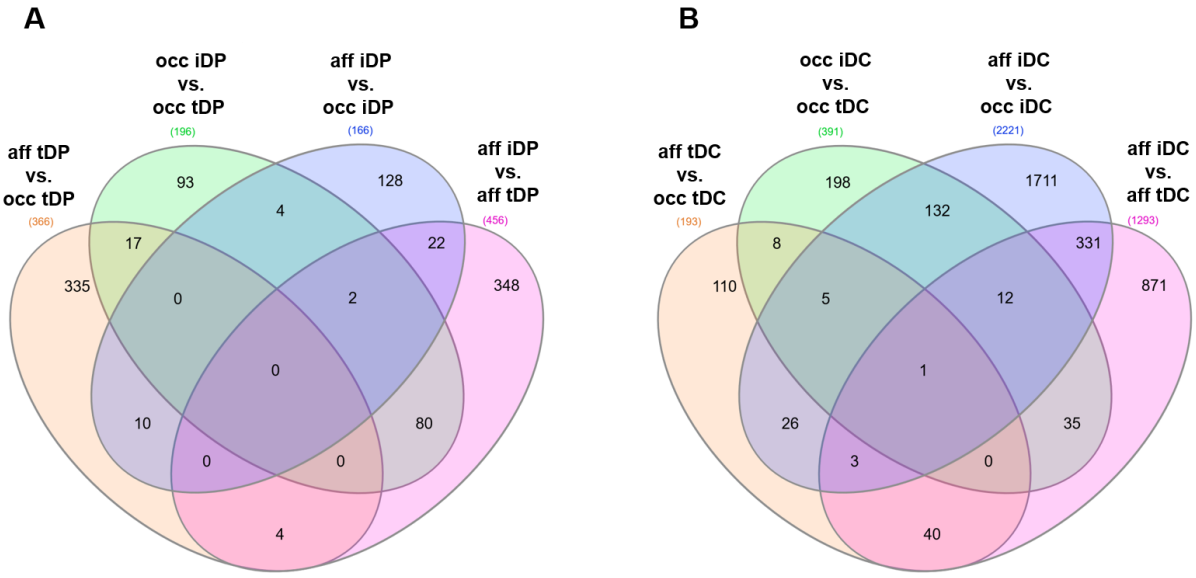

Figure 3.21 Final number of differentially regulated genes in different comparisons of affected and occipital terminal and intermediate hair follicles of male pattern androgenetic alopecia patients. **A:** Differentially regulated genes in the dermal papilla (DP) of affected (aff) and occipital (occ) intermediate (i) and terminal (t) hair follicles (HFs) of male pattern androgenetic alopecia (mpAGA) patients (Pts) in different comparisons. Aff tDP versus occ tDP revealed 366 differentially regulated genes which represent the different "baselines" of either pathological or physiological miniaturization. Occ iDP versus occ tDP represents the genes involved in physiological miniaturization and revealed 196 differentially regulated genes. Aff iDP versus occ iDP revealed 166 differentially regulated genes which are found in iHFs' DPs after both ways of miniaturization. Lastly, aff iDP versus aff tDP represents the genes involved in pathological miniaturization and revealed 456 differentially regulated genes. Only genes with counts per million (CPM) value lower than 0.5 and fold changes (FCs) higher than 2 and lower than 0.5 have been taken into account for this evaluation. **B:** Differentially regulated genes in the dermal cup (DC) of aff and occ i/ tHFs of mpAGA Pts in different comparisons. Aff tDC versus occ tDC revealed 193 differentially regulated genes which represent the different "baselines" of either pathological or physiological miniaturization. Occ iDC versus occ tDC represents the genes involved in physiological miniaturization and revealed 391 differentially regulated genes. Aff iDC versus occ iDC revealed 2,221 differentially regulated genes which are found in iHFs' DPs after both ways of miniaturization. Lastly, aff iDC versus aff tDC represents the genes involved in pathological miniaturization and revealed 1,293 differentially regulated genes. Only genes with counts per million (CPM) value lower than 0.5 and fold changes (FCs) higher than 2 and lower than 0.5 have been taken into account for this evaluation.

3.4 Selection of possible male pattern androgenetic alopecia target genes

The selection of potential target genes was based on the comparison of the differentially regulated genes shown in **Chapter 3.3.2** with the already published literature. Therefore, genes affiliated with signaling pathways which are potentially involved in HF physiology, HC, hair loss and androgen signaling where investigated. The finally picked genes for further investigation, differentially regulated in the DP and/ or the DC of at least 66.6 % of all analysed Pts, were namely *ALDH1A2*, *TGFβ1I1* and *SYT1*. All three of them were counterchecked in the data retrieved from the transcriptomic analysis of 10 nM T treated HFs (see **Chapter 3.3.1**) to see if these genes are T responsive.

3.4.1 Validation of aldehyde dehydrogenase 1 family member A2 as potential male pattern androgenetic alopecia target gene

ALDH1A2 is an enzyme which is known to convert retinaldehyde into retinoic acid [213,214] and cutaneous retinoic acid was shown to determine HF development and HF down growth in mice [215]. Moreover, already published results of a combined treatment of minoxidil together with all-trans-retinoic acid (tretinoin) suggest positive effects in mpAGA Pts [216–218]. High levels of the *ALDH1A2* gene were found in the *in situ* RNAseq data for the DC of aff iHFs, obtained from LCM derived mpAGA Pts' HFs (see **Figure 3.22**).

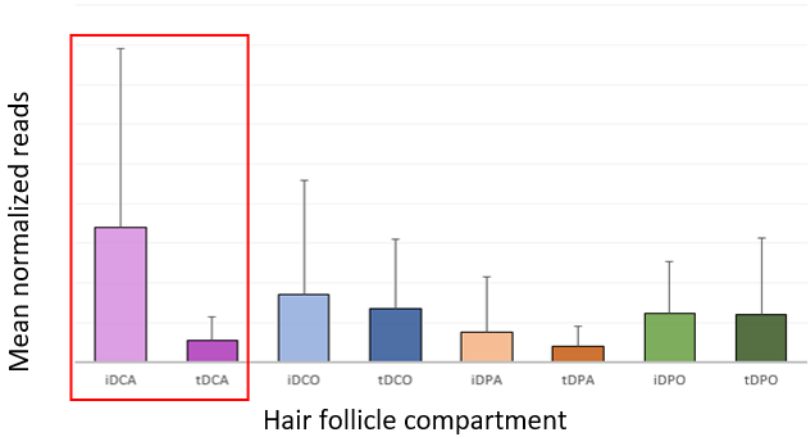

Figure 3.22 Validation of the aldehyde dehydrogenase 1 family member A2 gene expression in selected compartments of male pattern androgenetic alopecia patients' hair follicles. Laser capture microdissection obtained *in situ* data revealed high gene expression of aldehyde dehydrogenase 1 family member A2 in the intermediate dermal cup of hair follicles from the affected scalp of male pattern androgenetic alopecia patients. i= intermediate, t= terminal, DC= dermal cup, DP= dermal papilla, A= affected, O= occipital.

To confirm the localized gene expression of *ALDH1A2* and *TGFβ1I1*, RNA *in situ* hybridization was performed (see **Chapter 3.4.2**) in occ tHFs from healthy volunteers. Most prominently mRNA expression of *ALDH1A2* could have been detected in the DP, DC, IRS and HMg (see **Figure 3.23**, displayed by red dots and indicated exemplarily by red arrows) as expected from the data obtained from RNAseq (see **Figure 3.22**). Furthermore, *in situ* hybridization was also performed in occ and aff t/ iHFs from mpAGA Pts. The localization of *ALDH1A2* mRNA was similar to the previous localization in healthy volunteers' HFs, but the expression was stronger. As expected from the RNAseq results a higher expression was seen in aff HFs compared to occ HFs (see **Figure 3.24**, displayed by red dots).

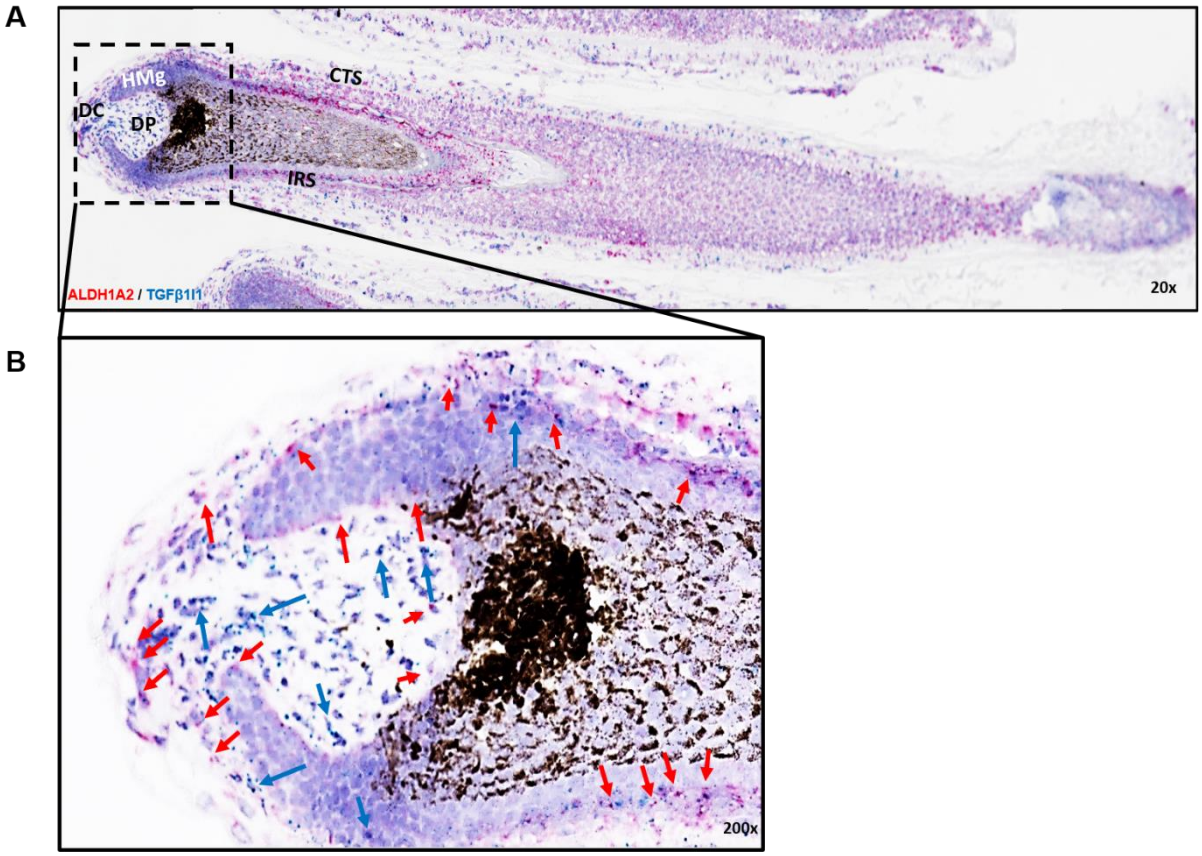

Figure 3.23 mRNA expression of aldehyde dehydrogenase 1 family member A2 and transforming growth factor beta-1-induced transcript 1 in terminal occipital hair follicles by *in situ* hybridization. A: *In situ* hybridization of aldehyde dehydrogenase 1 family member A2 (*ALDH1A2*) and transforming growth factor beta-1-induced transcript 1 (*TGFβ1I1*) performed in occipital terminal hair follicles of healthy volunteers. Magnification 20x. **B**: mRNA expression of *ALDH1A2* is most prominently detected in the dermal cup (DC), the dermal papilla (DP), the inner root sheath (IRS) and the germinative hair matrix (HMg), and is visualized by red dots. *ALDH1A2* expression is exemplarily indicated by red arrows. mRNA expression of *TGFβ1I1* is most prominently detected in the DP, the DC, the IRS and the connective tissue sheath and is visualized by blue dots. Magnification 200x .DP= dermal papilla, DC= dermal cup, HMg= germinative hair matrix, IRS= inner root sheath, CTS= connective tissue sheath.

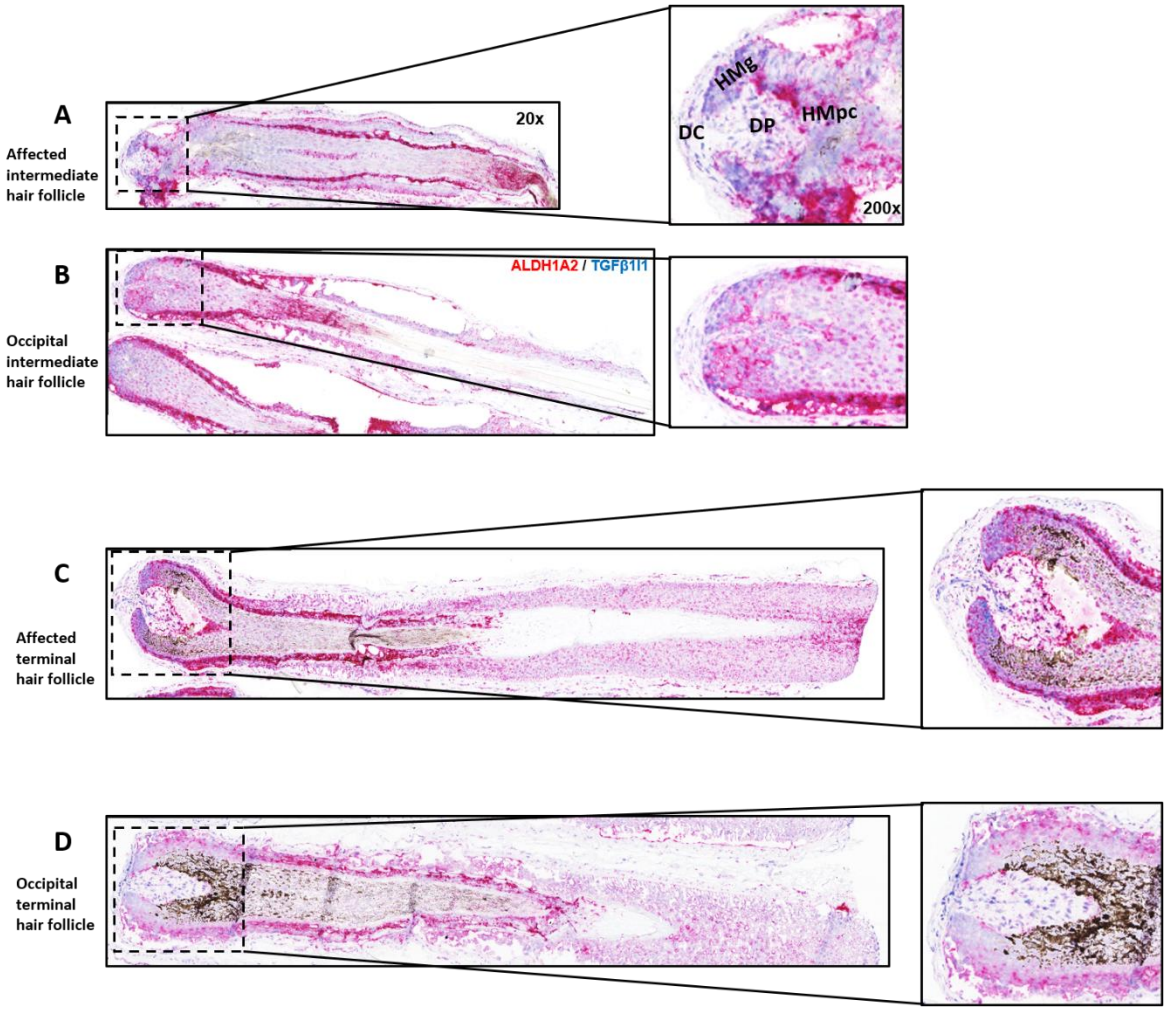

Figure 3.24 mRNA expression of aldehyde dehydrogenase 1 family member A2 and transforming growth factor beta-1-induced transcript 1 in occipital and affected terminal and intermediate hair follicles from male pattern androgenetic alopecia patients by *in situ* hybridization. A: *In situ* hybridization of aldehyde dehydrogenase 1 family member A2 (*ALDH1A2*) and transforming growth beta-1-induced transcript 1 in affected (aff) intermediate (i) hair follicles (HFs) of male pattern androgenetic alopecia (mpAGA) patients (Pts). **B**: *In situ* hybridization of *ALDH1A2* and *TGFβ1I1* in occipital (occ) iHFs of mpAGA Pts. **C:** *In situ* hybridization of *ALDH1A2* and *TGFβ1I1* in aff terminal (t) HFs of mpAGA Pts. **D**: *In situ* hybridization of *ALDH1A2* and *TGFβ1I1* in aff tHFs of mpAGA Pts. mRNA expression of *ALDH1A2* is most prominently detected in the dermal cup (DC), the dermal papilla (DP), the inner root sheat (IRS) and the germinative hair matrix (HMg), and is visualized by red dots. mRNA expression of TGFβ1I1 is most prominently detected in the DP, the DC, the IRS and the connective tissue sheath (CTS) and is visualized by blue dots. DP= dermal papilla, DC= dermal cup, HMg= germinative hair matrix, HMpc= germinative hair matrix.

Amongst the genes which are involved in the pathological miniaturization (comparison between aff iHFs compartments and aff tHFs compartments), *ALDH1A2* was found to be differentially regulated in all three validated Pts' (Pt8, Pt13 and pt25) DCs according to the chosen criteria for upregulated genes (FC > 2 and CPM <0.5) and downregulated genes (FC < 0.5 and CPM < 0.5) (see **Table 3.3**). A list of genes exclusively involved in the pathological miniaturization was used. Therefore, all genes found to be differentially regulated in physiological miniaturization (occ iHFs compartments versus occ tHFs compartments) and all genes which were found to be commonly differentially regulated between aff tHFs and occ tHFs were excluded from this list of genes. In addition, it was found to be differentially regulated after 10 nM T treatment in aff tHFs, aff iHFs and occ iHFs (see **Table 3.3**). *ALDH1A2* is suggested to be a T responsive gene.

Table 3.3 Gene expression results obtained from RNA sequencing after Laser capture micro dissection of fresh frozen hair follicle compartments and after 48 hours *ex vivo* culture with 10 nM testosterone of male pattern androgenetic alopecia patients hair follicles. Aldehyde dehydrogenase 1 family member A2 (*ALDH1A2*) was found to be differentially regulated amongst all for the comparison of the dermal cup (DC) successfully sequenced male pattern androgenetic alopecia patients (Pts) (Pt 8, Pt 13 and Pt 25). It was showing up in the list of genes retrieved from the analysis of genes exclusively involved in the pathological miniaturization. Moreover, *ALDH1A2* seems to be a testosterone (T) responsive gene, because it was found to be upregulated in affected (aff) terminal (t) hair follicles (HFs), aff intermediate (i) HFs and occipital (occ) iHFs after 10 nM T treatment *ex vivo*. Green background indicates a fold change (FC) > than 2 (upregulation) and red background indicated a FC < than 0.5 (downregulation) of the gene. ALDH1A2= aldehyde dehydrogenase 1 family member A2, FC= fold change, DC= dermal cup, aff= affected, occ= occipital, i= intermediate, t= terminal, Pt= patient, T= testosterone.

gene	FC of gene expression in situ in the DC of aff i compared to ver tHFs			FC of gene expression after 10 nM T treatment			
	Pt8	Pt13	Pt25	aff t	aff i	occ t	occ i
ALDH1A2	38,4621993	0,36017392	7,46562429	0,444678	4,111833	1,261638	0,121512

In line with the previous shown RNAseq obtained data is the detected protein expression of ALDH1A2 in occ and aff tHF and iHFs from mpAGA Pts. Its protein expression was found to be significantly higher in the DC of aff iHFs compared to aff tHFs of n= 3 mpAGA Pts' (namely Pt31, Pt33 and Pt36) fresh frozen HFs (see **Figure 3.25**). No changes in ALDH1A2 protein expression were found in the DP amongst all analysed HF types (see **Figure 3.25**). For this investigation mpAGA Pts' HFs were frozen in OCT after extraction and prepared for immunofluorescence staining (see **Chapter 2.1.3**). For detailed information of the staining procedure, please refer to **Chapter 2.6**. For the evaluation, the fluorescence expression intensity of the DP and the DC was measured and the FC was calculated. The value for occ tHFs was normalized to 1 for a more reliable comparison.

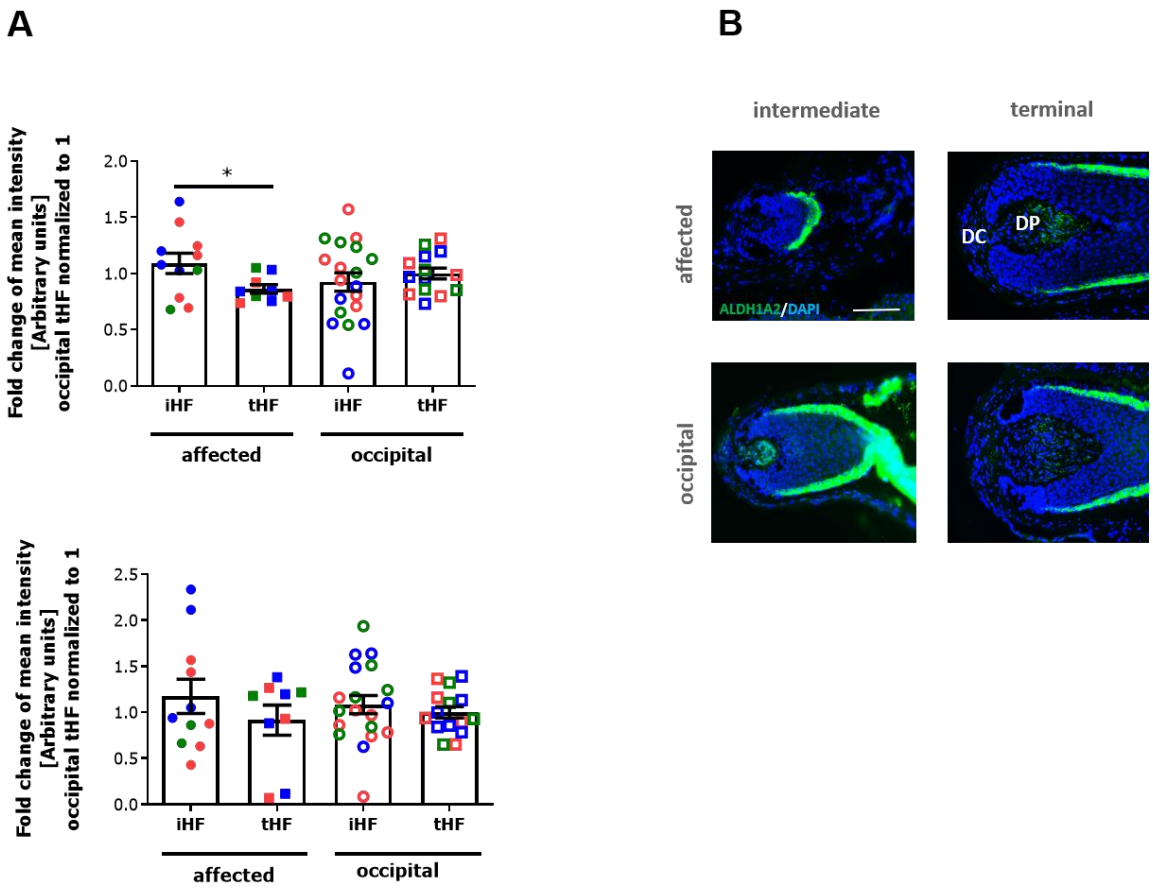

Figure 3.25 Aldehyde dehydrogenase 1 family member A2 protein expression in affected and occipital terminal and intermediate hair follicles of male pattern androgenetic alopecia patients. A: Graphs showing the fold change of fluorescence mean intensity in arbitrary units where the value for occipital (occ) terminal (t) hair follicles (HFs) was normalized to 1 for the expression of aldehyde dehydrogenase 1 family member A2 (ALDH1A2). A significant higher expression was detected in affected (aff) intermediate (i) HFs compared to aff tHFs in the dermal cup (DC). For the expression of ALDH1A2 in the dermal papilla (DP) no changes could have been detected. Mean±SEM, n= 9-19 HFs/ group from each donor, Graph Pad Prism 9, D'Agostino & Pearson omnibus normality test, data follows Gaussian distribution, ns; students' t-test *p<0.05. Pt31 displayed in blue, Pt 36 displayed in red, Pt33 displayed in green. **B:** Example pictures of the immunofluorescence staining for ALDH1A2 in aff and occ t/ iHFs of male pattern androgenetic alopecia (mpAGA) patients. The displayed scale bar indicates 100 µm. ALDH1A2= aldehyde dehydrogenase 1 family member A2, i= intermediate, t= terminal, HF= hair follicles, DAPI= 4′,6-Diamidin-2-phenylindol, DP= dermal papilla, DC= dermal cup.

3.4.2 Validation of transforming growth factor beta-1-induced transcript 1 as potential male pattern androgenetic alopecia target gene

In the human skin, TGFβ1I1 protein is mostly present in mesenchymal components including DPCs. The expression of TGFβ1I1 increases during cellular senescence and decreases during immortalization. Furthermore, its forced expression induces growth retardation and senescence cell-like morphology in fibroblasts [219]. It has been shown that the AR functions together with coactivators to activate target genes [220,221]. In addition, TGFβ1I1 is known to function as such an AR coactivator [222] and also to enhance androgen sensitivity in DPCs from the balding scalp of mpAGA Pts [223]. High levels of the *TGFβ1I1* gene were found in the *in situ* RNAseq data from LCM derived mpAGA Pts' HFs in all mesenchymal compartments (DP and DC), regardless to their scalp location or their physiological state (see **Figure 3.26**).

To confirm the obtained RNAseq results, *in situ* hybridization of *TGFβ1I1* together with *ALDH1A2* (see **Chapter 3.4.1**) was performed. mRNA expression was first checked in occ tHFs from healthy volunteers (see **Figure 3.23**, displayed by blue dots and exemplarily indicated by blue arrows) and also in occ and aff t/ iHFs deriving from mpAGA Pts (see **Figure 3.24**, displayed by blue dots). *TGFβ1I1* mRNA is most prominently expressed in mesenchymal compartments as namely the DP, DC and the CTS, but it was also localized in the HMg, HMpc and the IRS (see **Figure 3.23** and **Figure 3.24**). The expression in the mesenchymal compartment was expected according to the RNAseq results (see **Figure 3.26**).

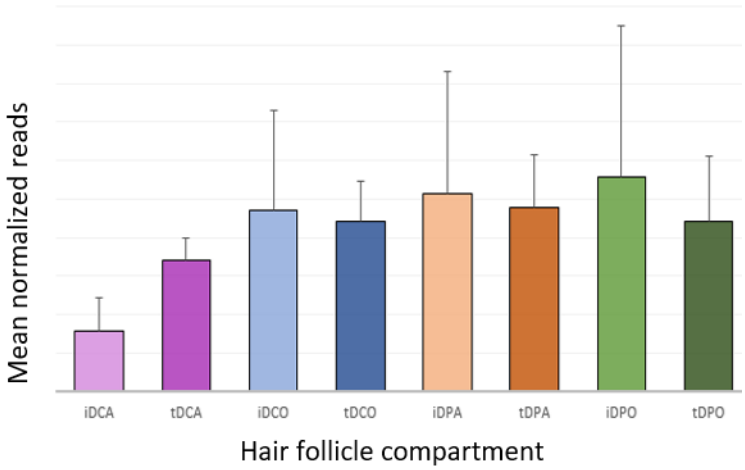

Figure 3.26 Validation of the transforming growth factor beta-1-induced transcript 1 gene expression in selected compartments of male pattern androgenetic alopecia patients' hair follicles. Laser capture microdissection obtained *in situ* data revealed high gene expression of transforming growth factor beta-1-induced transcript 1 in all mesenchymal compartments, namely dermal papilla and dermal cup of hair follicles from male pattern androgenetic alopecia patients, regardless of their scalp location or their physiological state. i= intermediate, t= terminal, DC= dermal cup, DP= dermal papilla, HMg= germinative hair matrix, HMpc= pre-cortical hair matrix, A= affected, O= occipital.

Table 3.4 Gene expression results obtained from RNA sequencing after laser capture microdissection of fresh frozen hair follicle compartments and after 48 hours *ex vivo* culture with 10 nM testosterone of male pattern androgenetic alopecia patients' hair follicles. A: Transforming growth factor beta-1-induced transcript 1 (*TGFβ1I1*) was found to be downregulated in two out of three for the comparison of the dermal cup (DC) successfully sequenced male pattern androgenetic alopecia (mpAGA) patients (Pts) (Pt 13 and Pt 15). It was showing up in the list of genes retrieved from the analysis of genes differentially regulated in the "pathological" miniaturized hair follicles (HFs). Moreover, *TGFβ1I1* seems not to be responsive to 10 nM testosterone (T) *ex vivo*. **B**: *TGFβ1I1* was found to be downregulated in three out of four for the comparison of the DC successfully sequenced mpAGA Pts (Pt 13, Pt 15 and Pt25). It was showing up in the list of genes retrieved from the analysis of genes differentially regulated in affected intermediate HFs versus occipital terminal HFs. Red background indicates a FC < than 0.5 (downregulation) of the gene. TGFβ1I1= transforming growth factor beta-1-induced transcript 1, FC= fold change, DC= dermal cup, aff= affected, occ= occipital, i= intermediate, t= terminal, Pt= patient, T= testosterone.

A

gene	FC of gene expression *in situ* in the DC of aff i compared to occ iHFs			FC of gene expression after 10 nM T treatment			
	Pt8	Pt13	Pt15	aff t	aff i	occ t	occ i
TGFβ1I1	0,85809223	0,31794591	0,44824925	1,15533806	0,95954047	1,09714507	1,00729405

B

gene	FC of gene expression *in situ* in the DC of aff i compared to occ tHFs				FC of gene expression after 10 nM T treatment			
	Pt8	Pt13	Pt15	Pt25	aff t	aff i	occ t	occ i
TGFβ1I1	0,66182511	0,32409646	0,33902294	0,22112785	1,15533806	0,95954047	1,09714507	1,00729405

The *TGFβ1I1* gene was shown to be differentially regulated in "pathological" miniaturized HFs (comparison between aff iHFs compartments with occ iHFs compartments as well as in the comparison between aff iHFs with occ tHFs compartments). *TGFβ1I1* was found to be differentially regulated in two out of three (aff iHFs versus occ iHFs, see **Table 3.4 A**) and three out of four (aff iHFs versus occ tHFs, see **Table 3.4 B**) validated mpAGA Pts' (Pt8, Pt13, Pt15 and Pt25) DCs according to the chosen criteria for downregulated genes (FC < 0.5 and CPM < 0.5) (see **Table 3.4**). Therefore, a list of genes exclusively displaying differentially regulated genes in "pathological" miniaturized HFs have been used. *TGFβ1I1* was not found to be responsive to a short-term 10 nM T treatment (see **Table 3.4**).

For the protein expression data of TGFβ1I1 a strong inter-donor variation was detected. Pooling the results for protein expression together from three mpAGA Pts (namely Pt31, Pt33 and Pt36), no difference in the expression intensity was detected between occ and aff t/ iHFs DPs or DCs (see **Figure 3.27 A**). By eliminating the results of protein expression intensity from Pt31, the obtained results confirm the higher expression of TGFβ1I1 in the DC of aff tHFs compared to aff iHFs. In these Pts (Pt33 and Pt36), comparable differential expression was found also in the DP at protein level (see **Figure 3.27 B**). The obtained results for the protein expression are not in line with the detected mRNA expression of *TGFβ1I1*, where a slightly higher expression was found in the aff iDP compared to the aff tDP and the expression in occ HF compartments (t/ i) was shown to be higher than in compartments from aff HFs. For the protein expression intensity detection, mpAGA Pts' HFs were frozen in OCT after extraction and prepared for immunofluorescence staining (see **Chapter 2.1.3**). For detailed information

of the staining procedure, please refer to **Chapter 2.6**. For the evaluation, the fluorescence expression intensity of the DP and the DC was measured and the FC was calculated. The value for occ tHFs was normalized to 1 for a more reliable comparison.

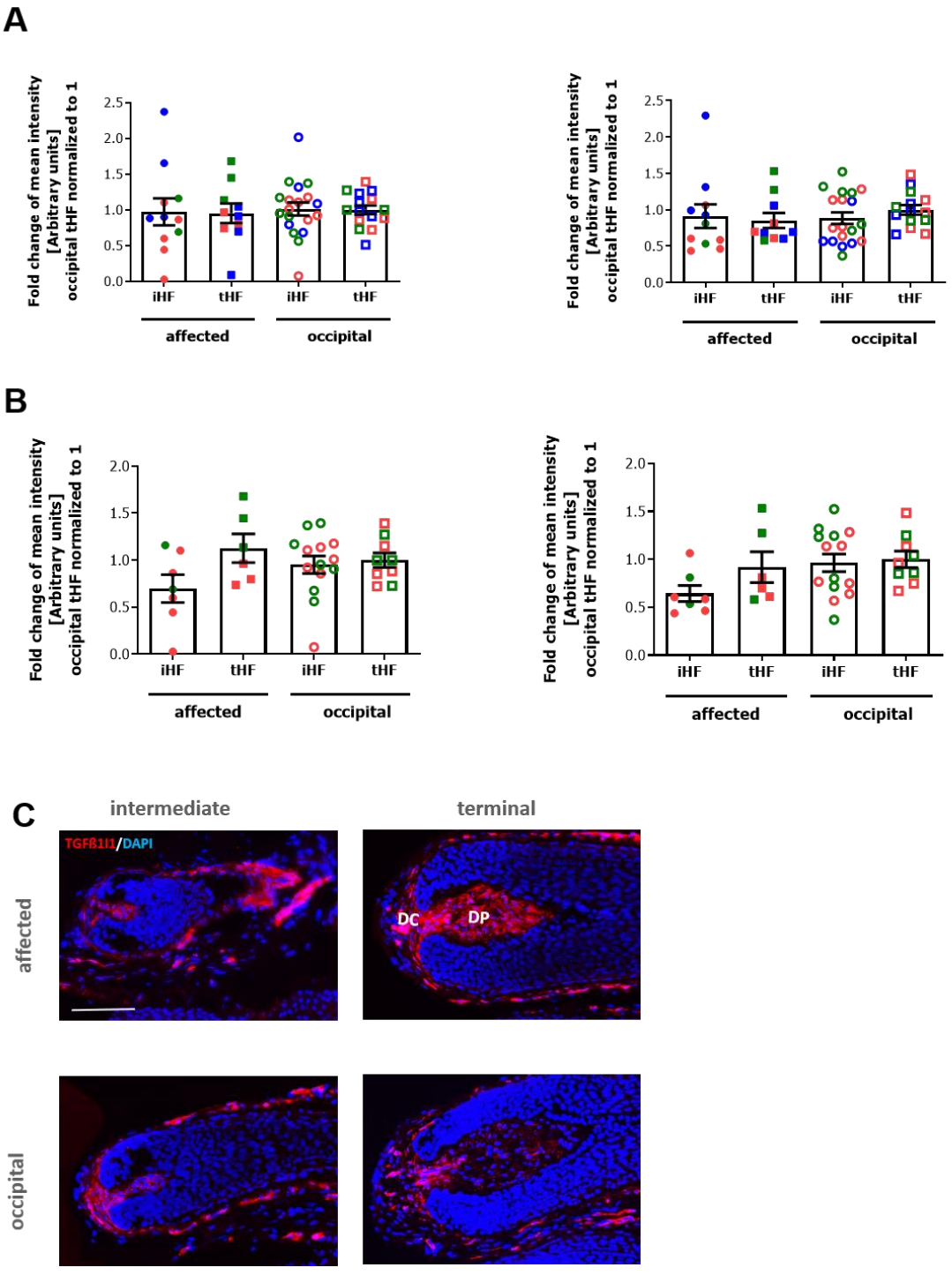

Figure 3.27 Transforming growth factor beta-1-induced transcript 1 protein expression in affected and occipital terminal and intermediate hair follicles of male pattern androgenetic alopecia patients. A: Displayed results for the pooled evaluation of all three analyzed patients (Pts) (patient 31, patient 33 and patient 36). Graphs showing the fold change (FC) of fluorescence mean intensity in arbitrary units where the value for occipital (occ) terminal (t) hair follicles (HFs) was normalized to 1 for the expression of transforming growth factor beta-1-induced transcript 1 (TGFβ1I1). No change in expression intensity was detected. **B:** Displayed results for the pooled evaluation of only the two Pts showing the same tendency in their results (patient 33 and patient 36). Graphs showing the FC of fluorescence mean intensity in arbitrary units where the value for occ tHFs was normalized to 1 for the expression of TGFβ1I1. A tendential higher expression was detected in affected (aff) terminal (t) HFs compared to aff intermediate (i) HFs in the dermal cup and the dermal papilla. Mean±SEM, n= 6-19 HFs/ group from each donor, Graph Pad Prism 9, D'Agostino & Pearson omnibus normality test, data follows Gaussian distribution; students' t-test ns. Pt31 displayed in blue, Pt 36 displayed in red, Pt33 displayed in green**. C:** Example pictures of the immunofluorescence staining for TGFβ1I1 in aff and occ t/ iHFs of male pattern androgenetic alopecia Pts. The displayed scale bar indicates 100 µm. TGFβ1I1= transforming growth factor beta-1-induced transcript 1, i= intermediate, t= terminal, HF= hair follicles, DAPI= 4′,6-Diamidin-2-phenylindol; DC= dermal cup, DP= dermal papilla.

3.4.3 Validation of synaptotagmin 1 as potential male pattern androgenetic alopecia target gene

In the human body, SYT was shown to be mostly expressed in the brain, where it is known to mediate calcium-dependent release of neurotransmitters and modulates synaptic vesicle endocytosis [194]. It was demonstrated, that SYT1 is required for stress induced fibroblast growth factor 1 (FGF1) and interleukin 1α (IL1α) release [224,225]. Moreover, it was shown, that fibroblasts respond to FGF1 treatment with limited proliferation and tend to express a large amount of cell cycle inhibitors [224,225]. It was suggested that SYT1 is indirectly involved the inhibition of proliferation and cell cycle.

On gene level, *SYT1* was found in the retrieved *in situ* RNAseq data to be mostly expressed in the DP of mpAGA HFs. Regardless to their scalp location, the level of *SYT1* seems to be higher in iDPs as compared to tDPs (see **Figure 3.28**).

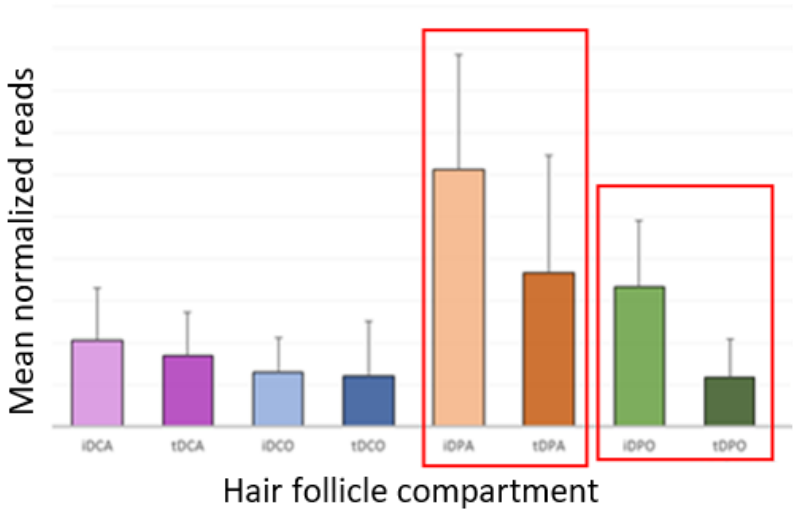

Figure 3.28 Validation of the synaptotagmin 1 gene expression in selected compartments of male pattern androgenetic alopecia patients hair follicles. Laser capture microdissection obtained *in situ* data revealed high levels of gene expression of synaptotagmin 1 in the dermal papilla of hair follicles from male pattern androgenetic alopecia patients, regardless to their scalp location. i= intermediate, t= terminal, DC= dermal cup, DP= dermal papilla, HMg= germinative hair matrix, HMpc= pre-cortical hair matrix, A= affected, O= occipital.

To confirm the obtained RNAseq results, *in situ* hybridization of *SYT1* (blue dots) (see **Chapter 3.4.1**) was performed. mRNA expression was first checked in occ tHFs from healthy volunteers (see **Figure 3.29**, *SYT1* displayed by blue dots, exemplarily indicated by blue arrows) and also in occ and aff t/ iHFs deriving from mpAGA Pts (see **Figure 3.30**, *SYT1* displayed by blue dots, exemplarily indicated by blue arrows).

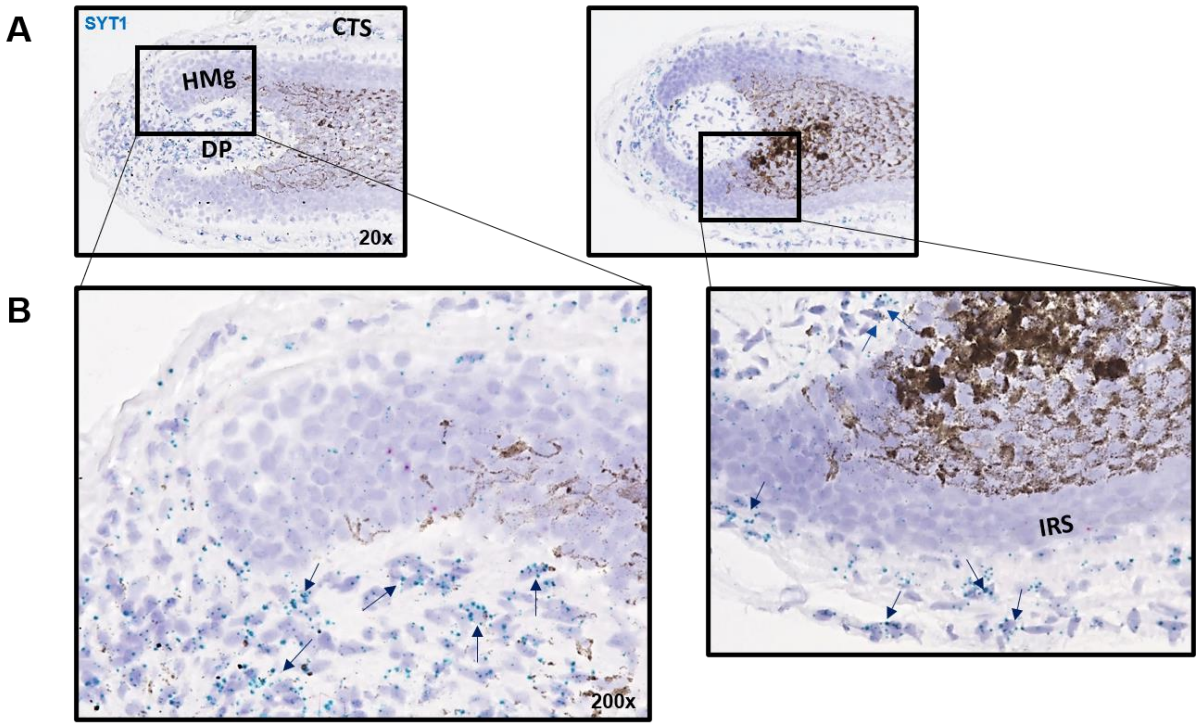

Figure 3.29 mRNA expression of synaptotagmin 1 in terminal occipital hair follicles by *in situ* hybridization. A: *In situ* hybridization of synaptotagmin 1 (*SYT1*) performed in occipital terminal hair follicles of healthy volunteers. Magnification 20x. **B:** mRNA expression of *SYT1* is most prominently detected in the dermal papilla and is visualized by blue dots and exemplarily indicated by blue arrows. DP= dermal papilla, HMg= germinative hair matrix, IRS= inner root sheath, CTS= connective tissue sheath, SYT1= synaptotagmin 1.

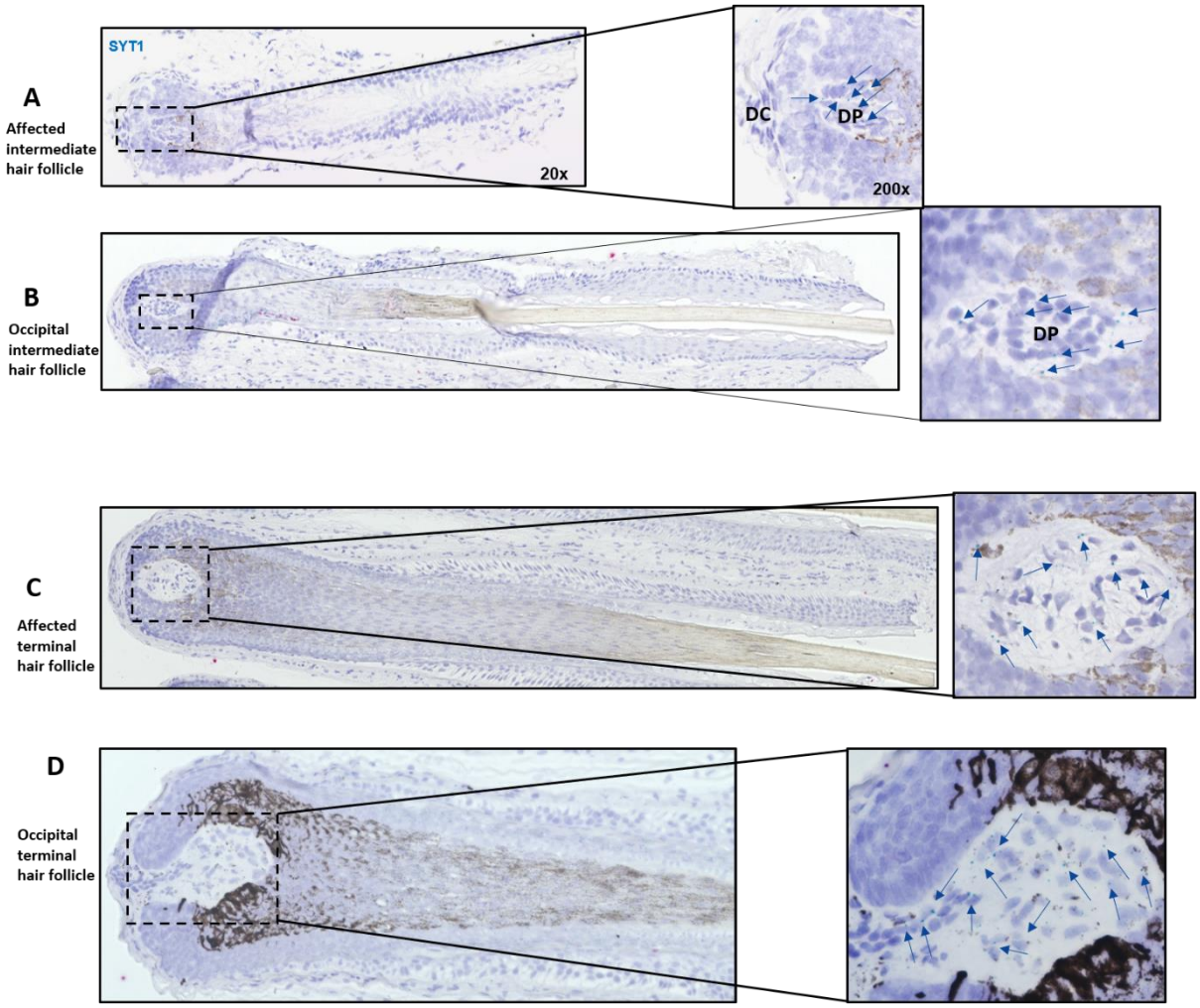

Figure 3.30 mRNA expression of synaptotagmin 1 in occipital and affected terminal and intermediate hair follicles from male pattern androgenetic alopecia patients by *in situ* hybridization. A: *In situ* hybridization of synaptotagmin 1 (*SYT1*) in affected (aff) intermediate (i) hair follicles (HFs) of male pattern androgenetic alopecia (mpAGA) patients (Pts). **B**: *In situ* hybridization of *SYT1* in occipital (occ) iHFs of mpAGA Pts. **C:** *In situ* hybridization of *SYT1* in aff terminal (t) HFs of mpAGA Pts. **D**: *In situ* hybridization of *SYT1* in aff tHFs of mpAGA Pts. mRNA expression of *SYT1* is most prominently detected in the dermal papilla and is visualized by blue dots and exemplarily indicated by blue arrows. DP= dermal papilla.

The *SYT1* gene was shown to be differentially regulated in the DPs of tHFs deriving from different scalp locations. This points towards genetically different starting conditions for "pathological" miniaturization and "physiological" miniaturization. *SYT1* was found to be differentially regulated in all five (see **Table 3.5**) validated mpAGA Pts' (Pt10, Pt19, Pt20, Pt24 and Pt25) DPs according to the chosen criteria for upregulated (FC > 2 and CPM < 0.5) and downregulated genes (FC < 0.5 and CPM < 0.5). The treatment with 10 nM T for 48 h caused a decreased gene expression of *SYT1* in aff tHFs and occ iHFs, and an increased gene expression in aff iHFs (see **Table 3.5**). This leads to the fact that *SYT1* is a T responsive gene.

Table 3.5 Gene expression results obtained from RNA sequencing after laser capture microdissection of fresh frozen hair follicle compartments and after 48 hours *ex vivo* culture with 10 nM testosterone of male pattern androgenetic alopecia patients' hair follicles. Synaptotagmin 1 (*SYT1*) was found to be differentially regulated amongst all for the comparison of the dermal papilla (DP) successfully sequenced male pattern androgenetic alopecia patients (Pts) (Pt10, Pt19, Pt20, Pt24 and Pt25). It was showing up in the list of genes retrieved from the analysis of genes exclusively involved in the difference between both types of terminal hair follicles (HFs). Moreover, *SYT1* seems to be a testosterone (T) responsive gene because it was found to be downregulated in affected (aff) terminal (t) HFs and occipital (occ) intermediate (i) HFs and upregulated in aff iHFs after 10 nM T treatment *ex vivo*. Green background indicates a fold change (FC) > than 2 (upregulation) and red background indicates a FC < than 0.5 (downregulation) of the gene. SYT1= synaptotagmin 1, FC= fold change, DC= dermal cup, aff= affected, occ= occipital, i= intermediate, t= terminal, Pt= patient, T= testosterone.

gene	FC of gene expression *in situ* in the DP of aff compared to occ tHFs					FC of gene expression after 10 nM T treatment			
	Pt10	Pt19	Pt20	Pt24	Pt25	aff t	aff i	occ t	occ i
SYT1	7,57210603	4,66393807	0,43680751	13,3211528	4,04271951	0,49079144	3,0730135	1,38475479	0,14633894

The SYT1 protein expression in mpAGA Pts' HFs, showed a huge variability between the examined donors. Two out of three donors (Pt31 and Pt33) show a lower expression of SYT1 in the DP of occ iHFs as compared to occ tHFs. While in another pair of Pts (Pt33 and Pt36) show a tendential higher SYT1 protein expression in the DC of aff tHFs as compared to aff iHFs. For all three investigated Pts, a significant higher expression of SYT1 protein was found in the occ iDP compared to occ tDPs (see **Figure 3.31**).

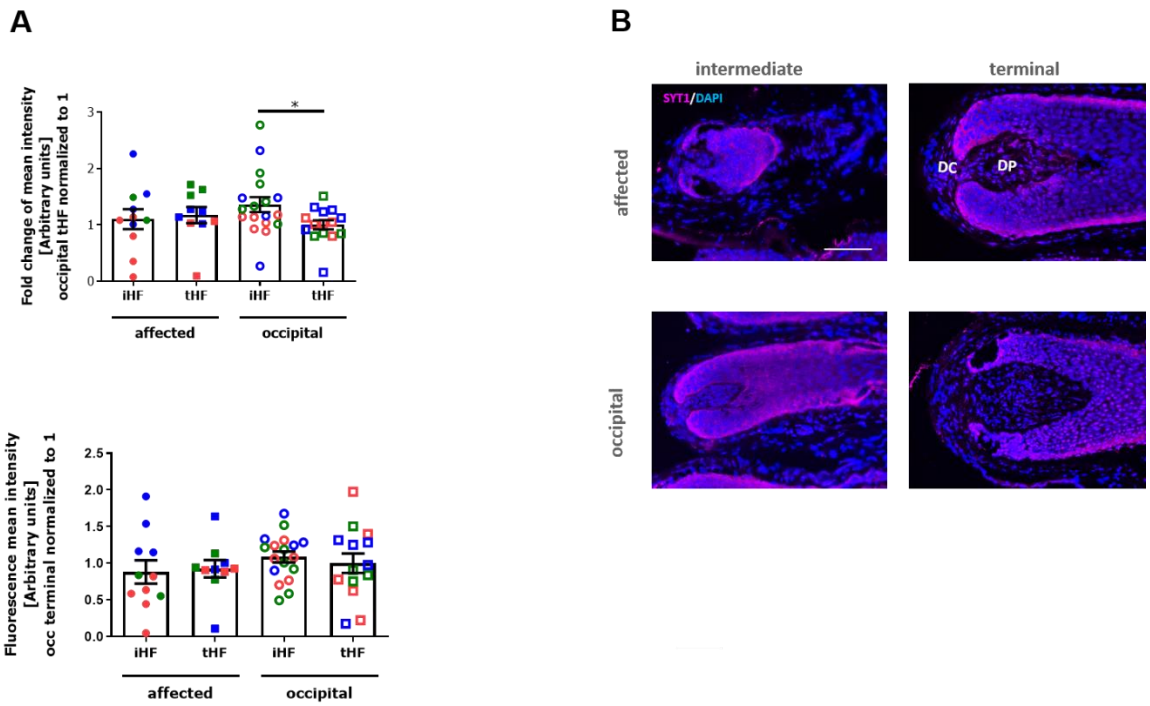

Figure 3.31 Synaptotagmin 1 protein expression in affected and occipital terminal and intermediate hair follicles of male pattern androgenetic alopecia patients. A: Graphs showing the fold change of fluorescence mean intensity in arbitrary units where the value for occipital (occ) terminal (t) hair follicles (HFs) was normalized to 1 for the expression of synaptotagmin 1 (SYT1). A significant higher expression was detected in occ intermediate (i) HFs compared to occ tHFs in the dermal papilla. For the expression of SYT1 in the dermal cup only tendential changes could have been detected. Mean±SEM, n= 10-18 HFs/ group from each donor, Graph Pad Prism 9, D'Agostino & Pearson omnibus normality test, data follows Gaussian distribution; students' t-test *p<0.05. Pt31 displayed in blue, Pt 36 displayed in red, Pt33 displayed in green. **B:** Example pictures of the immunofluorescence staining for SYT1 in affected and occ t/ iHFs of male pattern androgenetic alopecia patients. The displayed scale bar indicates 100 µm. SYT1= synaptotagmin 1, i= intermediate, t= terminal, HF= hair follicles, DAPI= 4′,6-Diamidin-2-phenylindol, DC= dermal cup, DP= dermal papilla.

3.5 Silencing target genes in hair follicle *ex vivo* culture by small interfering RNA

The use of siRNA is one of the most established methods to posttranscriptional silence a certain gene. siRNAs are short single- or double-stranded RNA molecules which do not code for proteins. Once transfected to cells, they fuse with their complementary single-strand mRNA and prohibit their translation into proteins [226]. The successful gene silencing was defined by a knockdown of the target gene on mRNA level (validated by qRT-PCR) and on protein level (validated by immunofluorescence staining). To investigate the influence of the silenced genes, the HF elongation was measured. As one of the greatest hallmarks of mpAGA is HF miniaturization resulting from premature catagen induction, the determination of HC phases was done with the results of Ki-67/ TUNEL immunofluorescence staining according to Kloepper et al [199]. HC score was evaluated using arbitrary values (anagen= 100, early catagen= 200, mid catagen= 300, late catagen= 400, dystrophic catagen= 500). Furthermore, the impact of gene silencing on HM keratinocyte proliferation and apoptosis was checked.

3.5.1 Silencing of aldehyde dehydrogenase 1 family member A2 by small interfering RNA induces catagen

To investigate the influence of *ALDH1A2* knockdown on the HC, occ tHFs of healthy male donors (Pt44, Pt45 and Pt46; see **Table 2.1**) were cultured for 72 h with *ALDH1A2* or scrambled (control) siRNA. After the culture was finished, the success of the knockdown was checked by the mRNA expression of *ALDH1A2* in both groups. Therefore, RNA was extracted from the HFs of the corresponding experimental groups (see **Chapter 2.3.2**) to check the knockdown on mRNA level by qRT-PCR. In two out of three experiments (Pt45 and Pt46), the knockdown of *ALDH1A2* was possible to be detected on the mRNA level (see **Figure 3.32**).

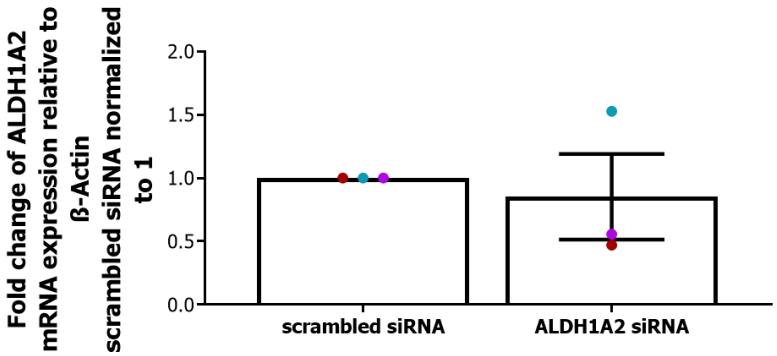

Figure 3.32 Aldehyde dehydrogenase 1 family member A2 expression referenced to the housekeeping gene beta-actin after 72 hours siRNA treatment. This figure shows the fold change of aldehyde dehydrogenase 1 family member A2 (*ALDH1A2*) mRNA expression in relation to the expression of the housekeeping gene beta-actin. Scrambled siRNA was normalized to 1. In two out of three patients (Pts) (namely Pt45 and Pt46), *ALDH1A2* knockdown was detected on mRNA level. Mean±SEM, n= 3 donors, Graph Pad Prism 9, D'Agostino & Pearson omnibus normality test, data does not follow Gaussian distribution; students' t-test ns. Pt44 displayed in blue, Pt45 displayed in purple, Pt46 displayed in red. ALDH1A2= aldehyde dehydrogenase 1 family member A2; β-Actin= beta-actin.

To examine the influence of the *ALDH1A2* siRNA induced gene knockdown on its protein expression, occ tHF were incubated for 72 h with either scrambled siRNA (control group) or *ALDH1A2* siRNA. After 72 h of HF *ex vivo* culture, the HFs were frozen in OCT and cut on a Leica cryostat and immunofluorescence staining was performed (see **Chapter 2.6**). On protein level, one can observe a significant 50 % knockdown in the DC and a significant 40 % knockdown in DP in n= 3 examined donors (see **Figure 3.33**).

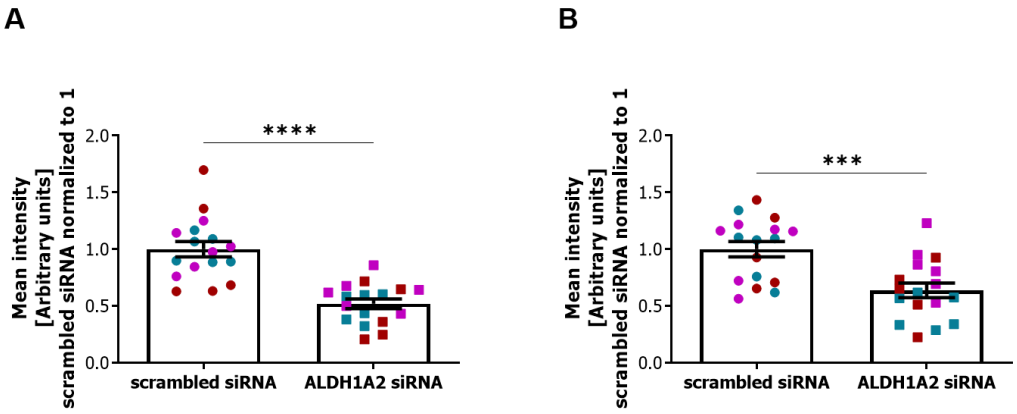

Figure 3.33 Aldehyde dehydrogenase 1 family member A2 protein expression in occipital terminal hair follicles after 72 hours siRNA treatment. A: Graph is showing the fold change of fluorescence mean intensity in arbitrary units where the value for occipital (occ) terminal (t) hair follicles (HFs) was normalized to 1 for the expression of aldehyde dehydrogenase 1 family member A2 (ALDH1A2) in the dermal cup (DC). A significant lower expression was detected in the group treated with *ALDH1A2* siRNA compared to the control group (treated with scrambled siRNA) in the DC. **B:** Graphs showing the fold change of fluorescence mean intensity in arbitrary units where the value for occ t HFs was normalized to 1 for the expression of ALDH1A2 in the dermal papilla (DP). A significant lower expression was detected in the group treated with *ALDH1A2* siRNA compared to the control group (treated with scrambled siRNA) in the DP. ALDH1A2= aldehyde dehydrogenase 1 family member A2. Mean±SEM, n= 17 HFs/ group from n= 3 donors, Graph Pad Prism 9, D'Agostino & Pearson omnibus normality test, data follows Gaussian distribution; students' t-test ***p<0.001; ****p<0.0001. Pt44 displayed in blue, Pt45 displayed in purple, Pt46 displayed in red.

For checking whether the silencing of *ALDH1A2* is affecting the HF growth, throughout the duration of the culture, the length of each HF was measured on D0, D1, D3 and D4. The percentage of growth was calculated and pooled together from all analyzed Pts. Statistical analysis has been performed using GraphPad Prism 9. The Mann-Whitney test showed a significant reduction of HF growth on D4 for the *ALDH1A2* knock out group compared to the control group. This trend could have been already observed on D2 of the culture (see **Figure 3.34**).

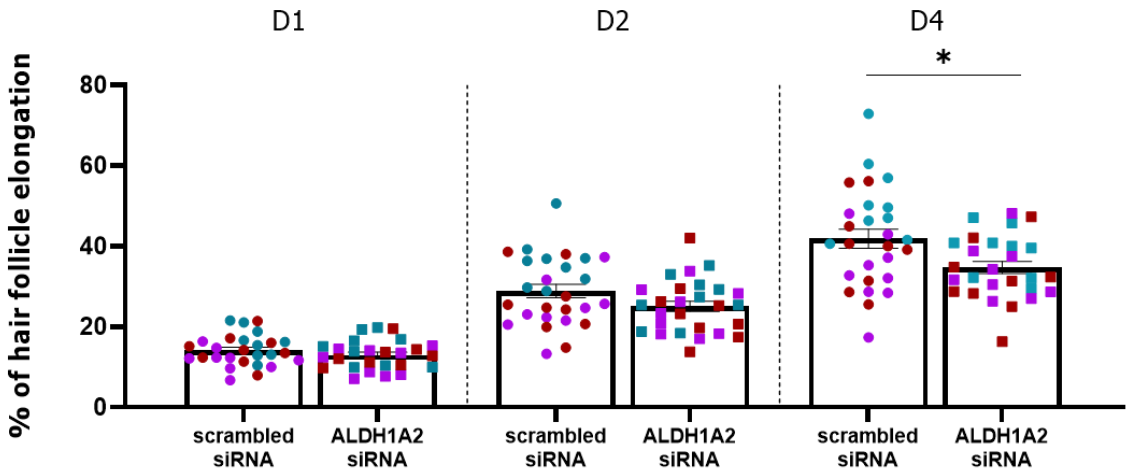

Figure 3.34 Knockdown of aldehyde dehydrogenase 1 family member A2 significantly reduces hair growth after 72 hours. Graph shows the pooled hair follicle (HF) elongation data of n= 3 healthy volunteers on day 1 (D1), D2 and D4 of HF *ex vivo* culture. On D1 (before siRNA treatment) no notably differences appeared between the HFs of both groups. On D2, a trend towards a reduced HF growth of aldehyde dehydrogenase 1 family member A2 (*ALDH1A2*) siRNA treated HFs could have been observed, compared to HFs in the control group (treated with scrambled siRNA). By the end of the HF *ex vivo* culture (D4) the HF growth is significantly reduced in HFs treated with *ALDH1A2* siRNA compared to HFs from the control group. Mean±SEM, n= 17-18 HFs/ group/ donor from n= 3 donors, Graph Pad Prism 9; D'Agostino & Pearson omnibus normality test, n too small to determine whether the data follows Gaussian distribution; Mann-Whitney test *p<0.005. Pt44 displayed in blue, Pt45 displayed in purple, Pt46 displayed in red. ALDH1A2= aldehyde dehydrogenase 1 family member A2.

As previously described in **Chapter 3.1.3**, all HFs were assigned to certain HC phases at the end of the 72 h of siRNA treatment. Additionally, the HC score was calculated as described in **Chapter 3.1.3**. The pooled results of n= 3 donors showed a significant promotion of catagen in HFs treated with *ALDH1A2* siRNA compared to HFs treated with scrambled siRNA (see **Figure 3.35**).

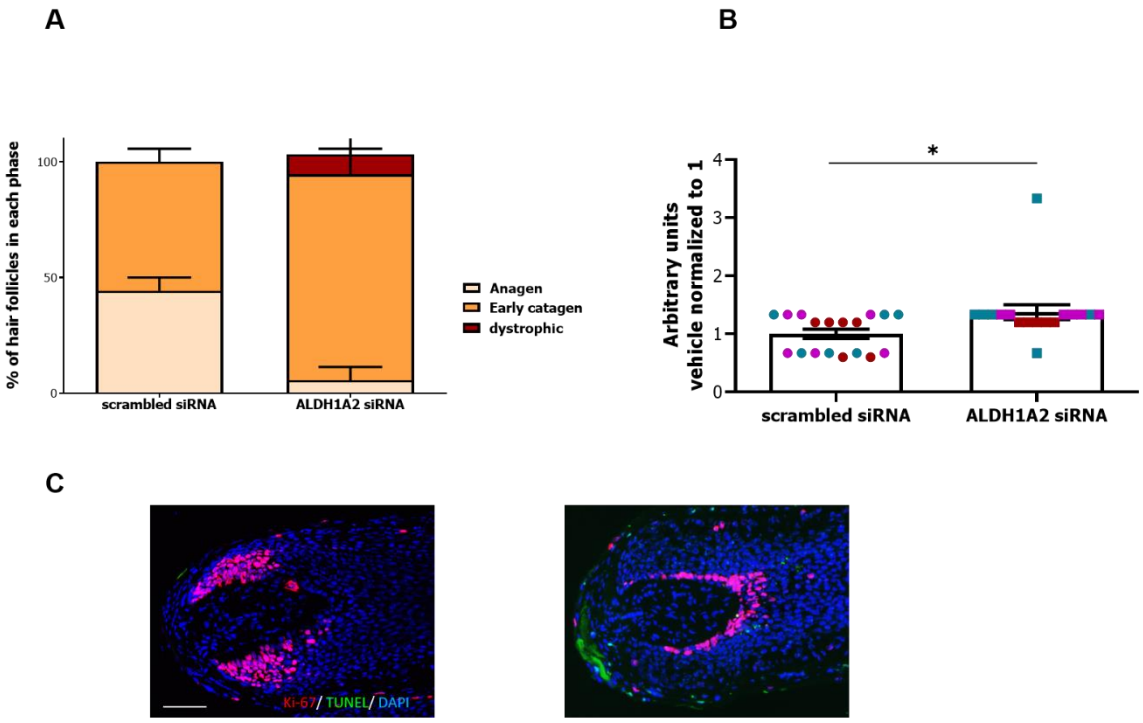

Figure 3.35 Knockdown of aldehyde dehydrogenase 1 family member A2 significantly induces catagen transition after 72 hours. A: This graph shows the pooled microscopic hair cycle (HC) staging of hair follicles (HFs) treated for 72 hours with scrambles siRNA (control) or aldehyde dehydrogenase 1 family member A2 (*ALDH1A2*) siRNA. *ALDH1A2* knockdown showed compared to the control group a clear reduction of HFs in anagen phase as well as a distinct increase of HFs in catagen phase. **B:** This graph displays the pooled HC score of HFs treated for 72 hours with scrambled and *ALDH1A2* siRNA. The comparison of both experimental groups showed a significantly higher HC score for the *ALDH1A2* siRNA treated HFs which indicates a significant increase in HFs in catagen phase. Mean±SEM, n= 17-18 HFs/ group from n= 3 donors, Graph Pad Prism 9; D'Agostino & Pearson omnibus normality test, data does not follow Gaussian distribution; Mann-Whitney test *p<0.005. Pt44 displayed in blue, Pt45 displayed in purple, Pt46 displayed in red. To determine the hair cycle score, arbitrary values are assigned to HFs in different hair cycle phases: Anagen= 100, early catagen= 200, mid catagen= 300, late catagen= 400, dystrophic catagen= 500. ALDH1A2= aldehyde dehydrogenase 1 family member A2. **C:** Representative images of HFs after 72 hours of siRNA treatment (scrambled siRNA- left picture; *ALDH1A2 siRNA*-right picture). The HF on left picture representing the control group, fulfills clear anagen criteria (e.g. germinative hair matrix keratinocyte proliferation, no dermal papilla cell emigration). The HF on the right picture represents ALDH1A2 siRNA treated HFs and demonstrates the present catagen induction. ALDH1A2= aldehyde dehydrogenase 1 family member A2, Ki-67= marker of proliferation Ki-67; TUNEL= terminal desoxynucleotidyl transferase-mediated deoxyuridine triphosphate-biotin nick end labelling, DAPI= 4′,6-Diamidin-2-phenylindol Displayed scale bar indicates 100 µm.

The last evaluation performed to investigate the influence of *ALDH1A2* knockdown on HFs was the examination of HM keratinocyte proliferation and apoptosis. Herefor a Ki-67/ TUNEL immunofluorescence staining was performed as described in **Chapter 2.6** and **Chapter 3.1.3**. Analyzing the HFs from both experimental groups of n= 3 Pts, a highly significant reduction in the percentage of proliferative (Ki-67 positive) cells in the HMg was detected, what supports the previous results regarding catagen induction (see **Figure 3.36 A**). The percentage of apoptotic (TUNEL positive) cells was not affected by the knockdown of *ALDH1A2* (see **Figure 3.36 B**).

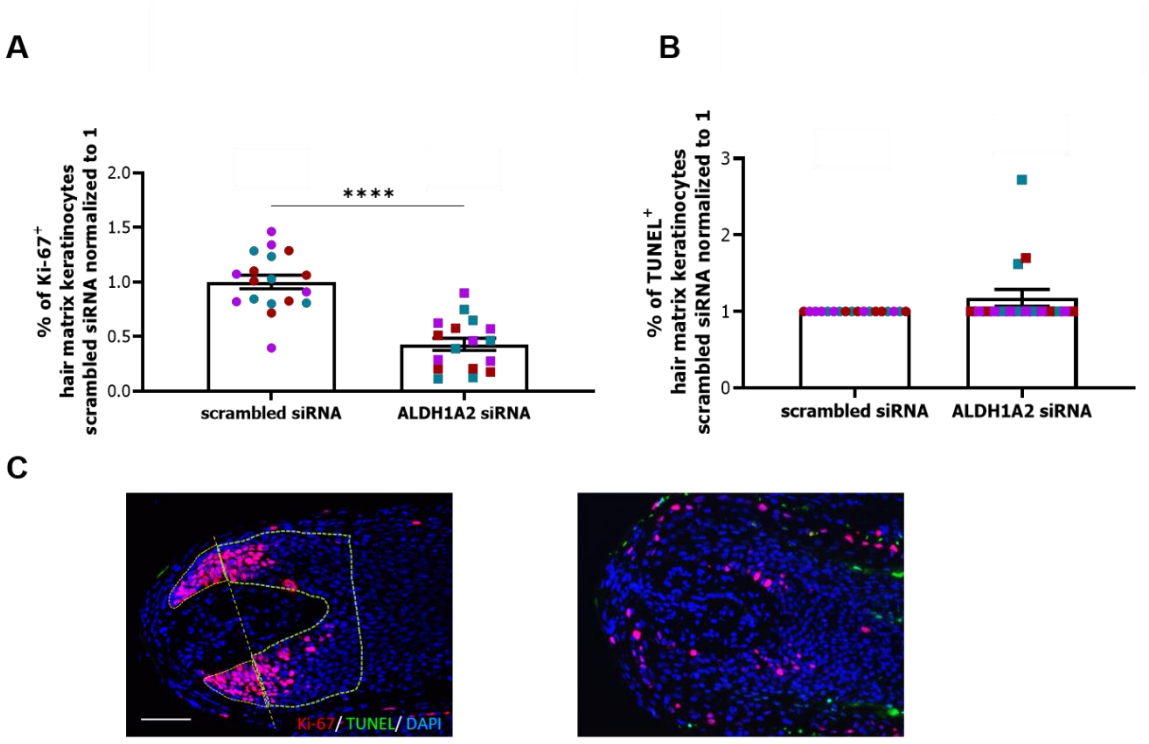

Figure 3.36 Knockdown of aldehyde dehydrogenase 1 family member A2 significantly reduces hair matrix keratinocyte proliferation. A: This graph shows the pooled evaluation of Ki-67 positive cells in both examined experimental groups. It shows a highly significant reduction in Ki-67 positive (proliferative) hair matrix keratinocytes after the treatment with aldehyde dehydrogenase 1 family member A2 (*ALDH1A2*) siRNA. **B:** This graph shows the percentage of TUNEL positive (apoptotic) cells after the treatment with either scrambled or *ALDH1A2* siRNA. No changes could have been detected regarding the apoptosis of hair matrix keratinocytes. **C:** Representative images of Ki-67/ TUNEL staining reflecting the results shown in the graphs of panel A and B. Mean±SEM, n= 17-18 HFs/ group from n= 3 donors, Graph Pad Prism 9; D'Agostino & Pearson omnibus normality test, data does not follow Gaussian distribution; Mann-Whitney test ****p<0.0001. Pt44 displayed in blue, Pt45 displayed in purple, Pt46 displayed in red. ALDH1A2= aldehyde dehydrogenase 1 family member A2, Ki-67= marker of proliferation Ki-67; TUNEL= terminal desoxynucleotidyl transferase-mediated deoxyuridine triphosphate-biotin nick end labelling, DAPI= 4′,6-Diamidin-2-phenylindol. Displayed scale bar indicates 100 µm.

3.5.2 Silencing of transforming growth factor beta 1 induced transcript 1 by small interfering RNA has no impact on the hair cycle

Investigating the effects of *TGFβ1I1* knockdown, by siRNA, in occ tHFs of healthy male volunteers, showed no impact on HC related criteria as elongation, changes in HC phases or changes in HM keratinocytes proliferation and apoptosis. To confirm the successful knockdown, qRT-PCR was performed and the TGFβ1I1 protein expression was evaluated in n= 2 donors (namely Pt44 and Pt45; see **Table 2.1**). The culture was performed as previously described in **Chapter 2.5.2**. After 72 h treatment with either *TGFβ1I1* or scrambled siRNA, the RNA was extracted and qRT-PCR was performed as previously described (see **Chapter 2.3.2**). The results of the qRT-PCR showed a successful knockdown of *TGFβ1I1* for one out of the two donors. Pt44 showed a reduction in *TGFβ1I1* mRNA of nearly 50 % (see **Figure 3.37**), while Pt46 showed an increase of *TGFβ1I1* mRNA of nearly 50 % (see **Figure 3.37**).

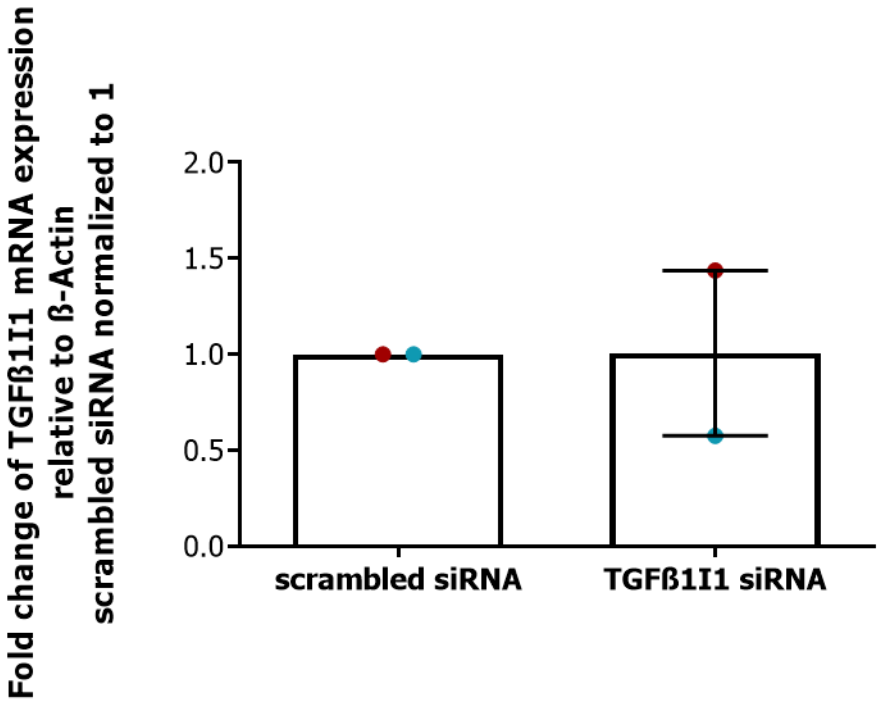

Figure 3.37 Transforming growth factor beta 1 induced transcript 1 mRNA expression referenced to the housekeeping beta-actin expression after 72 hours siRNA treatment. This figure shows the fold change of transforming growth factor beta 1 induced transcript 1 (*TGFβ1I1*) mRNA expression in relation to the expression of the housekeeping gene beta-actin. Scrambled siRNA was normalized to 1. In Pt44 a *TGFβ1I1* knockdown of approximately 50 % was detected, whereas for Pt45 the knockdown did not work. Mean±SEM, n= 12 HFs/ group from n= 2 donors, Graph Pad Prism 9, D'Agostino & Pearson omnibus normality test, data does not follow Gaussian distributionMann-Whitney test, ns. Pt44 displayed in blue, Pt46 displayed in red. TGFβ1I1= transforming growth factor beta 1 induced transcript 1; β-Actin= beta-actin.

After evaluating the impact of *TGFβ1I1* knockdown on its mRNA expression, also its protein expression was evaluated. In OCT embedded HFs were cryosectioned and a fluorescence staining was performed as previously described in **Chapter 2.6**. No reduction in protein expression was detected neither in the DP nor in the DC of Pt44 or Pt46 (see **Figure 3.38**).

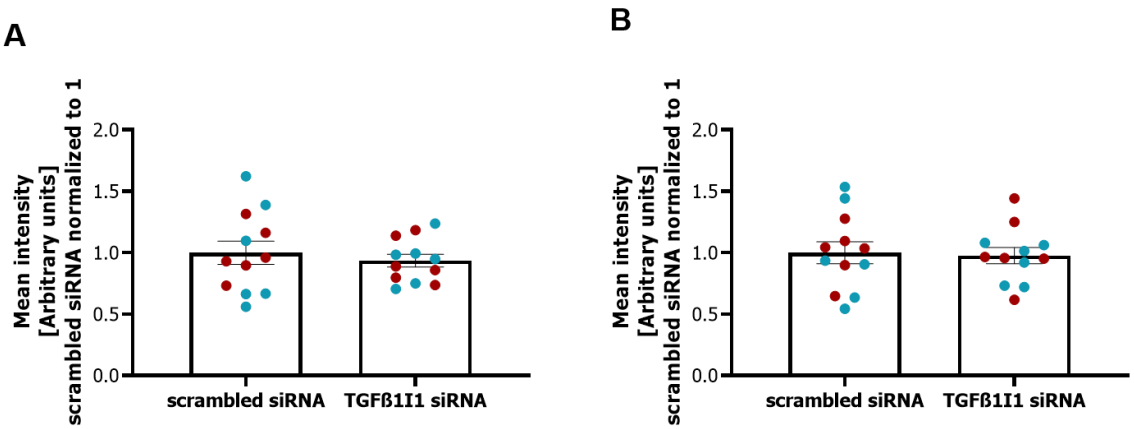

Figure 3.38 Transforming growth factor beta 1 induced transcript 1 protein expression in occipital terminal hair follicles after 72 hours siRNA treatment. **A:** Graph is showing the fold change of fluorescence mean intensity in arbitrary units, where the value for occipital (occ) terminal (t) hair follicles (HFs) was normalized to 1 for the expression of transforming growth factor beta 1 induced transcript 1 (TGFβ1I1) in the dermal cup (DC). No reduction in expression was detected in the group treated with *TGFβ1I1* siRNA compared to the control group (treated with scrambled siRNA) in the DC. **B:** Graph is showing the fold change of fluorescence mean intensity in arbitrary units where the value for occ tHFs was normalized to 1 for the expression of TGFβ1I1 in the dermal papilla (DP). No reduction in expression was detected in the group treated with *TGFβ1I1* siRNA compared to the control group (treated with scrambled siRNA) in the DP. TGFβ1I1= transforming growth factor beta 1 induced transcript 1. Mean±SEM, n= 12 HFs/ group from n= 2 donors, Graph Pad Prism 9, D'Agostino & Pearson omnibus normality test, data does not follow Gaussian distribution; Mann-Whitney test, ns. Pt44 displayed in blue, Pt46 displayed in red.

Moreover, treating the HFs with *TGFβ1I1* siRNA, also did not affect the HF elongation in a significant manner (see **Figure 3.39**). One can observe a decent growth throughout the days of the HF *ex vivo* culture in both experimental groups. Between the scrambled siRNA treated control group and the *TGFβ1I1* siRNA treated group, a slight tendential reduction in HF elongation was observed after 72 h (see **Figure 3.39**).

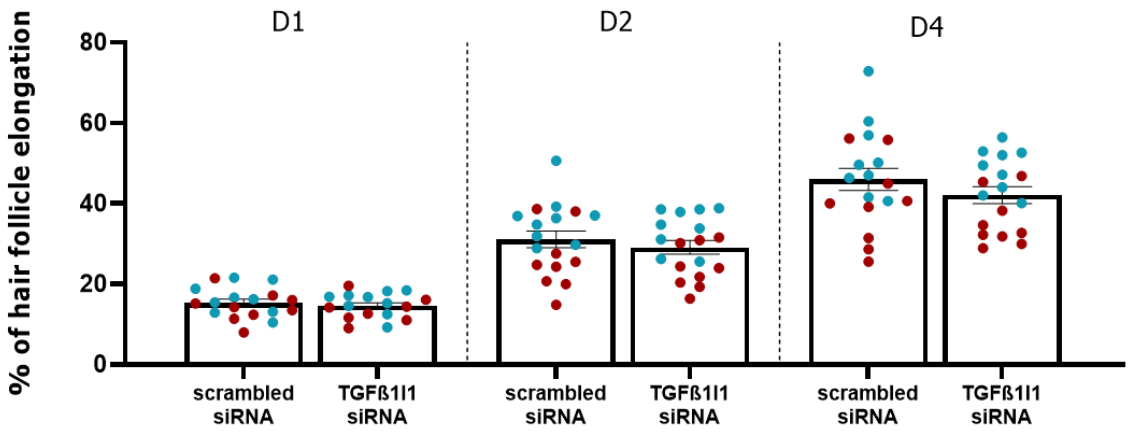

Figure 3.39 Knockdown of transforming growth factor beta 1 induced transcript 1did not significantly impact on hair follicle elongation after 72 hours. Graph shows the pooled hair follicle (HF) elongation data of n= 2 healthy volunteers on day 1 (D1), D2 and D4 of HF *ex vivo* culture. On D1 (before siRNA treatment) no notably differences appeared between the HFs of both experimental groups. On D2, a trend towards a reduced HF growth of transforming growth factor beta 1 induced transcript 1 (*TGFβ1I1*) siRNA treated HFs could have been observed, compared to HFs in the control group (treated with scrambled siRNA). By the end of the HF *ex vivo* culture (D4) the HF growth is tendentially reduced in HFs treated with *TGFβ1I1* siRNA compared to HFs from the control group. Mean±SEM, n= 17-18 HFs/ group/ donor from n= 2 donors, Graph Pad Prism 9; D'Agostino & Pearson omnibus normality test, data follows Gaussian distribution; unpaired t-test, ns; One-way ANOVA test, p< 0.0001. Pt44 displayed in blue, Pt46 displayed in red, TGFβ1I1= transforming growth factor beta 1 induced transcript 1.

As previously described in **Chapter 3.1.3**, in the end of the HF *ex vivo* culture, all HFs were assigned to certain HC phases. The HC score additionally was calculated as described in **Chapter 3.1.3**. The pooled results of n= 2 donors showed a tendential promotion of catagen transition in HFs treated with *TGFβ1I1* siRNA compared to HFs treated with scrambled siRNA. This shows off in a higher percentage of HFs in catagen phase (see **Figure 3.40 A**), a higher HC score (see **Figure 3.40 B**) and microscopically analyzed catagen typical Ki-67 expression in *TGFβ1I1* siRNA treated HFs (see **Figure 3.40 C**).

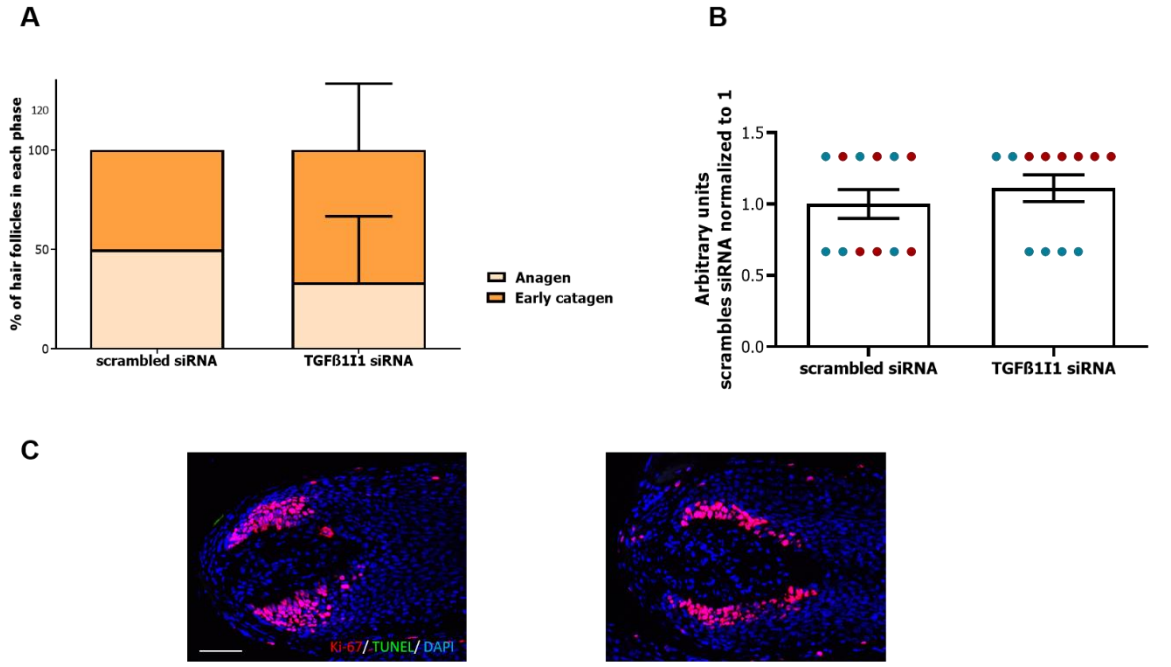

Figure 3.40 Knockdown of transforming growth factor beta 1 induced transcript 1 tendentially induces catagen transition after 72 hours. A: This graph shows the pooled microscopic hair cycle (HC) staging of hair follicles (HFs) treated for 72 hours with scrambled siRNA (control) or transforming growth factor beta 1 induced transcript 1 (*TGFβ1I1*) siRNA in n= 2 healthy donors. *TGFβ1I1* knockdown showed compared to the control group a tendential reduction of HFs in anagen phase as well as a distinct increase of HFs in catagen phase. **B:** This graph displays the pooled HC score of HFs treated for 72 hours with scrambled and *TGFβ1I1* siRNA. The comparison of both experimental groups showed a tendentially higher HC score for the *TGFβ1I1* siRNA treated HFs which indicates a tendential increase in HFs in catagen phase. Mean±SEM, n= 12 HFs/ group/ donor from n= 2 donors, Graph Pad Prism 9; D'Agostino & Pearson omnibus normality test, data does not follow Gaussian distribution; Mann-Whitney test, ns. Pt44 displayed in blued, Pt46 displayed in red. For determine the hair cycle score, arbitrary values are assigned to HFs in different hair cycle phases: anagen= 100, early catagen= 200, mid catagen= 300, late catagen= 400, dystrophic catagen= 500. TGFβ1I1= transforming growth factor beta 1 induced transcript 1. **C:** Representative images of HFs after 72 hours of siRNA treatment (scrambled-left picture; *TGFβ1I1*-right picture). The HF on left picture representing the control group, fulfills clear anagen criteria (e.g. germinative hair matrix keratinocyte proliferation, no dermal papilla cell emigration). The HF on the right picture represents TGFβ1I1 siRNA treated HFs and demonstrates the present catagen transition. Ki-67= marker of proliferation Ki-67; TUNEL= terminal desoxynucleotidyl transferase-mediated deoxyuridine triphosphate-biotin nick end labelling, DAPI= 4′,6-Diamidin-2-phenylindol, TGFβ1I1= transforming growth factor beta 1 induced transcript 1. Displayed scale bar indicates 100 µm.

After a tendential decrease in anagen HFs was observed, the influence of *TGFβ1I1* knockdown on HM keratinocytes proliferation was evaluated. For the reason, a Ki-67/ TUNEL immunofluorescence staining was performed as described in **Chapter 2.6** and **Chapter 3.1.3**. The pooled results of n= 2 Pts showed that a 72 h incubation with *TGFβ1I1* siRNA has no impact on HM keratinocytes proliferation or apoptosis (see **Figure 3.40**).

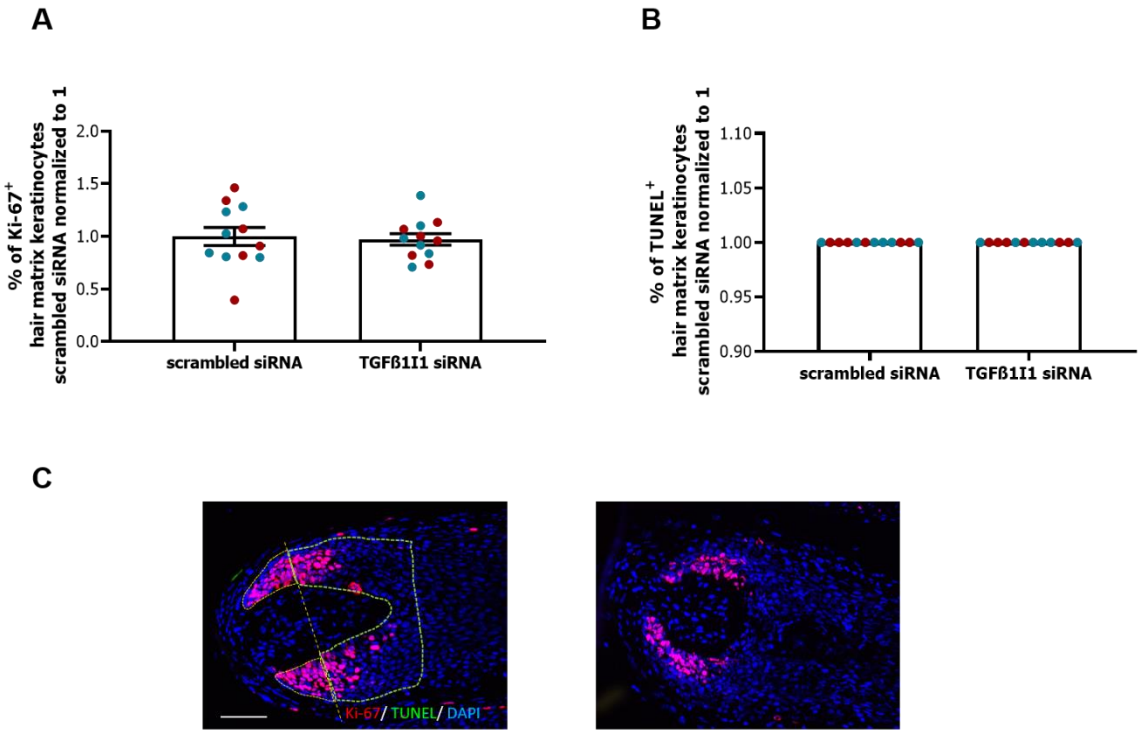

Figure 3.41 Knockdown of transforming growth factor beta 1 induced transcript 1 does not affect hair matrix keratinocyte proliferation or apoptosis. A: This graph shows the pooled evaluation of Ki-67 positive cells in both examined experimental groups. It shows no change in Ki-67 positive (proliferative) hair matrix keratinocytes after the treatment with transforming growth factor beta 1 induced transcript 1 (*TGFβ1I1*) siRNA. **B:** This graph shows the percentage of TUNEL positive (apoptotic) cells after the treatment with either scrambled or *TGFβ1I1* siRNA. No changes could have been detected regarding the apoptosis. **C:** Representative images of Ki-67/ TUNEL staining reflecting the results shown in the graphs of panel **A** and **B**. Mean±SEM, n= 12 HFs/ group/ donor from n= 2 donors, Graph Pad Prism 9; D'Agostino & Pearson omnibus normality test data does not follow Gaussian distribution; Mann-Whitney test, ns. Pt44 displayed in blue, Pt46 displayed in red. TGFβ1I1 = transforming growth factor beta 1 induced transcript 1. Ki-67= marker of proliferation Ki-67; TUNEL= terminal desoxynucleotidyl transferase-mediated deoxyuridine triphosphate-biotin nick end labelling, DAPI= 4′,6-Diamidin-2-phenylindol, TGFβ1I1= transforming growth factor beta 1 induced transcript 1. Displayed scale bar indicates 100 µm.

4 Discussion

mpAGA is the most prevalent form of hair loss in men. The progressive miniaturization of HFs is characterized by a premature catagen induction [63–68].

The driving force behind the initiation of HF miniaturization is known to be the activation of the AR by T or its more potent metabolite DHT [55,76,78]. T was considered to trigger certain responses in aff scalp HFs of mpAGA Pts, which leads to stepwise miniaturization and results in balding in this distinct scalp area [55–57]. The mechanisms behind this miniaturization of HFs from the aff area of mpAGA patients remain unraveled. Therefore, HFs from the occ scalp are claimed to be androgen-insensitive" [200].

4.1 Testosterone influences not only hair follicles from the affected scalp but also hair follicles from the occipital scalp in male pattern androgenetic alopecia patients *ex vivo*

This thesis aimed to establish a HF *ex vivo* organ culture model to investigate the immediate changes regarding HC related parameters on the protein level and the gene expression level after T exposure. Previous studies demonstrated that too high levels of T (5 µg/ ml) suppress the proliferation of HM keratinocytes and HS elongation *ex vivo*[66]. The model developed during this thesis should serve as a model for testing drugs for mpAGA treatment. Therefore, it was crucial to work with physiological realistic T concentrations. The first experiment was carried out with a concentration of 10 nM T, based on the experiments performed by Miranda et al. [227]. This thesis aimed to investigate the immediate influence of T treatment, so we cultured the HFs for 24 h with 10 nM T. Allthough no change was observed regarding HF elongation, no changes on the protein level of HC related parameters, but the treatment with 10 nM T for 24 h was sufficient to see changes in the HFs' transcriptomic profile (see **Chapter 3.2**). To see effects by T on the protein level on the HC or the HS production, a longer duration of the culture or an increase of T concentration was necessary.

For retrieving the most reliable results, we aimed to mimic the most natural dose of T. As the concentration of T in the blood of mpAGA Pts is in the same range like in healthy Pts [79–87] we opted for a treatment concentration of 30 nM T and a treatment duration of 48 h to investigate changes on HC related parameters on the protein level. Therefore, HFs from the aff and occ scalp of mpAGA Pts were microdissected and treated with 30 nM T *ex vivo*.

As previously shown in the literature, the level of circulating T does not vary too much between the occ and aff scalp area in mpAGA Pts [85–87]. The much higher level of DHT in the treated HF groups from the aff scalp (see **Figure 3.1**) reflects first of all the fact, that in the aff scalp area the DHT concentration is higher compared to the occ area [78,88]. As previously reported, activity of 5α-R in the aff scalp of mpAGA patients the is higher compared to their occ scalp and to healthy controls [89]. As alredy proven, HFs *ex vivo* are able to convert T to its much more potent metabolite DHT. This thesis successfully showed that microdissected HFs deriving from mpAGA Pts aff scalp are able to convert T to DHT *ex vivo* (see **Figure 3.1**)[78]. These results where necessary to exclude any unspecific actions of T on the HFs and to validate the used *ex vivo* organ culture model. Moreover, it confirms the already published higher activity of 5α-R, the enzyme which converts T to DHT [55,76,78], in the aff scalp area [89].

For the longest time, occ HFs of mpAGA Pts were claimed to be T- insensitive[200]. This thesis demonstrates that HFs from the occ scalp area are not less affected by T compared to HFs from the aff area. A tendentially increased proliferation of HM keratinocytes as it was seen in occ iHFs (see **Figure 3.4**), is associated with prolongation of the anagen phase[199]. Together with a significant reduction of apoptosis markers casp3 (see **Figure 3.12**) and TUNEL (see **Figure 3.11**) in the DC, a protective effect of T on occ HFs of mpAGA Pts can be hypothesized. These findings can also be a hint towards unravelling the andorogen paradoxon. This paradoxon says that in one distinct part of the body androgens trigger the transcription of hair growth inhibiting factors, such as TGFβ1 and lead to HF miniaturization and hair loss. Whereas in other areas (axillary area, pubic area and beard area), androgens lead to the transcription of growthfactors like IGF1 and induce hair growth (see **Figure1.5**).

This thesis furthermore confirms the lately reported effect of androgens on the inductive role of DP cells by Ceruti *et al* [204]. It was stated that androgens cause a downregulation of BMP2 and BMP4 that leads to an impairment of DP inductivity [204]. This was confirmed by the previous shown significant lower AP activity in the aff iHFs after T treatment (see **Figure 3.6 A**) and a tendential lower versican expression in aff t/ iHFs and occ iHFs (see **Figure 3.6 B)**. On the one hand, AP activity has been lately associated with Wnt signaling [228], one of the major pathways promoting hair growth [125]. This is also reflected by its significant downregulation in aff iHFs (see **Figure 3.6 A**), when those HFs are known to have altered growth abilities and are miniaturized in size already. On the other hand, versican expression is associated with matrix assembly and cell-matrix interaction, characteristic for anagen VI HFs [229]. This is mirrored by the decreased versican expression in the DPs of aff and occ iHFs (see **Figure 3.6 B**) due to their reduced DP size and vellus- like characteristics [193]. The tendentially reduced versican expression in the DPs of aff tHFs (see **Figure 3.6 B**)

reflects the initiation of the miniaturization process induced by T. While versican expression was shown to be reduced in catagen HFs, the reduction in DPCs of aff tHFs (see **Figure 3.6 B**) can be the first indication towards catagen induction as a first direct consequence of T.

Although an altered HC [63–65], resulting in premature catagen induction [63–68] is one of the known and most prominent hallmarks of mpAGA, no significant effect of 30 nM T treatment *ex vivo,* on HF elongation (see **Figure 3.2**) or the HC (see **Figure 3.3**) could have been detected in the cultured mpAGA HFs. To see a dependably effect on the HC and on HS production in this organ culture model, the duration of the culture would need to be extended as seen in previous publications [66–68] or the used concentration of T would need to be increased [66]. But with regard to evaluate the disease specific and naturally appearing impact of T in HFs *ex vivo*, an elevation of the used T concentration would not be recommended.

The more a healthy HF switches from anagen to catagen phase, the more DP fibroblasts migrate out of its DP into the DC [199]. This results in a lower number of DP fibroblasts and a higher number of DC cells as well as a higher number of DP stalk cells where DP fibroblasts accumulate during their emigration in catagen phase [199]. With the onset of another HC, the emigrated DP cells will be restored so the efflux and influx of DPCs is balanced throughout the HC [199] (see **Figure 1.7 A**). One of the greatest hallmarks of mpAGA is the impaired efflux and influx of DPCs [12,120,121] (see **Figure 1.7 B**).
While the data in this thesis indicates that T may indeed promote DP fibroblast emigration in aff iHFs (see **Figure 3.10 A**), it also suggests that other events seem to be involved in the reduction of fibroblast numbers in the DPs of aff iHFs as the numbers of cells in the DCs and DP stalks of aff iHFs remained unaffected by T (see **Figure 3.10 B** and **C**).
Interestingly, quantitative observations revealed TUNEL-positive cells in the CTS and the DC of aff and occ HFs from all Pts (see **Figure 3.3 C**). The treatment with 30 nM T *ex vivo* increased significantly the percentage of TUNEL-positive cells in the DC of aff tHFs and decreased it significantly in the DC of occ tHFs and tendentially in the DC of aff iHFs (see **Figure 3.11 A**). These observations only partially overlap with the obtained results by labeling casp3. This revealed a significant decrease in the percentage of casp3 positive cells in occ t and iHFs' DCs (see **Figure 3.12 A**). This discrepancy may derive from the fact that the TUNEL technique is known to detect DNA fragmentation, a process which is not only occurring during apoptosis, but also in cells, where DNA damage is induced by other means [230]. Moreover, the TUNEL technique can also label non-apoptotic nuclei showing signs of active gene transcription [190,191]. Instead, casp3 is expressed by a cell during the so called "point of no return" towards apoptosis, even when no morphological changes happened yet [190]. Therefore, this thesis clearly showed that apoptosis of DC fibroblasts is

prevented by T in t and iHFs from the occ scalp, and suggests a possible induction of apoptosis or DNA damage in cells of the DC of aff tHFs following the treatment with 30 nM T. Interestingly, a significant increase of casp3 positive cells was detected in the DP of those aff tHFs (see **Figure 3.12 B**). One could speculate that while the apoptosis process may be induced in the DP fibroblasts of those HFs following T exposure, the nuclei fragmentation in these cells may occur in the DC where the DP fibroblasts have emigrated to in the meantime.
Quite intriguing is also the tendential decrease in the percentage of TUNEL-positive (see **Figure 3.11 A**) and casp3-positive cells (see **Figure 3.12 A**) detected in the DC of aff iHFs. This suggests that a sort of homeostasis might be recreated in miniaturized HFs. This might prevent specialized fibroblasts to undergo apoptosis. This hypothesis is underlined by the fact that the number of DPCs of aff iHFs is significantly reduced aft T treatment (see **Figure 3.10 A**), whereas no apoptosis could have been observed in the DPs of aff iHFs (see **Figure 3.11 B** and **Figure 3.12 B**).

Taken together, this thesis revealed different effects of T treatment, not only in HFs from different scalp locations, but also inter-follicular variability depending on the HF size within the same scalp location. While in aff tHFs T may induce apoptosis and migration of DP fibroblasts into the DC, in aff iHFs, T may primarily affect the inductive potential of DP fibroblasts impairing also their number within the DP. This underlines the fact that in aff tHFs the miniaturization process still needs to be initiated and executed, whereas in aff iHFs the miniaturization process is already ongoing and needs to be “maintained” or even pushed forward.
All these described findings are summarized in **Figure 4.1**.

In conclusion, this thesis proved the used organ culture model as a valid tool for testing anti-androgenetic alopecia drugs in the future. Moreover, this model could also be used for studies using T in combination with an AR antagonist like cyproterone acetate [227] and study the impact of T under those circumstances on HC related parameters as mentioned above.

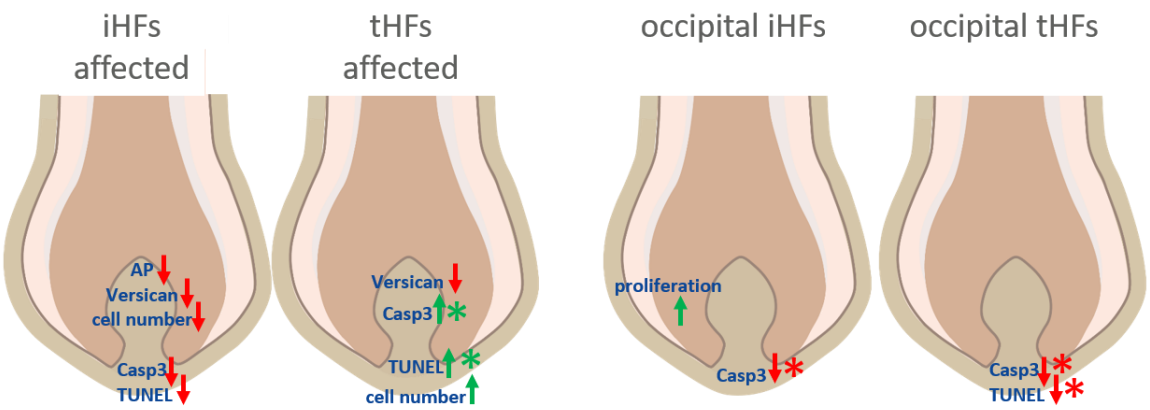

Figure 4.1 Effects of 30 nM testosterone treatment on intermediate and terminal affected and occipital hair follicles *ex vivo*. The scheme indicates the effects on protein level, caused by 30 nM testosterone (T) treatment *ex vivo* on intermediate (i) and terminal (t) hair follicles (HFs) from the occipital (occ) and affected (aff) scalp regions from male pattern androgenetic alopecia (mpAGA) patients. In aff iHFs a tendential decrease of alkaline phosphatase activity as well as a tendential lower expression of versican and a lower cell number in the dermal papilla (DP) was observed. In the dermal cup (DC) of those HFs, a decreased percentage of caspase3 (casp3) and TUNEL positive cells was evaluated. In aff tHFs, a tendential decrease in versican expression as well as a significant increase of casp3 positive cells was observed in the DP. In the DC of aff tHFs, a significant increase of TUNEL positive cells as well as a tendential increase in the total cell number was seen. In occ iHFs, a tendential increase in proliferative hair matrix keratinocytes as well as a significant decrease of casp3 positive cells in the DC could be observed, whereas in the DC of occ tHFs a significant lower percentage of casp3- and TUNEL positive cells was present. i= intermediate, HFs= hair follicles, AP= alkaline phosphatase activity, Casp3= cleaved caspase 3, *= significance, red arrows= decrease, green arrows= increase. Image was created with Adobe Illustrator.

Having a closer look on the expression of defined HC related genes, like marker of proliferation *Ki-67* [231], *CASP3* [232], *ALPL* [202], *VCAN* [193] and *BMP2/ 4* [204], after the initial 10 nM T treatment (see **Figure 3.16**) and compare them to the changes on protein level (see **Figure 4.1**), these results point out, that the retrieved data from the RNAseq has to be considered to be a “snapshot” of gene expression. Therefore, for this thesis, the fact of differential gene regulation was more important than the direction of gene regulation (up- or down regulation). One needs always to consider that all HFs were harvested from mpAGA Pts scalp where a certain concentration of T was constantly present. The obtained changes in gene expression (either up- or downregulation) are necessarily a consequence of T and entitles it as a T responsive gene.

Despite the fact that the samples for RNAseq after 10 nM T treatment were harvested from mpAGA Pts having similar disease severity (see **Table 2.1**), the PCA reveals inter-individual variations in the transcriptome of the analyzed samples (see **Figure 3.19**). This suggests inter-individual variations in organ culture condition adaptation and response to T treatment. No sample cluster could be identified separating aff and occ HFs treated with T (see **Figure 3.19**) which assumes that occ HFs are more sensitive to androgens than previously

supposed. This led to the suggestion that other components besides androgen-sensitivity may be involved in mpAGA development in aff scalp.

In conclusion, this thesis confirms, that T impacts on the development and progression of mpAGA as previously shown in the literature [55,76,78]. Moreover, a potential new mechanism involved in pathological HF miniaturization in mpAGA was introduced: apoptosis of emigrated DP fibroblasts within the DP and the DC. This leads to the assumption, that in aff tHFs, where the miniaturization process was just initiated by the T treatment, emigrating DP fibroblasts might undergo programmed cell death which further potentiates miniaturization.

In addition, this project showed that occ HFs are not as androgen insensitive as widely accepted. In contrast to HFs from the beared, axillary and pubic area (where T triggers a vellus to terminal conversion) or HFs from the aff scalp (where T induces the terminal to vellus conversion) T seems to have a more protective role on HFs from the occ area.

4.2 RNAseq from laser capture microdissected hair follicle compartments revealed potential targets for androgenetic alopecia managment

Besides androgens also genetic factors play a key role in the pathobiology of mpAGA [137]. As it is known to be one of the most heritable complex traits [138], during the last decades, scientists were interested in revealing genes which are involved in the development of this disease.

To unravel mpAGA target genes, it is necessary to prevent the HF from miniaturization in the earliest stage possible. If the disease-typical miniaturization has progressed too far, the HF loses the connection to the APM [117,118] which makes its the miniaturization irreversible.

For disclosure of those potential target genes, different techniques have been used over the time, such as DNA sequencing from whole scalp tissue biopsies [106], microarray analysis from whole scalp tissue biopsies [156,160,233,234] and “plucked HFs” [109], RNA analysis via Northern blot of microdissected HFs [89] and immunostainings of scalp biopsies [130]. All of those techniques have inveterate limitations towards their exclusiveness of the discovered genes. By using whole scalp tissue biopsies, one will discover genes which are also differentially regulated in this disease in other compartments of the skin and not exclusively in the HF. By using “plucked HFs” (correctly: plucked HSs, where the biggest part of the HF mesenchyme and substantial components of the HF epithelium like the bulge and most of

the HM are missing) [243], one might miss important genes which are differentially regulated during the mpAGA progression in the missing HF compartment. Immunostainings of scalp biopsies are displaying only the impact on the protein expression. It is not nescessarily given, that the protein expression displays exactly the gene expression changes. Changes on protein level appear much later than changes in the gene expression.

The overall aim of this thesis was the identification of potential new anti-mpAGA target genes so the avbove mentioned limitations need to be solved in this thesis. Therefore, RNAseq from LCM derived distinct HF compartments (see **Chapter 2.2**) was performed. Using this technique, one can ensure to only obtain results from differentially regulated genes in the compartment of interest. By working very precisely and carefully, "cross-contaminations" by genes differentially regulated in surrounding tissue or compartments can be avoided completely. A negative aspect of this technique was the large number of HFs which were needed from one mpAGA Pt to isolate enough RNA to perform RNAseq.

This technique allows a more detailed look on the genetical differences and similarities of aff/ occ t/ iHFs (see **Figure 3.19**). The shown final PCA of all analyzed and used results (see **Figure 2.19** based on **Table 3.2**) reveals a clustering of differentially regulated genes per HF compartment rather than per scalp location. These findings further confirm that those selected HF compartments have different transcriptomic profiles, by greater separation of epithelial versus mesenchymal compartments. These results underline even more the importance of analyzing the different HF compartments separately rather than bulk HF analysis. Bioinformatical analysis (see **Chapter 2.4**) of the retrieved raw data, revealed several differentially regulated genes in the DP and DC of the different HF types.

The finally chosen genes for further investigation towards their potential role in mpAGA biogenesis are *ALDH1A2*, *TGFβ1I1* and *SYT1*. The pattern of expression of these targets was confirmed on the gene level by *in situ* hybridization (see **Figure 3.24** and **Figure 3.30**) and on the protein level by immunofluorescence staining (see **Figure 3.25**, **Figure 3.27** and **Figure 3.31**) which further revealed that these proteins are functional in the defined HF compartment.

ALDH1A2 codes for an enzyme which converts retinaldehyde into retinoic acid [213,214]. Murine studies showed cutaneous retinoic acid to be involved in HF down growth and development [215]. The protein expression (see **Figure 3.25 A**) as well as the gene expression level (see **Figure 3.22**) of ALDH1A2 occurred to be significantly lower in aff tHFs compared to aff iHFs DCs. This fininding seems to be surprising in in the first moment because aff iHFs of mpAGA are known to be smaller in size and are not anchored as deep in the skin as tHFs [75]. The miniaturization process in aff tHF has not been carried out yet, but is "pre-

programmed". The significant lower concentration of ALDH1A2 in aff tHFs DCs might show the first indication for the initiation of pathological miniaturization of aff tHFs in mpAGA.

If androgens are as crucial for mpAGA as Hamilton's study [55] suggested and as the relative efficacy of finasteride in halting mpAGA progression suggests as well [172], why does only a small subset of Pts experiencing a full hair growth recovery after suppressing the conversion of T to DHT? After these observations, it has been shown that the AR can function together with coactivators to activate target genes [220,221]. *TGFβ1I1* is known to code for an AR coactivator [222] which also enhances the androgen sensitivity in DPCs from aff scalp HFs [223].

These findings are also in line with the RNAseq results provided by this thesis and suggests *TGFβ1I1* already to be important for the progression of mpAGA. The previously shown high levels of *TGFβ1I1* expression in fibroblasts of the mesenchymal compartments of HFs (see **Figure 3.26)** and especially in the DP of aff t/ iHFs [89–93] was confirmed by the above shown results. Regaring the observed protein expression of TGFβ1I1 (see **Figure 3.27**), it seems to be not only important for the progression of mpAGA, furthermore, it might be also involved in the initiation of the miniaturization process of aff tHFs. This can be hypothezised by the distinct higher protein expression in the DC of aff tHFs from two validated mpAGA Pts (see **Figure 3.27 B**).

As widely appreciated, pathologically miniaturized HFs show altered growth abilities resulting from an altered HC [126,127] induced by premature termination of the anagen phase [63–68]. Treatment of fibroblasts, like in the mesenchymal compartments of the HF, with FGF1, showed limited proliferation and were shown to express large numbers of cell cycle inhibitors [224,225]. The mostly in the brain expressed mediator of neurotransmitter release [194], SYT1, was demonstrated to be required for FGF1 release as consequence to stress [224,225]. This thesis showed *SYT1* to be mostly expressed in the DP of aff and occ HFs (see **Figure 3.28**). Interestingly, in HFs from both scalp locations, the gene expression is higher in the iDP compared to the tDP. This might indicate that SYT1 as well as its known stress induced FGF1 release[224,225] is not exclusively being involved in the miniaturization process in mpAGA, but also in the physiological miniaturization. This is why this thesis suggests SYT1 to be indirectly involved in the inhibition of proliferation and retardation of the cell cycle in HF miniaturization processes in general.

In conclusion, this thesis proves RNAseq from LCM derived single HF compartments as the most reliable technique to study the transcriptomic events in such a complex disease. With this technique it was possible to identify compartment specific regulated genes which might be involved in the pathogenesis of mpAGA.

4.3 Knockdown of aldehyde dehydrogenase 1 family member A2 and transforming growth factor beta 1 induced transcript 1 by small interfering RNAs suggested their involvement in male pattern androgenetic alopecia pathobiology

The manipulation of a certain target gene is the first step to study its involvement in a process of interest. The knockdown of either ALDH1A2 or TGFβ1I1 with siRNA combined with the previously seen gene regulation from RNAseq revealed first insights into both of their roles in the HC and allows to speculate about their involvement in mpAGA development.

Retinoic acid was discovered a long time ago to be critically involved in several developmental and maintaining processes in different tissues, containing also skin and hair [235,236]. The synthesis of all-*trans* retinoic acid (tretinoin) was shown to be degraded in cultured dermal fibroblasts [237]. This shown degradation suggests a limitation of the delivery of retinoic acid to the HF which makes a local synthesis crucial for the HF's normal development and function [238]. ALDH1A2 is an enzyme known to convert retinaldehyde into retinoic acid [213,214]. Tretinoin, the end product of this enzymatic cascade, has been shown to have positive effects on mpAGA Pts when applied together with minoxidil [217,218].

Silencing the first chosen target gene, *ALDH1A2* showed a significant catagen promoting effect (see **Figure 3.35**) together with a significant reduced proliferation of HM keratinocytes (see **Figure 3.36**). These findings corroborated with the observation of significantly reduced ALDH1A2 protein expression in aff tHFs as compared to aff iHFs (see **Figure 3.25**).

In conclusion, one could speculate that the elevation of local ALDH1A2 levels can be beneficial for keeping HFs in anagen phase and might also prevent HFs from miniaturization by avoiding premature catagen induction. But the chosen dose would need to be evaluated carefully, because also the stimulation of DPCs with tretinoin was recently also shown to have catagen inductive and proliferation inhibiting effects [239].

By knocking down the second chosen target *TGFβ1I1* no changes on protein level could have been detected. Taking into consideration that on the mRNA level the knockdown by siRNA was only successful in one out of two donors (see **Figure 3.37**) and no changes on the protein level could have been detected neither in the DP nor in the DC (see **Figure 3.38**), one could speculate that one donor might be a non-responder to the siRNA. But contemplating the tendential decrease of HFs in anagen phase (see **Figure 3.40**), suggests *TGFβ1I1* to also host an important role in the HC. The tendential catagen promoting effect is underlined by the observed downregulation of *TGFβ1I1* in the RNAseq data of the DC from aff iHFs compared to occ iHFs and also in the DC of aff iHFs compared to occ tHFs

(see **Table 3.4**). Moreover, on the protein level a tendential lower expression of TGFβ1I1 was seen in the DP and the DC of aff iHFs from two out of three analyzed mpAGA Pts (see **Figure 3.27**).

The results of this thesis regarding the knockdown of *TGFβ1I1* suggest to continue this experiment in HFs from mpAGA Pts. Possibly, the reduced androgen sensitivity of DPCs from occ healthy HFs [89–93] can be a valid explanation for the rather weak results after gene knockdown. One can assume the already higher androgen sensitivity of aff HFs of mpAGA Pts [89–93] would be affected more by the deprivation from a known AR co-activator [222].

Thus, premature catagen induction is one of the greatest hallmarks of mpAGA development [63–68]. The results of both siRNA induced knockdown experiments are very encouraging and promote *ALDH1A2* and *TGFβ1I1* to be promising target genes in mpAGA research.

Conclusively, this thesis revealed robust data, regarding the importance of ALDH1A2 and TGFβ1I1 in the HC and their possible contribution in mpAGA pathobiology. The shown results encourage follow-up studies to stimulate the gene-expression or manipulate the protein expression in a positive way in aff mpAGA HFs to investigate if the disease-typical miniaturization can (at least partially) be reversed and HFs can be prevented from premature catagen induction. This might lead other than the already FDA approved treatments not only to an inhibiton of the disease progression but also to reverse HF miniaturization and to promote stimulation of hair regrowth.

6 References

1. Di Meglio, P., Perera, G. K. & Nestle, F. O. The multitasking organ: recent insights into skin immune function. *Immunity* **35**, 857–869 (2011).
2. Heath, W. R. & Carbone, F. R. The skin-resident and migratory immune system in steady state and memory: innate lymphocytes, dendritic cells and T cells. *Nat Immunol* **14**, 978–985 (2013).
3. Sterry / Paus / Burgdorf | Thieme Clinical Companions: Dermatology | 1. Auflage | 2006 | 978-3-13-135911-7. https://www.sack.de/sterry-paus-burgdorf-thieme-clinical-companions-dermatology/9783131359117.
4. Ji, S., Zhu, Z., Sun, X. & Fu, X. Functional hair follicle regeneration: an updated review. *Signal Transduct Target Ther* **6**, 66 (2021).
5. Patzelt, A. & Lademann, J. Drug delivery to hair follicles. *Expert Opin Drug Deliv* **10**, 787–797 (2013).
6. Schneider, M. R., Schmidt-Ullrich, R. & Paus, R. The hair follicle as a dynamic miniorgan. *Curr Biol* **19**, R132-142 (2009).
7. Stenn, K. S. & Paus, R. Controls of hair follicle cycling. *Physiol Rev* **81**, 449–494 (2001).
8. Plikus, M. V. *et al.* Epithelial stem cells and implications for wound repair. *Semin Cell Dev Biol* **23**, 946–953 (2012).
9. Schmidt-Ullrich, R. & Paus, R. Molecular principles of hair follicle induction and morphogenesis. *Bioessays* **27**, 247–261 (2005).
10. Shimomura, Y. & Christiano, A. M. Biology and genetics of hair. *Annu Rev Genomics Hum Genet* **11**, 109–132 (2010).
11. Jing, J. *et al.* Expression of decorin throughout the murine hair follicle cycle: hair cycle dependence and anagen phase prolongation. *Exp Dermatol* **23**, 486–491 (2014).
12. Paus, R. & Foitzik, K. In search of the 'hair cycle clock': a guided tour. *Differentiation* **72**, 489–511 (2004).

13. Poblet, E., Ortega, F. & Jiménez, F. The arrector pili muscle and the follicular unit of the scalp: a microscopic anatomy study. *Dermatol Surg* **28**, 800–803 (2002).

14. Purba, T. S. *et al.* Human epithelial hair follicle stem cells and their progeny: current state of knowledge, the widening gap in translational research and future challenges. *Bioessays* **36**, 513–525 (2014).

15. Schneider, M. R. The first description of the hair follicle bulge by Franz von Leydig. *Dermatology* **223**, 29–31 (2011).

16. Langbein, L. & Schweizer, J. Keratins of the human hair follicle. *Int Rev Cytol* **243**, 1–78 (2005).

17. Moll, R., Divo, M. & Langbein, L. The human keratins: biology and pathology. *Histochem Cell Biol* **129**, 705–733 (2008).

18. Panteleyev, A. A., Jahoda, C. A. & Christiano, A. M. Hair follicle predetermination. *J Cell Sci* **114**, 3419–3431 (2001).

19. Slominski, A. *et al.* Hair follicle pigmentation. *J Invest Dermatol* **124**, 13–21 (2005).

20. Tobin, D. J. The cell biology of human hair follicle pigmentation. *Pigment Cell Melanoma Res* **24**, 75–88 (2011).

21. Alonso, L. & Fuchs, E. The hair cycle. *J. Cell. Sci.* **119**, 391–393 (2006).

22. Panteleyev, A. A. Putting the Human Hair Follicle Cycle on the Map. *J. Invest. Dermatol.* **136**, 4–6 (2016).

23. Paus, R. & Cotsarelis, G. The biology of hair follicles. *N. Engl. J. Med.* **341**, 491–497 (1999).

24. Blanpain, C., Lowry, W. E., Geoghegan, A., Polak, L. & Fuchs, E. Self-renewal, multipotency, and the existence of two cell populations within an epithelial stem cell niche. *Cell* **118**, 635–648 (2004).

25. Botchkarev, V. A. & Kishimoto, J. Molecular control of epithelial-mesenchymal interactions during hair follicle cycling. *J. Investig. Dermatol. Symp. Proc.* **8**, 46–55 (2003).

26. Inui, S., Fukuzato, Y., Nakajima, T., Yoshikawa, K. & Itami, S. Identification of androgen-inducible TGF-beta1 derived from dermal papilla cells as a key mediator in androgenetic alopecia. *J. Investig. Dermatol. Symp. Proc.* **8**, 69–71 (2003).

27. Paladini, R. D., Saleh, J., Qian, C., Xu, G.-X. & Rubin, L. L. Modulation of Hair Growth with Small Molecule Agonists of the Hedgehog Signaling Pathway. *Journal of Investigative Dermatology* **125**, 638–646 (2005).

28. Plikus, M. V. *et al.* Cyclic dermal BMP signalling regulates stem cell activation during hair regeneration. *Nature* **451**, 340–344 (2008).

29. Kimura-Ueki, M. *et al.* Hair cycle resting phase is regulated by cyclic epithelial FGF18 signaling. *J. Invest. Dermatol.* **132**, 1338–1345 (2012).

30. Hsu, Y.-C., Pasolli, H. A. & Fuchs, E. Dynamics between stem cells, niche, and progeny in the hair follicle. *Cell* **144**, 92–105 (2011).

31. Botchkarev, V. A. *et al.* Noggin is required for induction of the hair follicle growth phase in postnatal skin. *FASEB J.* **15**, 2205–2214 (2001).

32. Greco, V. *et al.* A two-step mechanism for stem cell activation during hair regeneration. *Cell Stem Cell* **4**, 155–169 (2009).

33. Oshimori, N. & Fuchs, E. Paracrine TGF-β signaling counterbalances BMP-mediated repression in hair follicle stem cell activation. *Cell Stem Cell* **10**, 63–75 (2012).

34. Plikus, M. V. *et al.* Self-organizing and stochastic behaviors during the regeneration of hair stem cells. *Science* **332**, 586–589 (2011).

35. Zhou, L. *et al.* Activation of β-Catenin Signaling in CD133-Positive Dermal Papilla Cells Drives Postnatal Hair Growth. *PLoS ONE* **11**, e0160425 (2016).

36. Botchkarev, V. A. & Paus, R. Molecular biology of hair morphogenesis: development and cycling. *J. Exp. Zool. B Mol. Dev. Evol.* **298**, 164–180 (2003).

37. Hibberts, N. A., Messenger, A. G. & Randall, V. A. Dermal papilla cells derived from beard hair follicles secrete more stem cell factor (SCF) in culture than scalp cells or dermal fibroblasts. *Biochem. Biophys. Res. Commun.* **222**, 401–405 (1996).

38. Peters, E. M. J. *et al.* Kit is expressed by epithelial cells in vivo. *J. Invest. Dermatol.* **121**, 976–984 (2003).

39. Kawano, M. *et al.* Comprehensive analysis of FGF and FGFR expression in skin: FGF18 is highly expressed in hair follicles and capable of inducing anagen from telogen stage hair follicles. *J. Invest. Dermatol.* **124**, 877–885 (2005).

40. Cotsarelis, G. & Millar, S. E. Towards a molecular understanding of hair loss and its treatment. *Trends Mol Med* **7**, 293–301 (2001).

41. Kamimura, A. & Takahashi, T. Procyanidin B-3, isolated from barley and identified as a hair-growth stimulant, has the potential to counteract inhibitory regulation by TGF-beta1. *Exp. Dermatol.* **11**, 532–541 (2002).

42. Randall, V. & Botchkareva, N. The Biology of Hair Growth. in *Cosmetic Applications of Laser and Light-Based Systems* 3–35 (2009). doi:10.1016/B978-0-8155-1572-2.50006-3.

43. Trüeb, R. M. Molecular mechanisms of androgenetic alopecia. *Exp. Gerontol.* **37**, 981–990 (2002).

44. Chiang, C. *et al.* Essential role for Sonic hedgehog during hair follicle morphogenesis. *Dev. Biol.* **205**, 1–9 (1999).

45. Oro, A. E. *et al.* Basal cell carcinomas in mice overexpressing sonic hedgehog. *Science* **276**, 817–821 (1997).

46. DasGupta, R. & Fuchs, E. Multiple roles for activated LEF/TCF transcription complexes during hair follicle development and differentiation. *Development* **126**, 4557–4568 (1999).

47. Zhou, P., Byrne, C., Jacobs, J. & Fuchs, E. Lymphoid enhancer factor 1 directs hair follicle patterning and epithelial cell fate. *Genes Dev.* **9**, 700–713 (1995).

48. Wilson, N., Hynd, P. I. & Powell, B. C. The role of BMP-2 and BMP-4 in follicle initiation and the murine hair cycle. *Exp. Dermatol.* **8**, 367–368 (1999).

49. Ito, M., Kizawa, K., Hamada, K. & Cotsarelis, G. Hair follicle stem cells in the lower bulge form the secondary germ, a biochemically distinct but functionally equivalent progenitor cell population, at the termination of catagen. *Differentiation* **72**, 548–557 (2004).

50. Müller-Röver, S. *et al.* A comprehensive guide for the accurate classification of murine hair follicles in distinct hair cycle stages. *J Invest Dermatol* **117**, 3–15 (2001).

51. Zhang, Y. V., Cheong, J., Ciapurin, N., McDermitt, D. J. & Tumbar, T. Distinct self-renewal and differentiation phases in the niche of infrequently dividing hair follicle stem cells. *Cell Stem Cell* **5**, 267–278 (2009).

52. Blanpain, C. & Fuchs, E. Epidermal homeostasis: a balancing act of stem cells in the skin. *Nat. Rev. Mol. Cell Biol.* **10**, 207–217 (2009).

53. Sinclair, R. Male pattern androgenetic alopecia. *BMJ* **317**, 865–869 (1998).

54. Vañó-Galván, S. *et al.* Frequency of the Types of Alopecia at Twenty-Two Specialist Hair Clinics: A Multicenter Study. *Skin Appendage Disord* **5**, 309–315 (2019).

55. Hamilton, J. B. Patterned Loss of Hair in Man: Types and Incidence. *Annals of the New York Academy of Sciences* **53**, 708–728 (1951).

56. Kim, J. Y., Kim, M. H., Hong, S. P. & Park, B. C. Characteristics of nonbalding scalp zones of androgenetic alopecia in East Asians. *Clinical and Experimental Dermatology* **40**, 279–285 (2015).

57. Norwood, O. T. Male pattern baldness: classification and incidence. *South. Med. J.* **68**, 1359–1365 (1975).

58. Inui, S. Trichoscopy for common hair loss diseases: algorithmic method for diagnosis. *J Dermatol* **38**, 71–75 (2011).

59. Inui, S. Trichoscopy: a new frontier for the diagnosis of hair diseases. *Expert Review of Dermatology* **7**, 429–437 (2012).

60. Lacarrubba, F., Micali, G. & Tosti, A. Scalp dermoscopy or trichoscopy. *Curr Probl Dermatol* **47**, 21–32 (2015).

61. Whiting, D. A. Possible mechanisms of miniaturization during androgenetic alopecia or pattern hair loss. *J. Am. Acad. Dermatol.* **45**, S81-86 (2001).

62. Miranda, B. H., Tobin, D. J., Sharpe, D. T. & Randall, V. A. Intermediate hair follicles: a new more clinically relevant model for hair growth investigations. *Br. J. Dermatol.* **163**, 287–295 (2010).

63. Ellis, J. A., Sinclair, R. & Harrap, S. B. Androgenetic alopecia: pathogenesis and potential for therapy. *Expert Rev Mol Med* **4**, 1–11 (2002).

64. Guarrera, M. & Rebora, A. The Higher Number and Longer Duration of Kenogen Hairs Are the Main Cause of the Hair Rarefaction in Androgenetic Alopecia. *Skin Appendage Disord* **5**, 152–154 (2019).

65. Kaufman, K. D. Androgens and alopecia. *Molecular and Cellular Endocrinology* **198**, 89–95 (2002).

66. Fischer, T. W., Hipler, U. C. & Elsner, P. Effect of caffeine and testosterone on the proliferation of human hair follicles in vitro. *Int. J. Dermatol.* **46**, 27–35 (2007).

67. Fischer, T. W. *et al.* Differential effects of caffeine on hair shaft elongation, matrix and outer root sheath keratinocyte proliferation, and transforming growth factor-β2/insulin-like growth factor-1-mediated regulation of the hair cycle in male and female human hair follicles in vitro. *Br. J. Dermatol.* **171**, 1031–1043 (2014).

68. Kwack, M. H., Ahn, J. S., Kim, M. K., Kim, J. C. & Sung, Y. K. Dihydrotestosterone-Inducible IL-6 Inhibits Elongation of Human Hair Shafts by Suppressing Matrix Cell Proliferation and Promotes Regression of Hair Follicles in Mice. *J Invest Dermatol* **132**, 43–49 (2012).

69. Randall, V. A. Androgens and hair growth. *Dermatol Ther* **21**, 314–328 (2008).

70. El-Domyati, M., Attia, S., Saleh, F. & Abdel-Wahab, H. Androgenetic alopecia in males: a histopathological and ultrastructural study. *J Cosmet Dermatol* **8**, 83–91 (2009).

71. Whiting, D. A. Diagnostic and predictive value of horizontal sections of scalp biopsy specimens in male pattern androgenetic alopecia. *J. Am. Acad. Dermatol.* **28**, 755–763 (1993).

72. Sueki, H., Stoudemayer, T., Kligman, A. M. & Murphy, G. F. Quantitative and ultrastructural analysis of inflammatory infiltrates in male pattern alopecia. *Acta Derm. Venereol.* **79**, 347–350 (1999).

73. Jaworsky, C., Kligman, A. M. & Murphy, G. F. Characterization of inflammatory infiltrates in male pattern alopecia: implications for pathogenesis. *British Journal of Dermatology* **127**, 239–246 (1992).

74. Klein, L. M., Lavker, R. M., Matis, W. L. & Murphy, G. F. Degranulation of human mast cells induces an endothelial antigen central to leukocyte adhesion. *Proc Natl Acad Sci U S A* **86**, 8972–8976 (1989).

75. Sinclair, R. Androgenetic alopecia. Modelling progression and regrowth. *Exp. Dermatol.* **25**, 424–425 (2016).

76. Ayob, S. M. & Messenger, A. G. Androgens, hair loss and eugenics: a tale of discovery and American social history. *Exp. Dermatol.* **24**, 412–413 (2015).

77. Bayne, E. K. *et al.* Immunohistochemical localization of types 1 and 2 5alpha-reductase in human scalp. *Br. J. Dermatol.* **141**, 481–491 (1999).

78. Poór, V., Juricskay, S. & Telegdy, E. Urinary steroids in men with male-pattern alopecia. *J. Biochem. Biophys. Methods* **53**, 123–130 (2002).

79. Bang, H. J. *et al.* Comparative studies on level of androgens in hair and plasma with premature male-pattern baldness. *J Dermatol Sci* **34**, 11–16 (2004).

80. Fernandes, A. L. *et al.* Effect of time of day on performance, hormonal and metabolic response during a 1000-M cycling time trial. *PLoS One* **9**, e109954 (2014).

81. Guo, H., Gao, W. V., Endo, H. & McElwee, K. J. Experimental and early investigational drugs for androgenetic alopecia. *Expert Opin Investig Drugs* **26**, 917–932 (2017).

82. Harman, S. M. *et al.* Longitudinal effects of aging on serum total and free testosterone levels in healthy men. Baltimore Longitudinal Study of Aging. *J. Clin. Endocrinol. Metab.* **86**, 724–731 (2001).

83. Lis-Święty, A., Arasiewicz, H., Ranosz-Janicka, I. & Brzezińska-Wcisło, L. Serum androgens and prostate-specific antigen levels in androgenetic alopecia: is there a difference between frontal and vertex baldness? *J Eur Acad Dermatol Venereol* **32**, 1815–1818 (2018).

84. Vierhapper, H., Nowotny, P., Maier, H. & Waldhäusl, W. Production rates of dihydrotestosterone in healthy men and women and in men with male pattern baldness: determination by stable isotope/dilution and mass spectrometry. *J Clin Endocrinol Metab* **86**, 5762–5764 (2001).

85. Brown, W. A., Monti, P. M. & Corriveau, D. P. Serum testosterone and sexual activity and interest in men. *Arch Sex Behav* **7**, 97–103 (1978).

86. Horton, R., Shinsako, J. & Forsham, P. H. TESTOSTERONE PRODUCTION AND METABOLIC CLEARANCE RATES WITH VOLUMES OF DISTRIBUTION IN NORMAL ADULT MEN AND WOMEN. *Acta Endocrinol (Copenh)* **48**, 446–458 (1965).

87. Southren, A. L., Tochimoto, S., Carmody, N. C. & Isurugi, K. Plasma production rates of testosterone in normal adult men and women and in patients with the syndrome of feminizing testes. *J Clin Endocrinol Metab* **25**, 1441–1450 (1965).

88. Zhang, Y., Xu, J., Jing, J., Wu, X. & Lv, Z. Serum Levels of Androgen-Associated Hormones Are Correlated with Curative Effect in Androgenic Alopecia in Young Men. *Med Sci Monit* **24**, 7770–7777 (2018).

89. Sawaya, M. E. & Price, V. H. Different levels of 5alpha-reductase type I and II, aromatase, and androgen receptor in hair follicles of women and men with androgenetic alopecia. *J. Invest. Dermatol.* **109**, 296–300 (1997).

90. Ando, Y., Yamaguchi, Y., Hamada, K., Yoshikawa, K. & Itami, S. Expression of mRNA for androgen receptor, 5alpha-reductase and 17beta-hydroxysteroid dehydrogenase in human dermal papilla cells. *Br. J. Dermatol.* **141**, 840–845 (1999).

91. Ceruti, J. M., Leirós, G. J. & Balañá, M. E. Androgens and androgen receptor action in skin and hair follicles. *Mol. Cell. Endocrinol.* **465**, 122–133 (2018).

92. Kwon, O. S. *et al.* Expression of androgen receptor, estrogen receptor alpha and beta in the dermal papilla of human hair follicles in vivo. *J. Dermatol. Sci.* **36**, 176–179 (2004).

93. Randall, V. A., Thornton, M. J., Hamada, K. & Messenger, A. G. Mechanism of androgen action in cultured dermal papilla cells derived from human hair follicles with varying responses to androgens in vivo. *J. Invest. Dermatol.* **98**, 86S-91S (1992).

94. Hasegawa, T. *et al.* Developmental roles of the steroidogenic acute regulatory protein (StAR) as revealed by StAR knockout mice. *Mol. Endocrinol.* **14**, 1462–1471 (2000).

95. Patel, M. V., McKay, I. A. & Burrin, J. M. Transcriptional regulators of steroidogenesis, DAX-1 and SF-1, are expressed in human skin. *J. Invest. Dermatol.* **117**, 1559–1565 (2001).

96. Palmer, M. A., Blakeborough, L., Harries, M. & Haslam, I. S. Cholesterol homeostasis: Links to hair follicle biology and hair disorders. *Experimental Dermatology* **29**, 299–311 (2020).

97. Inui, S. & Itami, S. Androgen actions on the human hair follicle: perspectives. *Exp. Dermatol.* **22**, 168–171 (2013).

98. Inui, S., Fukuzato, Y., Nakajima, T., Yoshikawa, K. & Itami, S. Androgen-inducible TGF-beta1 from balding dermal papilla cells inhibits epithelial cell growth: a clue to understand paradoxical effects of androgen on human hair growth. *FASEB J.* **16**, 1967–1969 (2002).

99. Foitzik, K. *et al.* Control of murine hair follicle regression (catagen) by TGF-beta1 in vivo. *FASEB J.* **14**, 752–760 (2000).

100. Itami, S., Kurata, S. & Takayasu, S. Androgen induction of follicular epithelial cell growth is mediated via insulin-like growth factor-I from dermal papilla cells. *Biochem. Biophys. Res. Commun.* **212**, 988–994 (1995).

101. Philpott, M. P., Sanders, D. A. & Kealey, T. Effects of insulin and insulin-like growth factors on cultured human hair follicles: IGF-I at physiologic concentrations is an important regulator of hair follicle growth in vitro. *J. Invest. Dermatol.* **102**, 857–861 (1994).

102. Rhie, A. *et al.* Genetic variations associated with response to dutasteride in the treatment of male subjects with androgenetic alopecia. *PLoS ONE* **14**, e0222533 (2019).

103. Dhurat, R. *et al.* 5-Alpha reductase inhibitors in androgenetic alopecia: Shifting paradigms, current concepts, comparative efficacy, and safety. *Dermatologic Therapy* **33**, e13379 (2020).

104. Shanshanwal, S. J. S. & Dhurat, R. S. Superiority of dutasteride over finasteride in hair regrowth and reversal of miniaturization in men with androgenetic alopecia: A randomized controlled open-label, evaluator-blinded study. *Indian J Dermatol Venereol Leprol* **83**, 47–54 (2017).

105. Vañó-Galván, S. *et al.* Effectiveness and safety of oral dutasteride for male androgenetic alopecia in real clinical practice: A descriptive monocentric study. *Dermatol Ther* **33**, e13182 (2020).

106. Martinez-Jacobo, L. A. *et al.* Global Expression Profile and Global Genome Methylation Signatures in Male Patients with Androgenetic Alopecia. *J Eur Acad Dermatol Venereol* (2019) doi:10.1111/jdv.16169.

107. Penning, T. M. Mechanisms of drug resistance that target the androgen axis in castration resistant prostate cancer (CRPC). *J. Steroid Biochem. Mol. Biol.* **153**, 105–113 (2015).

108. Chéret, J. *et al.* Olfactory receptor OR2AT4 regulates human hair growth. *Nat Commun* **9**, 3624 (2018).

109. Hochfeld, L. M. *et al.* Insights into Male Androgenetic Alopecia: Differential Gene Expression Profiling of Plucked Hair Follicles and Integration with Genetic Data. *J. Invest. Dermatol.* **139**, 235–238 (2019).

110. Plikus, M. V. *et al.* Local circadian clock gates cell cycle progression of transient amplifying cells during regenerative hair cycling. *Proc Natl Acad Sci U S A* **110**, E2106–E2115 (2013).

111. Estrach, S., Cordes, R., Hozumi, K., Gossler, A. & Watt, F. M. Role of the Notch ligand Delta1 in embryonic and adult mouse epidermis. *J Invest Dermatol* **128**, 825–832 (2008).

112. Geyfman, M., Plikus, M. V., Treffeisen, E., Andersen, B. & Paus, R. Resting no more: re-defining telogen, the maintenance stage of the hair growth cycle. *Biol Rev Camb Philos Soc* **90**, 1179–1196 (2015).

113. Higgins, C. A., Westgate, G. E. & Jahoda, C. A. B. From telogen to exogen: mechanisms underlying formation and subsequent loss of the hair club fiber. *J. Invest. Dermatol.* **129**, 2100–2108 (2009).

114. Agabalyan, N. A., Rosin, N. L., Rahmani, W. & Biernaskie, J. Hair follicle dermal stem cells and skin-derived precursor cells: Exciting tools for endogenous and exogenous therapies. *Exp Dermatol* **26**, 505–509 (2017).

115. Rahmani, W. *et al.* Hair follicle dermal stem cells regenerate the dermal sheath, repopulate the dermal papilla, and modulate hair type. *Dev Cell* **31**, 543–558 (2014).

116. Tobin, D. J., Gunin, A., Magerl, M., Handijski, B. & Paus, R. Plasticity and cytokinetic dynamics of the hair follicle mesenchyme: implications for hair growth control. *J. Invest. Dermatol.* **120**, 895–904 (2003).

117. Torkamani, N., Rufaut, N. W., Jones, L. & Sinclair, R. Destruction of the arrector pili muscle and fat infiltration in androgenic alopecia. *Br J Dermatol* **170**, 1291–1298 (2014).

118. Yazdabadi, A., Whiting, D., Rufaut, N. & Sinclair, R. Miniaturized Hairs Maintain Contact with the Arrector Pili Muscle in Alopecia Areata but not in Androgenetic Alopecia: A Model for Reversible Miniaturization and Potential for Hair Regrowth. *Int J Trichology* **4**, 154–157 (2012).

119. Kure, K., Isago, T. & Hirayama, T. Changes in the sebaceous gland in patients with male pattern hair loss (androgenic alopecia). *J Cosmet Dermatol* **14**, 178–184 (2015).

120. Pantelireis, N. & Higgins, C. A. A bald statement - Current approaches to manipulate miniaturisation focus only on promoting hair growth. *Exp. Dermatol.* **27**, 959–965 (2018).

121. Paus, R. Therapeutic strategies for treating hair loss. *Drug Discovery Today: Therapeutic Strategies* **3**, 101–110 (2006).

122. Heilmann, S. *et al.* Androgenetic alopecia: identification of four genetic risk loci and evidence for the contribution of WNT signaling to its etiology. *J. Invest. Dermatol.* **133**, 1489–1496 (2013).

123. Ryu, S. *et al.* Mycophenolate antagonizes IFN-γ-induced catagen-like changes via β-catenin activation in human dermal papilla cells and hair follicles. *Int J Mol Sci* **15**, 16800–16815 (2014).

124. Hawkshaw, N. J. *et al.* Identifying novel strategies for treating human hair loss disorders: Cyclosporine A suppresses the Wnt inhibitor, SFRP1, in the dermal papilla of human scalp hair follicles. *PLoS Biol* **16**, e2003705 (2018).

125. Hawkshaw, N. J., Hardman, J. A., Alam, M., Jimenez, F. & Paus, R. Deciphering the molecular morphology of the human hair cycle: Wnt signalling during the telogen-anagen transformation. *Br J Dermatol* **182**, 1184–1193 (2020).

126. Lin, Z. *et al.* The pseudoreceptor BMP and activin membrane-bound inhibitor positively modulates Wnt/beta-catenin signaling. *J Biol Chem* **283**, 33053–33058 (2008).

127. Sekiya, T., Oda, T., Matsuura, K. & Akiyama, T. Transcriptional regulation of the TGF-beta pseudoreceptor BAMBI by TGF-beta signaling. *Biochem Biophys Res Commun* **320**, 680–684 (2004).

128. Fawzi, M. M. T., Mahmoud, S. B., Shaker, O. G. & Saleh, M. A. Assessment of tissue levels of dickkopf-1 in androgenetic alopecia and alopecia areata. *J Cosmet Dermatol* **15**, 10–15 (2016).

129. Kwack, M. H. *et al.* Dihydrotestosterone-inducible dickkopf 1 from balding dermal papilla cells causes apoptosis in follicular keratinocytes. *J. Invest. Dermatol.* **128**, 262–269 (2008).

130. Mahmoud, E. A., Elgarhy, L. H., Hasby, E. A. & Mohammad, L. Dickkopf-1 Expression in Androgenetic Alopecia and Alopecia Areata in Male Patients. *Am J Dermatopathol* **41**, 122–127 (2019).

131. Deplewski, D. & Rosenfield, R. L. Role of hormones in pilosebaceous unit development. *Endocr. Rev.* **21**, 363–392 (2000).

132. Marshall, W. A. & Tanner, J. M. Variations in the Pattern of Pubertal Changes in Boys. *Arch Dis Child* **45**, 13–23 (1970).

133. Elliott, K., Stephenson, T. J. & Messenger, A. G. Differences in hair follicle dermal papilla volume are due to extracellular matrix volume and cell number: implications for the control of hair follicle size and androgen responses. *J Invest Dermatol* **113**, 873–877 (1999).

134. Cotsarelis, G. Gene expression profiling gets to the root of human hair follicle stem cells. *J. Clin. Invest.* **116**, 19–22 (2006).

135. Chi, W., Wu, E. & Morgan, B. A. Dermal papilla cell number specifies hair size, shape and cycling and its reduction causes follicular decline. *Development* **140**, 1676–1683 (2013).

136. Tsuboi, R. *et al.* Autologous cell-based therapy for male and female pattern hair loss using dermal sheath cup cells: A randomized placebo-controlled double-blinded dose-finding clinical study. *J. Am. Acad. Dermatol.* **83**, 109–116 (2020).

137. Cranwell, W. & Sinclair, R. Male Androgenetic Alopecia. in *Endotext* (eds. Feingold, K. R. et al.) (MDText.com, Inc., 2000).

138. Pirastu, N. *et al.* GWAS for male-pattern baldness identifies 71 susceptibility loci explaining 38% of the risk. *Nat Commun* **8**, 1584 (2017).

139. Nyholt, D. R., Gillespie, N. A., Heath, A. C. & Martin, N. G. Genetic basis of male pattern baldness. *J. Invest. Dermatol.* **121**, 1561–1564 (2003).

140. Chumlea, W. C. *et al.* Family history and risk of hair loss. *Dermatology (Basel)* **209**, 33–39 (2004).

141. Goren, A. *et al.* Social selection favours offspring prone to the development of androgenetic alopecia. *J. Biol. Regul. Homeost. Agents* **31**, 1013–1016 (2017).

142. Yap, C. X. *et al.* Misestimation of heritability and prediction accuracy of male-pattern baldness. *Nat Commun* **9**, (2018).

143. Prodi, D. A. *et al.* EDA2R is associated with androgenetic alopecia. *J. Invest. Dermatol.* **128**, 2268–2270 (2008).

144. Hayes, V. M. *et al.* The E211 G>A androgen receptor polymorphism is associated with a decreased risk of metastatic prostate cancer and androgenetic alopecia. *Cancer Epidemiol. Biomarkers Prev.* **14**, 993–996 (2005).

145. Hillmer, A. M. *et al.* Genetic variation in the human androgen receptor gene is the major determinant of common early-onset androgenetic alopecia. *Am. J. Hum. Genet.* **77**, 140–148 (2005).

146. Levy-Nissenbaum, E., Bar-Natan, M., Frydman, M. & Pras, E. Confirmation of the association between male pattern baldness and the androgen receptor gene. *Eur J Dermatol* **15**, 339–340 (2005).

147. Ghassemi, M., Ghaffarpour, G. H. & Ghods, S. The effect of GGC and CAG repeat polymorphisms on the androgen receptor gene in response to finasteride therapy in men with androgenetic alopecia. *J Res Med Sci* **24**, 104 (2019).

148. Azzouni, F., Godoy, A., Li, Y. & Mohler, J. The 5 alpha-reductase isozyme family: a review of basic biology and their role in human diseases. *Adv Urol* **2012**, 530121 (2012).

149. Heilmann-Heimbach, S., Hochfeld, L. M., Paus, R. & Nöthen, M. M. Hunting the genes in male-pattern alopecia: how important are they, how close are we and what will they tell us? *Exp. Dermatol.* **25**, 251–257 (2016).

150. Hillmer, A. M. *et al.* Susceptibility variants for male-pattern baldness on chromosome 20p11. *Nat. Genet.* **40**, 1279–1281 (2008).

151. Liu, F. *et al.* Prediction of male-pattern baldness from genotypes. *Eur. J. Hum. Genet.* **24**, 895–902 (2016).

152. Richards, J. B. *et al.* Male-pattern baldness susceptibility locus at 20p11. *Nat Genet* **40**, 1282–1284 (2008).

153. Hagenaars, S. P. *et al.* Genetic prediction of male pattern baldness. *PLoS Genet.* **13**, e1006594 (2017).

154. Heilmann-Heimbach, S. *et al.* Meta-analysis identifies novel risk loci and yields systematic insights into the biology of male-pattern baldness. *Nat Commun* **8**, 14694 (2017).

155. Puc, J. *et al.* Ligand-dependent enhancer activation regulated by topoisomerase-I activity. *Cell* **160**, 367–380 (2015).

156. Dey-Rao, R. & Sinha, A. A. A genomic approach to susceptibility and pathogenesis leads to identifying potential novel therapeutic targets in androgenetic alopecia. *Genomics* **109**, 165–176 (2017).

157. Brockschmidt, F. F. *et al.* Susceptibility variants on chromosome 7p21.1 suggest HDAC9 as a new candidate gene for male-pattern baldness. *The British Journal of Dermatology* **165**, 1293–1302 (2011).

158. Ellis, J. A., Panagiotopoulos, S., Akdeniz, A., Jerums, G. & Harrap, S. B. Androgenic correlates of genetic variation in the gene encoding 5alpha-reductase type 1. *J Hum Genet* **50**, 534–537 (2005).

159. Hillmer, A. M. *et al.* Genome-wide scan and fine-mapping linkage study of androgenetic alopecia reveals a locus on chromosome 3q26. *Am. J. Hum. Genet.* **82**, 737–743 (2008).

160. Mirmirani, P. *et al.* Similar Response Patterns to 5%Topical Minoxidil Foam in Frontal and Vertex Scalp of Men with Androgenetic Alopecia: A Microarray Analysis. *Br J Dermatol* **172**, 1555–1561 (2015).

161. Festa, E. *et al.* Adipocyte lineage cells contribute to the skin stem cell niche to drive hair cycling. *Cell* **146**, 761–771 (2011).

162. Higgins, C. A. *et al.* FGF5 is a crucial regulator of hair length in humans. *Proc. Natl. Acad. Sci. U.S.A.* **111**, 10648–10653 (2014).

163. Lei, M. *et al.* Modulating hair follicle size with Wnt10b/DKK1 during hair regeneration. *Exp. Dermatol.* **23**, 407–413 (2014).

164. Platz, E. A., Pollak, M. N., Willett, W. C. & Giovannucci, E. Vertex balding, plasma insulin-like growth factor 1, and insulin-like growth factor binding protein 3. *J Am Acad Dermatol* **42**, 1003–1007 (2000).

165. Schmidt, B. A. & Horsley, V. Intradermal adipocytes mediate fibroblast recruitment during skin wound healing. *Development* **140**, 1517–1527 (2013).

166. Li, R. *et al.* Six novel susceptibility Loci for early-onset androgenetic alopecia and their unexpected association with common diseases. *PLoS genetics* **8**, e1002746 (2012).

167. Han, J. *et al.* A Genome-Wide Association Study Identifies Novel Alleles Associated with Hair Color and Skin Pigmentation. *PLoS Genet* **4**, (2008).

168. Mella, J. M., Perret, M. C., Manzotti, M., Catalano, H. N. & Guyatt, G. Efficacy and safety of finasteride therapy for androgenetic alopecia: a systematic review. *Arch Dermatol* **146**, 1141–1150 (2010).

169. Rossi, A. *et al.* Finasteride, 1 mg daily administration on male androgenetic alopecia in different age groups: 10-year follow-up. *Dermatol Ther* **24**, 455–461 (2011).

170. Rossi, A. *et al.* Multi-therapies in androgenetic alopecia: review and clinical experiences. *Dermatol Ther* **29**, 424–432 (2016).

171. Chen, K.-Y. *et al.* Androgenetic alopecia is associated with increased scalp hardness. *J Eur Acad Dermatol Venereol* (2020) doi:10.1111/jdv.16194.

172. Diani, A. R. *et al.* Hair growth effects of oral administration of finasteride, a steroid 5 alpha-reductase inhibitor, alone and in combination with topical minoxidil in the balding stumptail macaque. *J. Clin. Endocrinol. Metab.* **74**, 345–350 (1992).

173. Bunagan, M. J. K., Banka, N. & Shapiro, J. Hair transplantation update: procedural techniques, innovations, and applications. *Dermatol Clin* **31**, 141–153 (2013).

174. Jiménez-Acosta, F. & Ponce, I. [Follicular unit hair transplantation: current technique]. *Actas Dermosifiliogr* **101**, 291–306 (2010).

175. Vogel, J. E. *et al.* Hair restoration surgery: the state of the art. *Aesthet Surg J* **33**, 128–151 (2013).

176. Dicle, Ö., Bilgic Temel, A. & Gülkesen, K. H. Platelet-rich plasma injections in the treatment of male androgenetic alopecia: A randomized placebo-controlled crossover study. *J Cosmet Dermatol* **19**, 1071–1077 (2020).

177. Gentile, P. & Garcovich, S. Autologous activated platelet-rich plasma (AA-PRP) and non-activated (A-PRP) in hair growth: a retrospective, blinded, randomized evaluation in androgenetic alopecia. *Expert Opin Biol Ther* **20**, 327–337 (2020).

178. Paththinige, N. D., Akarawita, J. K. W. & Jeganathan, G. The Clinical Efficacy and Safety of Autologous Activated Platelet-Rich Plasma Injection in Androgenetic Alopecia. *Skin Appendage Disord* **6**, 19–24 (2020).

179. Siah, T. W. *et al.* Growth factor concentrations in platelet-rich plasma for androgenetic alopecia: An intra-subject, randomized, blinded, placebo-controlled, pilot study. *Exp. Dermatol.* **29**, 334–340 (2020).

180. Suchonwanit, P., Chalermroj, N. & Khunkhet, S. Low-level laser therapy for the treatment of androgenetic alopecia in Thai men and women: a 24-week, randomized, double-blind, sham device-controlled trial. *Lasers Med Sci* **34**, 1107–1114 (2019).

181. Yoon, J. S., Ku, W. Y., Lee, J. H. & Ahn, H. C. Low-level light therapy using a helmet-type device for the treatment of androgenetic alopecia: A 16-week, multicenter, randomized, double-blind, sham device-controlled trial. *Medicine (Baltimore)* **99**, e21181 (2020).

182. Egger, A. *et al.* Examining the Safety and Efficacy of Low-Level Laser Therapy for Male and Female Pattern Hair Loss: A Review of the Literature. *Skin Appendage Disord* **6**, 259–267 (2020).

183. Fukuoka, H., Narita, K. & Suga, H. Hair Regeneration Therapy: Application of Adipose-Derived Stem Cells. *Curr Stem Cell Res Ther* **12**, 531–534 (2017).

184. Dhurat, R. *et al.* An Open-Label Randomized Multicenter Study Assessing the Noninferiority of a Caffeine-Based Topical Liquid 0.2% versus Minoxidil 5% Solution in Male Androgenetic Alopecia. *Skin Pharmacol Physiol* **30**, 298–305 (2018).

185. Fischer, T. W. *et al.* New effects of caffeine on CRH-induced stress along the intrafollicular classical HPA-axis (CRH-R1/2, IP3 -R, ACTH, MC-R2) and the neurogenic non-HPA-axis (substance P, p75NTR and TrkA) in ex vivo human male androgenetic scalp hair follicles. *Br. J. Dermatol.* (2020) doi:10.1111/bjd.19115.

186. Iwabuchi, T. *et al.* Topical adenosine increases the proportion of thick hair in Caucasian men with androgenetic alopecia. *J Dermatol* **43**, 567–570 (2016).

187. Lisztes, E. *et al.* Adenosine Promotes Human Hair Growth and Inhibits Catagen Transition In Vitro: Role of the Outer Root Sheath Keratinocytes. *J Invest Dermatol* **140**, 1085-1088.e6 (2020).

188. Auber, L. VII.—The Anatomy of Follicles Producing Wool-Fibres, with special reference to Keratinization. *Earth and Environmental Science Transactions of The Royal Society of Edinburgh* **62**, 191–254 (1952).

189. Eschbach, S., Hofmann, C., Maerz, M., Maier, U.-G. & Sitte, P. Molecular Cloning. A Laboratory Manual. 2. Auflage. Hrsg. von J. Sambrook, E. F. Fritsch, T. Maniatis, Cold Spring Harbor Laboratory Press, Cold Spring Harbour 1989, $ 115. ISBN 0-87969-309-6. *Biologie in unserer Zeit* **20**, 285–285 (1990).

190. Duan, W. R. *et al.* Comparison of immunohistochemistry for activated caspase-3 and cleaved cytokeratin 18 with the TUNEL method for quantification of apoptosis in histological sections of PC-3 subcutaneous xenografts. *J Pathol* **199**, 221–228 (2003).

191. Kockx, M. M. Apoptosis in the atherosclerotic plaque: quantitative and qualitative aspects. *Arterioscler Thromb Vasc Biol* **18**, 1519–1522 (1998).

192. Yang, Y. *et al.* Versican gene: regulation by the β-catenin signaling pathway plays a significant role in dermal papilla cell aggregative growth. *J Dermatol Sci* **68**, 157–163 (2012).

193. Soma, T., Tajima, M. & Kishimoto, J. Hair cycle-specific expression of versican in human hair follicles. *J Dermatol Sci* **39**, 147–154 (2005).

194. Baker, K. *et al.* SYT1-associated neurodevelopmental disorder: a case series. *Brain* **141**, 2576–2591 (2018).

195. Handjiski, B. K., Eichmüller, S., Hofmann, U., Czarnetzki, B. M. & Paus, R. Alkaline phosphatase activity and localization during the murine hair cycle. *Br J Dermatol* **131**, 303–310 (1994).

196. Caserini, M., Radicioni, M., Leuratti, C., Annoni, O. & Palmieri, R. A novel finasteride 0.25% topical solution for androgenetic alopecia: pharmacokinetics and effects on plasma androgen levels in healthy male volunteers. *Int J Clin Pharmacol Ther* **52**, 842–849 (2014).

197. Itami, S., Kurata, S. & Takayasu, S. 5 alpha-reductase activity in cultured human dermal papilla cells from beard compared with reticular dermal fibroblasts. *J. Invest. Dermatol.* **94**, 150–152 (1990).

198. Itami, S., Kurata, S., Sonoda, T. & Takayasu, S. Characterization of 5 alpha-reductase in cultured human dermal papilla cells from beard and occipital scalp hair. *J. Invest. Dermatol.* **96**, 57–60 (1991).

199. Kloepper, J. E. *et al.* Methods in hair research: how to objectively distinguish between anagen and catagen in human hair follicle organ culture. *Exp Dermatol* **19**, 305–312 (2010).

200. Khunkhet, S., Chanprapaph, K., Rutnin, S. & Suchonwanit, P. Histopathological Evidence of Occipital Involvement in Male Androgenetic Alopecia. *Frontiers in Medicine* **8**, (2021).

201. Ohyama, M., Zheng, Y., Paus, R. & Stenn, K. S. The mesenchymal component of hair follicle neogenesis: background, methods and molecular characterization. *Exp. Dermatol.* **19**, 89–99 (2010).

202. Iida, M., Ihara, S. & Matsuzaki, T. Hair cycle-dependent changes of alkaline phosphatase activity in the mesenchyme and epithelium in mouse vibrissal follicles. *Dev Growth Differ* **49**, 185–195 (2007).

203. Rendl, M., Lewis, L. & Fuchs, E. Molecular dissection of mesenchymal-epithelial interactions in the hair follicle. *PLoS Biol.* **3**, e331 (2005).

204. Ceruti, J. M., Oppenheimer, F. M., Leirós, G. J. & Balañá, M. E. Androgens downregulate BMP2 impairing the inductive role of dermal papilla cells on hair follicle stem cells differentiation. *Mol Cell Endocrinol* **520**, 111096 (2021).

205. Xu, X., Lai, Y. & Hua, Z.-C. Apoptosis and apoptotic body: disease message and therapeutic target potentials. *Biosci Rep* **39**, BSR20180992 (2019).

206. Kerr, J. F., Wyllie, A. H. & Currie, A. R. Apoptosis: a basic biological phenomenon with wide-ranging implications in tissue kinetics. *Br J Cancer* **26**, 239–257 (1972).

207. Botchkareva, N. V., Ahluwalia, G. & Shander, D. Apoptosis in the hair follicle. *J Invest Dermatol* **126**, 258–264 (2006).

208. Matsuo, K., Mori, O. & Hashimoto, T. Apoptosis in murine hair follicles during catagen regression. *Arch Dermatol Res* **290**, 133–136 (1998).

209. Soma, T., Ogo, M., Suzuki, J., Takahashi, T. & Hibino, T. Analysis of apoptotic cell death in human hair follicles in vivo and in vitro. *J Invest Dermatol* **111**, 948–954 (1998).

210. Lindner, G. *et al.* Analysis of apoptosis during hair follicle regression (catagen). *Am J Pathol* **151**, 1601–1617 (1997).

211. Peter, M. E., Heufelder, A. E. & Hengartner, M. O. Advances in apoptosis research. *Proc Natl Acad Sci U S A* **94**, 12736–12737 (1997).

212. Nicholson, D. W. *et al.* Identification and inhibition of the ICE/CED-3 protease necessary for mammalian apoptosis. *Nature* **376**, 37–43 (1995).

213. Wang, X., Penzes, P. & Napoli, J. L. Cloning of a cDNA encoding an aldehyde dehydrogenase and its expression in Escherichia coli. Recognition of retinal as substrate. *J Biol Chem* **271**, 16288–16293 (1996).

214. Zhao, D. *et al.* Molecular identification of a major retinoic-acid-synthesizing enzyme, a retinaldehyde-specific dehydrogenase. *Eur J Biochem* **240**, 15–22 (1996).

215. Okano, J. *et al.* Cutaneous retinoic acid levels determine hair follicle development and downgrowth. *J Biol Chem* **287**, 39304–39315 (2012).

216. Sharma, A. *et al.* Tretinoin enhances minoxidil response in androgenetic alopecia patients by upregulating follicular sulfotransferase enzymes. *Dermatol Ther* **32**, e12915 (2019).

217. Kwon, O. S. *et al.* Promotive effect of minoxidil combined with all-trans retinoic acid (tretinoin) on human hair growth in vitro. *J Korean Med Sci* **22**, 283–289 (2007).

218. Bazzano, G. S., Terezakis, N. & Galen, W. Topical tretinoin for hair growth promotion. *J Am Acad Dermatol* **15**, 880–883, 890–893 (1986).

219. Varney, S. D. *et al.* Hic-5 is required for myofibroblast differentiation by regulating mechanically dependent MRTF-A nuclear accumulation. *J Cell Sci* **129**, 774–787 (2016).

220. Heinlein, C. A. & Chang, C. Androgen receptor (AR) coregulators: an overview. *Endocr Rev* **23**, 175–200 (2002).

221. Heinlein, C. A. & Chang, C. The roles of androgen receptors and androgen-binding proteins in nongenomic androgen actions. *Mol Endocrinol* **16**, 2181–2187 (2002).

222. Leach, D. A. *et al.* Hic-5 influences genomic and non-genomic actions of the androgen receptor in prostate myofibroblasts. *Mol Cell Endocrinol* **384**, 185–199 (2014).

223. Inui, S., Fukuzato, Y., Nakajima, T., Kurata, S. & Itami, S. Androgen receptor co-activator Hic-5/ARA55 as a molecular regulator of androgen sensitivity in dermal papilla cells of human hair follicles. *J Invest Dermatol* **127**, 2302–2306 (2007).

224. Mouta Carreira, C., Landriscina, M., Bellum, S., Prudovsky, I. & Maciag, T. The comparative release of FGF1 by hypoxia and temperature stress. *Growth Factors* **18**, 277–285 (2001).

225. Song, J. S. *et al.* Comparative gene expression analysis of the human periodontal ligament in deciduous and permanent teeth. *PLoS One* **8**, e61231 (2013).

226. Siomi, H. & Siomi, M. C. On the road to reading the RNA-interference code. *Nature* **457**, 396–404 (2009).

227. Miranda, B. H., Charlesworth, M. R., Tobin, D. J., Sharpe, D. T. & Randall, V. A. Androgens trigger different growth responses in genetically identical human hair follicles in organ culture that reflect their epigenetic diversity in life. *FASEB J.* **32**, 795–806 (2018).

228. Ryu, Y. C. *et al.* KY19382, a novel activator of Wnt/β-catenin signalling, promotes hair regrowth and hair follicle neogenesis. *Br J Pharmacol* **178**, 2533–2546 (2021).

229. du Cros, D. L., LeBaron, R. G. & Couchman, J. R. Association of versican with dermal matrices and its potential role in hair follicle development and cycling. *J Invest Dermatol* **105**, 426–431 (1995).

230. Crowley, L. C., Marfell, B. J. & Waterhouse, N. J. Detection of DNA Fragmentation in Apoptotic Cells by TUNEL. *Cold Spring Harb Protoc* **2016**, (2016).

231. Gerdes, J., Schwab, U., Lemke, H. & Stein, H. Production of a mouse monoclonal antibody reactive with a human nuclear antigen associated with cell proliferation. *International Journal of Cancer* **31**, 13–20 (1983).

232. Lei, M., Gao, X., Yang, L., Yang, T. & Lian, X. Gsdma3 gene is needed for the induction of apoptosis-driven catagen during mouse hair follicle cycle. *Histochem Cell Biol* **136**, 335–343 (2011).

233. Garza, L. A. *et al.* Prostaglandin D2 inhibits hair growth and is elevated in bald scalp of men with androgenetic alopecia. *Sci Transl Med* **4**, 126ra34 (2012).

234. Premanand, A. & Rajkumari, B. R. In silico analysis of gene expression data from bald frontal and haired occipital scalp to identify candidate genes in male androgenetic alopecia. *Arch Dermatol Res* **311**, 815–824 (2019).

235. Wolbach, S. B. & Howe, P. R. TISSUE CHANGES FOLLOWING DEPRIVATION OF FAT-SOLUBLE A VITAMIN. *J Exp Med* **42**, 753–777 (1925).

236. Frazier, C. N. CUTANEOUS LESIONS ASSOCIATED WITH A DEFICIENCY IN VITAMIN A IN MAN. *Arch Intern Med* **48**, 507 (1931).

237. Randolph, R. K. & Simon, M. Dermal fibroblasts actively metabolize retinoic acid but not retinol. *J Invest Dermatol* **111**, 478–484 (1998).

238. Everts, H. B., King, L. E., Sundberg, J. P. & Ong, D. E. Hair Cycle-Specific Immunolocalization of Retinoic Acid Synthesizing Enzymes Aldh1a2 and Aldh1a3 Indicate Complex Regulation. *Journal of Investigative Dermatology* **123**, 258–263 (2004).

239. Nan, W. *et al.* All-trans-retinoic acid inhibits mink hair follicle growth via inhibiting proliferation and inducing apoptosis of dermal papilla cells through TGF-β2/Smad2/3 pathway. *Acta Histochem* **122**, 151603 (2020).

7 Abstract

Male pattern androgenetic alopecia (mpAGA) is the most prevalent form of pattern hair loss in men. The known most crucial driving force for its development is known to be testosterone (T). With the onset of puberty, the serum T level in the blood raises and hair follicles (HFs) from distinct affected (aff) scalp locations (vertex and frontal scalp) start to progressivley miniaturize. These HFs become less pigmented, thinner and are miniaturizing until becoming vellus HFs. From this stage on, this miniaturization is irreversible because the HFs lose their arrector pili muscle connection. On the other side, HFs from the occipital (occ) scalp were known to be insensitive to androgens and would not follow this typical disease pattern.

During this project, an *ex vivo* organ culture model which can be used to investigate the influence of T on mpAGA HFs from different scalp locations, was established.

HFs from the aff scalp of mpAGA patients are known to convert T to its much more potent metabolite dehydrotestosterone (DHT). This thesis shows, that HFs, treated with 30 nM T *ex vivo*, keep their ability to convert T to DHT.

Immunofluorescence staining analyses in this thesis gave interesting insights on the early consequeces of exposure to 30 nM T *ex vivo*, happening in intermediate (i) and terminal (t) HFs from the aff scalp as well as in t/ iHFs from the occ scalp. iHFs from the aff area showed a decreased number of dermal papilla (DP) fibroblasts accompanied by a decreased DP inductivity, whereas aff tHFs show an increased DP fibroblast emigration accompanied by a significantly induced apoptosis of cells in the inductive dermal cup (DC). Interestingly, i/ tHFs from the occ scalp showed also strong responses to T treatment *ex vivo*. Their response appeared to be more protective than destructive showing in a lower number of DC cells, as well as an increased proliferation of hair matrix keratinocytes (occ iHFs) but also a significantly reduced level of apoptosis in the DC of occ i/ tHFs.

Moreover, RNAseq analysis after 10 nM T treatment confirmed the impact of T on gene expression in HFs regardless their scalp location. These analyses confirmed, that occ HFs are not T insensitive as widely suggested.

Furthermore, the differential regulation of potential mpAGA target genes in defined compartments of mpAGA aff and occ HFs was investigated. The DP and DC from mpAGA patients' t and i aff and occ HFs were microdissected and processed with a laser capture microdissector. From those obtained samples it was possible to generate a transcriptomic profile of all mentioned types of HFs DPs and DCs.

Based on these analyses, two promising possible new target genes for mpAGA were chosen based on literature research and knocked down in healthy human occ tHFs *ex vivo* to understand their impact on the hair cycle.

The first investigated target gene was aldehyde dehydrogenase 1 family member A2 (*ALDH1A2*) which is known to convert retinaldehyde into retinoic acid. The retrived results suggested this enzyme to be involved in hair cycle regulating processes, as a catagen induction was observed in all three tested donors. The second investigated target gene was transforming growth factor beta 1 induced transcript 1 (*TGFβ1I1*) which is known to act as an androgen receptor coactivator. This gene also has an impact on hair cycle related processes, indicated by a tendential decrease in the number of HFs in anagen phase. Both of these target genes gave promising results and deserve further investigation regarding their actual role in mpAGA.

In summary, this thesis promotes new insights into the development of the most common form of hair loss in men and identified two new target genes which possibly might serve as new potential treatment options for mpAGA.

8 Zusammenfassung

Die männliche androgenetische Alopezie (mpAGA) ist die häufigste Form des Haarausfalls bei Männern. Die wichtigste treibende Kraft für ihre Entwicklung ist bekanntermaßen Testosteron (T). Mit Beginn der Pubertät steigt der T-Serumspiegel im Blut an, und die Haarfollikel (HF) an bestimmten betroffenen (aff) Kopfhautstellen (Scheitel und Stirn) beginnen sich allmählich zu verkleinern. Diese HF werden weniger pigmentiert, dünner und verkleinern sich, bis sie zu Vellus-HF werden. Ab diesem Stadium ist die Miniaturisierung irreversibel, da die HF ihre Verbindung zum *Musculus arrector pili* verlieren. Auf der anderen Seite war bekannt, dass HF aus der okzipitalen Kopfhaut (occ) unempfindlich gegenüber Androgenen sind und diesem typischen Krankheitsbild nicht folgen.

Im Rahmen dieser Arbeit wurde ein *ex vivo* Organkulturmodell, mit dem der Einfluss von T auf mpAGA HF aus verschiedenen Kopfhautbereichen untersucht werden kann, etabliert.

Es ist bekannt, dass HF von der Kopfhaut von mpAGA Patienten T in seinen viel potenteren Metaboliten Dehydrotestosteron (DHT) umwandeln. Diese Arbeit zeigt, dass HF, die mit 30 nM T *ex vivo* behandelt wurden, ihre Fähigkeit, T in DHT umzuwandeln, behalten. Die Immunfluoreszenzfärbungen in dieser Arbeit geben interessante Einblicke in die frühen Folgen der Exposition mit 30 nM T *ex vivo*, die in intermediären (i) und terminalen (t) HF aus dem aff Bereich sowie in t/ iHFs aus dem occ Bereich auftraten. iHF aus dem aff-Bereich zeigten eine verringerte Anzahl von Fibroblasten der dermalen Papille (DP), begleitet von einer verringerten DP Induktivität. aff tHF hingegen zeigten eine erhöhte DP Fibroblastenemigration, begleitet von einer signifikant induzierten Apoptose von Zellen im induktiven dermalen Becher (DC). Interessanterweise zeigten i/ tHFs aus der occ Kopfhaut auch starke Reaktionen auf die T Behandlung *ex vivo*. Ihre Reaktion schien eher protektiv als destruktiv zu sein, was sich in einer geringeren Anzahl von DC Zellen sowie einer erhöhten Proliferation von Haarmatrixkeratinozyten (occ iHF), aber auch in einem signifikant reduzierten Apoptose Niveau in den DC von occ i/ tHF zeigte.

Darüber hinaus bestätigten RNAseq Analysen nach einer 10 nM T Behandlung die Auswirkungen von T auf die Genexpression in HF, unabhängig von ihrer Lage auf der Kopfhaut. Diese Analysen bestätigten, dass occ HF nicht, wie im Allgemeinen jedoch angenommen, T unempfindlich sind.

Darüber hinaus wurde die unterschiedliche Regulierung potenzieller mpAGA Zielgene in bestimmten Kompartimenten von mpAGA aff und occ HF untersucht. Die DP und DC von t und i aff und occ HF von mpAGA Patienten wurden mikrodissektiert und mit einem *Laser Capture Microdissector* bearbeitet. Aus den so gewonnenen Proben konnte ein transkriptomisches Profil aller genannten Typen von HF, DP und DC erstellt werden.

Auf der Grundlage dieser Analysen wurden zwei vielversprechende mögliche neue Zielgene für mpAGA basierend auf Literaturrecherchen ausgewählt und in gesunden menschlichen occ tHF *ex vivo* ausgeschaltet, um ihre Auswirkungen auf den Haarzyklus zu verstehen.

Das erste untersuchte Zielgen war Aldehyddehydrogenase 1 family member A2 (ALDH1A2), das dafür bekannt ist, Retinaldehyd in Retinsäure umzuwandeln. Die Ergebnisse deuten darauf hin, dass dieses Enzym an den den Haarzyklus regulierenden Prozessen beteiligt ist, da bei allen drei getesteten Spendern eine Katageninduktion beobachtet wurde. Das zweite untersuchte Zielgen war das durch den transformierenden Wachstumsfaktor beta 1 induzierte Transkript 1 (TGFβ1I1), von dem bekannt ist, dass es als Androgenrezeptor-Koaktivator wirkt. Dieses Gen hat auch Auswirkungen auf die mit dem Haarzyklus zusammenhängenden Prozesse, was sich in einer tendenziellen Abnahme der Anzahl der HF in der anagenen Phase zeigt. Beide Zielgene lieferten vielversprechende Ergebnisse und verdienen weitere Untersuchungen hinsichtlich ihrer tatsächlichen Rolle bei mpAGA.

Zusammenfassend lässt sich sagen, dass diese Arbeit neue Einblicke in die Entwicklung der häufigsten Form des Haarausfalls bei Männern ermöglicht und zwei neue Zielgene identifiziert hat, die möglicherweise als neue potenzielle Behandlungsoptionen für mpAGA dienen könnten.

List of figures

List of tables

Abstracts arose from this thesis

S. Altendorf, M. Fehrholz, M. Geyfman, N. Poloso, F. Jimenez, H. Erdmann, R. Paus, T. Bíró, M. Bertolini. New insights into androgenetic alopecia: Testosterone affects not only vertex but also occipital intermediate and terminal hair follicles of mpAGA patients *ex vivo.* Time to reformulate a current dogma? (31st European Academy of Dermatology and Venereology congress, oral presentation)

S. Altendorf, M. Fehrholz, M. Geyfman, N. Poloso, F. Jimenez, H. Erdmann, T. Bíro, R. Paus, M. Bertolini. Vertex and Occipital Intermediate and Terminal Hair Follicles from Androgenetic Alopecia Patients are Differentially Affected by Testosterone *ex vivo*. (Abstract accepted as poster number 564, for poster presentation at the 51st Annual Meeting of the European Society for Dermatological Research)

S. Altendorf, M. Geyfman, N. Poloso, F. Jimenez, H. Erdmann, R.Paus, M. Bertolini. Testosterone affects not only vertex, but also occipital intermediate and terminal hair follicles in mpAGA patients ex vivo – time to reconsider a current dogma? (Abstract accepted for poster presentation at the 12th Annual World Congress for Hair Research).

Publications generated during this thesis

Piccini, M. Sousa, S. Altendorf, F. Jimenez, A. Rossi, W. Funk, T. Bíró, R.Paus, J. Seibel, M. Jakobs, T. Yesilkaya, J. Edelkamp, M. Bertolini. Intermediate hair follicles from patients with female pattern hair loss are associated with nutrient insufficiency and a quiescent metabolic phenotype. Nutrients (submitted).

Publications in progress

Sabrina Altendorf, Marta Bertolini, Jennifer Hundt, Mikhail Geyfman, Neil Poloso, Ralf Paus. Frontiers in the pathobiology of male pattern androgenetic alopecia: Beyond the androgen horizon (Review)

Acknowledgements/ Danksagung

I want to thank **Dr. Marta Bertolini** and **Prof. Ralf Paus** for encouraging me for a long time to accept this challenge. Furthermore, I am so grateful that both of you gave me the opportunity to work on such an interesting and great project at Monasterium Laboratory. I would have never chosen a different lab to take this step. Thank you for teaching me how to work and think scientifficly, even when it is not alsway that easy.

Marta, from the first day we met, you have been my mentor and a great inspiration for me. And even more important, you became my friend. I want to thank you for supporting me in a very special way. You led me to where I am. Thank you for teaching me so incedably much. Without you, I would not have been able to bring this thesis to an end. Thank you for always having faith in my abilities.

Ich danke **Prof. Dr. Hauke Busch**, dass ich in seinem Institut meine Dissertation eireichen und verteidigen durfte.

Ein riesiger Dank gilt meiner Doktormutter **Prof. Dr. met. vet. habil. Jennifer Hundt**. Du hast keine Sekunde gezögert, meine Doktomutter zu werden, und dafür bin ich dir unendlich dankbar. Du warst immer für mich da und hast mich zu jeder Zeit mit allem unterstützt. Ich danke dir für alle nächtlichen online Korrektur-Sessions. Wir haben viel gelacht und immer viel Spaß bei der Arbeit gehabt. Das hat die Arbeit so sehr erleichtert. Jenny, ich danke dir, für all den Spaß den wir hatten, und die guten Gespräche, die wir geführt haben. Ich bedauere es sehr, dass wir uns pandemiebedingt nicht einmal sehen konnten.

Ein großer Dank geht auch an **Prof. Dr. rer. nat. Rudolf Manz** der den Posten des Zweitgutachter meiner Arbeit übernommen hat.

Furthermore, I would like to thank **Dr. Francisco Jimenez** and **Dr. Hanieh Erdmann** for providing the patients material. And a huge thank you goes to all **volunteer donors and patients** who consented in donating hair follicles. Without you, this thesis would not have been possible.

A special thank you goes to **all my colleagues in ML**.
Marta L, it was a pleasure to “sit in the same boat” with you my dear. Thank you for always being there and understand what it means to be trapped at the LCM and being desperate together. Thank you for becoming a friend. The time in our little office was special and we always had the best christmas decoration.
Janin, danke dass du stehts ein offense Ohr und eine Schulter für mich hattest. Unsere Montags-Heißgetränke haben jeden Montag erheblich versüßt. Danke, dass ich immer zu dir

kommen konnte.
Thomas, darling, what should I say? Thank you for always being available when I needed to talk. You were able to calm me down again by listening to me and having the best cigarette timing. Our 90s playlist rocks!

Ilaria, thank you for supporting me in every manner. I am so thankful that I had the opportunity to learn so much from you!
Ein großer Dank geht auch an **Markus**. Du warst immer geduldig mit mir, wenn mich Excel wieder geärgert hat. Und auch so hast du jedes Computer Problem gelöst bekommen.

Ein besonderer Dank gilt meinen Eltern, **Gisela** und **Ralf Altendorf**. Ihr habt mir immer versucht, alles im Leben zu ermöglichen und mich bei allem was ich gemacht habe immer unterstützt. Ohne euch wäre ich nicht der Mensch geworden der ich heute bin.

Ebenfalls möchte ich meiner Schwester **Simone Brümmer** danken. Danke, dass es dich gibt und wir immer ein Team waren und es auch immer sein werden! In allen Lebenslagen und ein Leben lang!

Auch meinem Partner, **Dennis Boosmann,** gilt ein ganz besonderer Dank. Danke für deine Liebe und deine Unterstützung, bei allem was ich mache und mir wieder in den Kopf gesetzt habe. Ohne dich hätte ich schon manches Mal aufgegeben und einfach alles hingeschmissen. Du hast viele von meinen Launen ertragen müssen, aber mir dennoch immer den Rücken freigehalten und auch niemals an mir gezweifelt und mir immer gesagt, dass ich alles schaffen kann was ich mir in den Kopf gesetzt habe. Wir sind und bleiben immer ein Team und können alles schaffen!

Ebenfalls von ganzem Herzen möchte ich meine Freundin **Ute Sroka** danken. Ich danke dir dafür, dass du immer an mich glaubst und immer für mich da bist. Danke für dein immer offenes Ohr und die Bereitschaft eine Flasche Vino zu öffnen, wenn die Verzweiflung wieder sehr groß war. Ebenfalls danke ich dir, dass du mich wieder auf Spur bringst und mir den Kopf zurechtrückst, wenn es notwendig ist. Wie wir immer sagen, wir haben uns nicht gesucht, aber dennoch gefunden. Und das ist auch gut so. Danke, dass du immer da bist. Du bist und bleibst meine Person!

Auch meiner Freundin **Sonja Erhard** möchte ich danken. Du begleitest mich nun schon seit mehr als 22 Jahren. Trotz großer Entfernung haben wir uns nie aus den Augen verloren und dafür bin ich unendlich dankbar. Ich weiß, ich kann dich jederzeit anrufen und du hast immer ein offenes Ohr für mich. Wie Honig an einem Blatt!

Abschließend möchte ich meinen Mädels, den **Green Mambas,** danken. Danke **Ute, Anna, Svetti, Keule** und **Ramona**, für all die schönen Abende und die schöne Zeit in sämtlichen Gärten und Pools, unsere mega driving dinners, unsere Fahrrad-Touren, Clubfahrten, Cocktailabende und Küchenpartys. Ihr habt es immer geschafft, mir den Kopf wieder frei zu machen und mich abzulenken, wenn ich es brauchte.

Nevertheless, I would like to thank all of my family, friends and colleagues I did not mention here by name. Luckily, there are too many to list, but everyone has contributed to this work.

Curriculum vitae

Sabrina Altendorf

BIOGRAPHICAL DETAILS

Name	Sabrina Altendorf
Birth date	12th December 1986
Email:	sabrina.altendorf@qima.com

EDUCATION

2008	Graduation from Gymnasium Weilheim with Abitur
2008 – 2011	Friedrich Alexander University Erlangen and Nürnberg 08/2011 Bachelor's Degree in Biology
2011 – 2014 01/2014	Ruhr- University Bochum Master's Degree in Biology and Molecular Lifesciences
Since 09/2022	University of Lübeck, external PhD student

WORKING EXPERIENCE

2011	Five months training at the research laboratory of Prof. Dr. Wolfgang Kreis in the Department of pharmaceutical biology at the Friedrich Alexander University Erlangen for the Bachelor's thesis project 'Optimization of the chromatographic conditions for the purification of recombinant P5βR from *E. coli*'
2013 – 2014	Eleven months training at the research laboratory of Prof. Dr. Ralf Erdmann in the Department of Systems Biochemistry at the Ruhr-University Bochum for the Master's thesis project 'functional characterization of human USP2'
2015 – 2016	Research technician in the Laboratory of Prof. Ralf Paus, Department of Dermatology in the University Hospital Münster, Germany

2016 – 2017	Research technician in the Laboratory of Dr. Marta Bertolini, Department of Dermatology in the University Hospital Münster, Germany
2017 – 2019	Research technician at Monasterium Laboratory, Skin & Hair research Solutions GmbH, Münster, Germany
09+12/2019	Guest Scientist at Mediteknia Hair Lab, Las Palmas de Gran Canaria, Las Palmas, Spain
Since 09/2019	External PhD student at the University of Lübeck, working at Monasterium Laboratory, Skin and Hair research Solution GmbH, Münster, Germany as 'Scientist in training'

PUBLICATIONS

1. I. Piccini, M. Sousa, S. Altendorf, F. Jimenez, A. Rossi, W. Funk, T. Bíró, R.Paus, J. Seibel, M. Jakobs, T. Yesilkaya, J. Edelkamp, M. Bertolini. Intermediate hair follicles from patients with female pattern hair loss are associated with nutrient insufficiency and a quiescent metabolic phenotype. Nutrients (submitted).

POSTER PRESENTATIONS

M. Bertolini, S. Altendorf, Y. Uchida, Q. Zhou, A. Rossi, K. Dornmair, R. Paus (2016): Towards the clonotype analysis of alopecia areata-specific, intralesional human CD8+ T-lymphocytes (accepted for Poster presentation at the46th Annual Meeting of the European Society for Dermatological research (ESDR), Munich, Germany)

S. Altendorf, M. Fehrholz, M. Geyfman, N. Poloso, F. Jimenez, H. Erdmann, T. Bíró, R. Paus, M. Bertolini (2022): Evidence that the dogma of androgen-"insensitive" occipital hair follicles in male pattern balding is unsustainable: Testosterone affects occipital intermediate and terminal hair follicles of androgenetic alopecia patients *ex vivo* (2nd 'Hair Biology & Translational Research in a Nutshell International Training course' organized by Monasterium Laboratory, Münster, Germany)